The Dissertation Committee for Insoo Hwang
certifies that this is the approved version of the following dissertation:

Multicell Coordination with Multiple Receive Antennas

Committee:

Robert W. Heath, Jr., Supervisor

Gustavo de Veciana

Sanjay Shakkottai

Scott Nettles

John Hasenbein

Multicell Coordination with Multiple Receive Antennas

by

Insoo Hwang, B.S.; M.S.E.E.

DISSERTATION

Presented to the Faculty of the Graduate School of

The University of Texas at Austin

in Partial Fulfillment

of the Requirements

for the Degree of

DOCTOR OF PHILOSOPHY

THE UNIVERSITY OF TEXAS AT AUSTIN

December 2013

Dedicated to my father.

Acknowledgments

I wish to thank my advisor Prof. Robert W. Heath, Jr., without whom this dissertation would not be possible. I also wish to thank the committee members Professors Gustavo de Veciana, Sanjay Shakkottai, Scott Nettles, and John Hasenbein. I thank the staff members of the WNCG office and the ECE department - Janet Preuss and Melanie Gulick.

Over my course of stay, I have had the privilege of collaborating with many people and I wish to express my gratitude for such opportunity. Specifically, I would like to thank those who have contributed to my intellectual development; they are Prof. Kyungwhoon Cheun, Prof. Vahid Tarokh, Dr. Bongyong Song, Dr. Heejin Roh, and many others. I would also like to thank my friends Jungho Ryu, Minchan Lee, Yongseok Yoo, Ramya Bhagavatula, Jaeweon Kim, Chan-Byoung Chae, and Behrang Nosrat-Makouei.

I would like to thank my mother, my wife Jinyoung and my two sons, Ian and Yireh, for their love and support. I would like to thank my father-in-law and mother-in-law for their prayers. I would like to thank Jesus Christ for loving me and showing His presence in my entire life.

Lastly, I would like to thank my father who started me in an electrical engineering career by encouraging me to choose POSTECH, and who I wish could have seen where this would lead.

Multicell Coordination with Multiple Receive Antennas

Publication No. _____

Insoo Hwang, Ph.D.
The University of Texas at Austin, 2013

Supervisor: Robert W. Heath, Jr.

In multicell coordinated networks where multiple base stations cooperate to jointly combat interference from adjacent cells and fading to receivers, one of the outstanding questions is what is the role of receive antenna and receiver processing. Multiple receive antennas not only enable additional degrees of freedom at each receiver to combat the other-cell interference but also can change the transmitter design because transmitter and receiver beamforming design is often closely coordinated. In this dissertation, we investigate the role of the multiple receive antennas in multicell cooperative systems under different interference conditions. We then present novel non-iterative and iterative coordinated beamforming and precoding algorithms with different receiver processing. We present comprehensive performance comparison of various multicell cooperative systems and explore the feasibility of achieving much higher throughput via hyper-densification of heterogeneous and small cell networks with mandatory multicell cooperation.

Table of Contents

Acknowledgments **v**

Abstract **vi**

List of Tables **x**

List of Figures **xi**

Chapter 1. Introduction **1**

1.1 Problem Statements 4

1.2 Summary of Contributions 6

1.2.1 Multicell Cooperation with Multiple Receive Antennas . 6

1.2.2 Interference-Aware Coordinated Precoding 7

1.2.3 Iterative Coordinated Beamforming 7

1.2.4 Comprehensive Performance Comparison 8

Chapter 2. Multicell Cooperation with Multiple Receive Antennas **9**

2.1 Introduction 9

2.2 Coordinated Beamforming Systems 12

2.2.1 Cellular Networks: CBF with No Data Sharing 12

2.2.2 Cellular Networks: JP with Perfect Data Sharing 15

2.2.3 Cognitive Networks 18

2.3 Advanced Receiver Algorithms 20

2.3.1 White Gaussian Interference: MMSE Filter 21

2.3.2 Colored Gaussian Interference: IW-MMSE or MMSE-IRC 22

2.3.3 Interference with Known Modulation Order: Joint Detection 25

2.4 Multicell Cooperation in Emerging Standards 26

2.4.1 CoMP Algorithms and Scenarios 27
2.4.2 Practical Issues in Receiver Processing 30
2.4.2.1 Feedback Channel Design 31
2.4.2.2 Downlink Reference Signal Design 32
2.4.2.3 Receiver Architecture 34
2.4.3 System Performance Evaluation Results 34
2.5 Fundamental Limits of Cooperation 36
2.6 Discussions 38

Chapter 3. Interference-Aware Coordinated Precoding 40
3.1 Introduction 40
3.2 System Model 42
3.3 Interference Aware-Coordinated Precoding 46
3.3.1 Dedicated Precoder Design 47
3.3.2 Common Precoder Design 48
3.3.3 Common Postcoder Design 49
3.4 Coordinated Precoding with MMSE-IRC 50
3.5 Simulations 51
3.6 Discussions 55

Chapter 4. Iterative Coordinated Beamforming 56
4.1 System Model and Problem Statement 57
4.2 Iterative CBF Algorithms 59
4.2.1 Maximizing Per-MS SINR 59
4.2.2 Maximizing Per-BS SLNR 61
4.2.3 Minimizing Sum-MSE (SMSE) 63
4.2.3.1 Max-SLNR beamforming and the transmit MMSE filter 67
4.2.3.2 Proof of convergence: 69
4.2.3.3 Comparison with non-iterative joint CBF: . . . 70
4.3 Iterative CBF with Limited Cooperation 71
4.4 Performance Comparison 74
4.5 Discussions 79

Chapter 5. Comprehensive Performance Comparison **81**
5.1 Further Evaluation of Coordinated Beamforming 82
5.2 Coordinated Beamforming vs. Joint Processing 85
5.3 Multicell Coordination in Heterogeneous Networks 88
5.3.1 Massive MIMO 88
5.3.2 Hyper-Dense HetSNets 89
5.3.3 Simulation Assumptions 91
5.3.4 Performance Comparison 94

Chapter 6. Conclusions and Future Work **105**
6.1 Conclusions 105
6.2 Future Work 107

Bibliography **112**

Vita **125**

List of Tables

2.1 Comparisons of receiver processing. Scenarios are I: Many interferers without dominant one, II: A few interferers with dominant one, and III: Single or a few strong interferers. Interference channel, interference plus noise variance, and interference covariance matrix are respectively denoted by $\boldsymbol{H}_I$, σ_I^2, and $\boldsymbol{R}_I$. MCS represents modulation and coding selection. 21

2.2 A summary of the characteristics for each CoMP algorithm. . 27

2.3 CoMP scenarios and supported algorithms in 3GPP LTE-Advanced [3]. The scenarios are I: Homogeneous network with intra-site coordination, II: Homogeneous network with high power RRHs, III: Heterogeneous with low power RRHs (different cell IDs) and IV: Heterogeneous with low power RRHs (same cell ID). . . . 30

2.4 Summary of precoding vector generation metrics in various CoMP and non-CoMP MIMO systems. The channel from the i-th base station to the j-th mobile station is denoted as $\boldsymbol{H}_{ij}$. vec and eig respectively represent the dominant eigenvector and eigenvalue. For JT with per-point feedback, inter-point phase information needs to be fed back to compute the transmit MCS at the base station. 31

2.5 Rank statistics - homogeneous (left column) and heterogeneous (right two columns) scenarios 35

2.6 Cell average and cell edge (5-percentile user) throughput performance comparison in homogeneous (left two columns) and heterogeneous (right two columns) scenarios. 36

4.1 Channel matrices, noise variances and beamforming vectors required to compute the transmit beamforming and receive combining vectors at the base station and the mobile station . . . 63

List of Figures

1.1 Coordinated multicell processing system model (a three cell scenario). Base stations (BSs) coordinate via inter-BS backhaul link to jointly combat the other-cell interference and to improve cell-edge user throughput. 2

1.2 A generic multicell MIMO receiver processing. LMMSE, MLD, and LLR represent linear minimum mean square error, maximum-likelihood detection and log-likelihood ratio, respectively. . . . 3

2.1 Coordinated multicell processing system model (a three cell scenario). The k-th receiver is in a coordinated beamforming scenario, the l-th receiver is under a joint processing scenario, and the m-th receiver is in spatial sensing scenario. 10

2.2 An illustration of IW-MMSE and MMSE-IRC processing. IW-MMSE is a two step approach for i) interference whitening and ii) LMMSE, while MMSE-IRC is a combined approach. Under the same estimation error, the two approaches result in the same symbol detection performance. 23

3.1 Equivalent two-user MIMO interference channel, (a) each base station transmits both dedicated and common messages. The dedicated message is for the desired mobile station, while the common message can be decoded at any mobile station and (b) a linear receiver structure. 43

3.2 Signaling flow chart of the proposed algorithm. 45

3.3 Sum rate performance comparison with full feedback. 52

3.4 Sum rate performance (common only). 53

3.5 Sum rate comparison with limited feedback. For the simulation, a non-uniform codebook with 3 bit quantization per real entry is used. 54

4.1 K User, K cell MIMO coordinated beamforming system model. 57

4.2 Sum rate comparison (SIR=0 dB, $K = N_{\mathrm{t}} = N_{\mathrm{r}} = 2$). 75

4.3 Sum rate under different numbers of iterations I - SNR at 5dB. 76

4.4 Sum rate under different numbers of iterations II - SNR at 20dB. 77

4.5 Sum throughput performance of proposed iterative CBF with limited cooperation. 78
4.6 Sum rate with limited cooperation ($K = 16, N_{\mathrm{t}} = N_{\mathrm{r}} = 4$). . . 79

5.1 Comparison of iterative coordinated beamforming algorithms with imperfect CSIR/CSIT due to channel estimation error and limited feedback. 82
5.2 Comparison between iterative and non-iterative coordinated beamforming algorithms in $N_{\mathrm{t}} = N_{\mathrm{r}} = K = 2$. 84
5.3 Block diagram of the proposed multicell joint processing. . . . 86
5.4 Sum throughput of linear and nonlinear joint processing with different numbers of antennas. The capacity with nonlinear precoding is obtained using the sum power iterative water-filling process [43]. Vector perturbation (VP) [32] is used as nonlinear precoding technique. 87
5.5 An illustration of base station distribution for 3-tier (red: macro, blue: pico, green: femto) HetSNets in (a) PPP and (b) MHP with voronoi tessellation of macro cells, and (c) their cell coverage performance comparison. In both cases, $\lambda_3 = 4\lambda_2 = 8\lambda_1$, where λ_i is the i-th tier's base station density. In MHP, the minimum distance in each tier is inversely proportional to its transmit power and the cell coverage performance is improved as the number of cells (N) in unit area is increased. 92
5.6 Performance comparison - massive MIMO (number of users per cell $K = 8$, number of cells $L = 4$, and inter-cell interference factor $\alpha = 0.1$) vs. dense small cells (1-tier, base stations are distributed by MHP with minimum distance $85m$, path loss exponent $\gamma = 4$). 'Best cell selection' means that each user selects the nearest base station and the unchosen base stations are turned off. 93
5.7 Performance comparison - dense small cells with and without multicell cooperation. In multicell Cooperation I, we assumed that each mobile station is capable of mitigating one dominant interferer, which is the strongest interference. In Coooperation II, each mobile station is capable of mitigating two dominant interferers. 95
5.8 PPP with $N = 500$ with voronoi tessellation of small cells. Blue dots represent mobile stations (500 users) and red dots represent the 8 mobile stations. 96
5.9 Area throughput with PPP distribution of small cells. 97

5.10 MHP with $N = 500$ with voronoi tessellation of small cells. Blue dots represent mobile stations (500 users) and red dots represent the 8 mobile stations. $50m$ minimum distance is enforced between small cells. The path loss exponent is 4. 98

5.11 Area throughput with MHP distribution of small cells. $50m$ minimum distance is enforced between small cells. 99

5.12 MHP with $N = 500$ with voronoi tessellation of small cells. Blue dots represent mobile stations (500 users) and red dots represent the 8 mobile stations. $85m$ minimum distance is enforced between small cells. 100

5.13 Area throughput with MHP distribution of small cells. $85m$ minimum distance is enforced between small cells. 101

5.14 SINR distribution. 102

6.1 The 1000x data challenge in three domains. 107

6.2 Multiple paths to the 1000x data throughput with projected gains. 108

Chapter 1

Introduction

In wireless cellular systems, a geographical region is broken down into multiple small cells so that each cell covers a fraction of the region. Within each cell, there is a base station dedicated to serve mobile stations within the vicinity of that cell. Under this cell structure, all voice and data traffic that the mobile stations request and generate will be transmitted to and from the base station dedicated to serving them. The mobile station may have a good link quality if the serving base station is in close proximity. The mobile station at the cell edge region, however, may experience poor link quality not only because of the degradation of desired signal strength due to path loss but also because of the higher out-of-cell interference. As the average cell size keeps decreasing due to the viral proliferation of small cells [1], mitigating the out-of-cell interference has become an interesting research area.

One of the performance indicators to decide the maximum rate at which the mobile stations and the base stations can communicate with each other is the received signal-to-interference-plus-noise-ratio (SINR); the higher the SINR, the higher the maximum rate. Transmissions from the neighboring base stations, however, result in out-of-cell interference, degrading the SINR, espe-

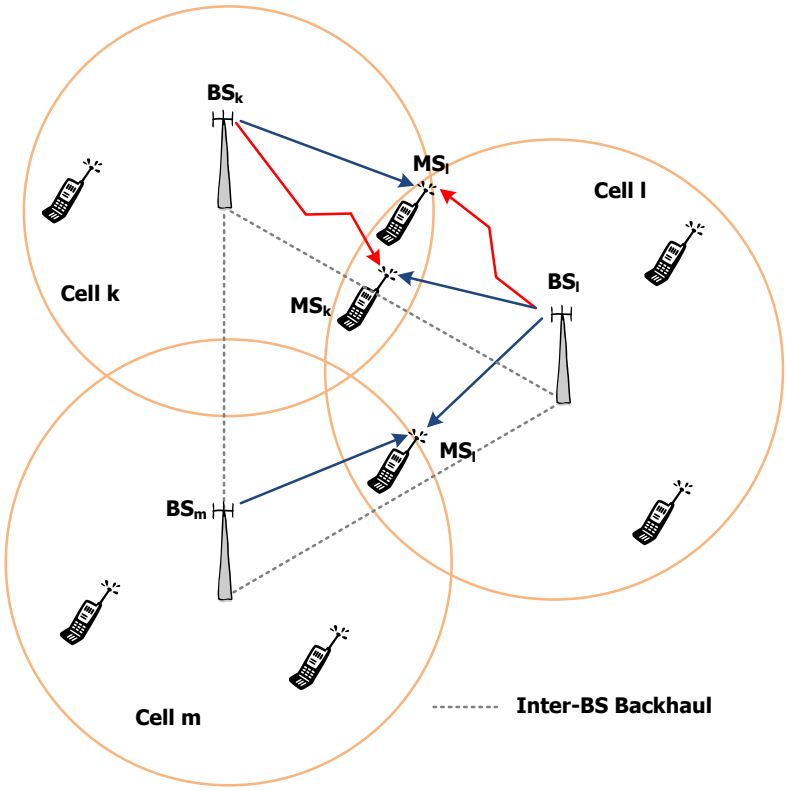

Figure 1.1: Coordinated multicell processing system model (a three cell scenario). Base stations (BSs) coordinate via inter-BS backhaul link to jointly combat the other-cell interference and to improve cell-edge user throughput.

cially for mobile stations located at the cell edge [20, 70, 82]. The co-channel deployment of base stations to avoid any frequency segmentation and thus improve spectral efficiency often causes higher out-of-cell interference. Suppressing such interference is important to improve the maximum transmission rate and user experience.

To reduce the effects of the out-of-cell interference, cooperation between base stations, called multicell cooperative processing, is being actively inves-

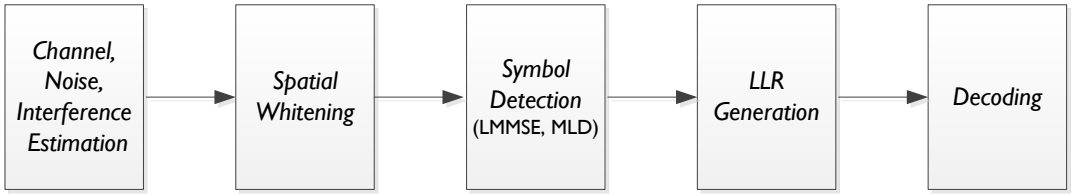

Figure 1.2: A generic multicell MIMO receiver processing. LMMSE, MLD, and LLR represent linear minimum mean square error, maximum-likelihood detection and log-likelihood ratio, respectively.

tigated [22, 30, 44, 46, 65, 70, 72, 83]. This base station cooperation requires an exchange of information such as downlink channel state and transmit data stream between nearby base stations. Multicell cooperation is considered as one of the important building blocks to achieve higher throughput in practical cellular systems such as 3GPP LTE-Advanced [3].

With the need for high spectral efficiency and the decrease in the price of radio frequency (RF) electronic components, the base and mobile stations are now equipped with more and more antennas. When both the base station and the mobile station can utilize multiple antennas, multiple-input multiple-output (MIMO) technologies can be used to provide high data rates and robustness. By combining beamforming or precoding techniques enabled by MIMO with the multicell cooperative processing, the received SINR per mobile station can be increased, thus further improving the overall system throughput. Since receiver processing plays a key role in the multicell cooperative system, the role of multiple receive antennas needs to be investigated in order

to fully understand and thus to achieve the full benefits of the multicell MIMO cooperative systems [28].

1.1 Problem Statements

A typical MIMO multicell cooperative processing system model is presented in Fig. 1.1. Prior work on multicell cooperative processing can be categorized as either 1) coordinated beamforming or 2) joint processing. In coordinated beamforming, base stations exchange only the downlink channel information, and each mobile station receives a stream of data from only one base station. The mobile station with coordinated beamforming is illustrated as MS_k in Fig. 1.1. In this case, the multicell MIMO channel is a MIMO interference channel and the goal of the coordinated beamforming is to design jointly optimized transmit and receive beamformers to minimize the effect of the out-of-cell interference. A number of coordinated beamforming algorithms have been proposed in the literature [9, 22, 30, 65, 69, 84].

In joint processing, data for a mobile station is available at more than one base station for a time-frequency resource [3]. In this case, downlink data streams as well as downlink channel information must be exchanged via inter-BS cooperation. The joint processing transforms the MIMO interference channel (in the coordinated case) into a MIMO broadcast channel because multiple coordinated base stations effectively form a distributed base stations,

virtually forming a super base station [1]. The capacity region of such systems is specified in [13, 76, 78]. The mobile station with the joint processing is illustrated as $\mathsf{MS_I}$ in Fig. 1.1. Prior work in [15, 44, 46, 71, 72, 83] is based on joint processing.

A generic multicell MIMO receiver processing is presented in Fig. 1.2. If the number of data streams designated to a receiver is smaller than the number of receive antennas, the receiver can use the receive antennas to combat the other-cell interference. Additional degrees of freedom at each receiver enable such operation, even with the use of linear receive filters [14, 49, 51]. When the number of receive antennas is equal to or less than the number of streams to decode, more advanced receiver algorithms to suppress the other-cell interference can also be used. The non-linear receiver processing can also be exploited when the channel is agile i.e. the channel coherence time is significantly shorter than the round-trip delay thus a full transmit-receive coordination is not feasible. Advanced receiver techniques can thus be complimentary to the full base station cooperation. As multiple receive antennas are being used nowadays, the receiver processing has become an important part in multicell cooperative systems. Despite the importance, however, the role of the receive antenna and its implications to multicell cooperative coordinated processing has not been fully understood.

[1] Such systems often refer to as distributed antenna systems (DAS).

1.2 Summary of Contributions

The main contribution of this dissertation is to investigate the role of multiple receive antennas and to propose joint transmit-receive beamforming/precoding algorithms in multicell MIMO cooperative systems. We first investigate the benefits of having multiple receive antennas in multicell cooperative systems [35]. This includes both linear receiver such as interference rejection combining [8] and advanced receiver techniques such as joint maximum likelihood [48]. We then propose novel receiver techniques that enable a simultaneous reception of two classes of messages, a private and a common [36]. We propose iterative coordinated beamforming techniques in which receiver beamforming can jointly be designed with transmit beamforming to combat the out-of-cell interference [37]. Finally, we present a comprehensive performance comparison of the multicell cooperation systems with other competing techniques under different circumstances.

We briefly introduce our main contributions below, which will be shown in detail in each subsequent chapter.

1.2.1 Multicell Cooperation with Multiple Receive Antennas

We investigate multicell cooperative systems with multiple receive antennas and advanced receiver techniques. In particular, coordinated beamforming (CBF), joint processing (JP) and spatial sensing (SS) techniques are introduced, explaining their potential use of multiple receive antennas. Asymptotic behavior of the sum rate with increasing number of receive an-

tennas is also analyzed. Advanced receiver algorithms, which include minimum mean square error (MMSE), interference rejection combining (IRC), interference whitening (IW) and joint detection (JD), in different interference statistics are also introduced. Multicell cooperative processing, coordinated multi-point (CoMP), as it is being envisioned by emerging wireless standards, are reviewed. We present system performance evaluation results with various multicell MIMO techniques and advanced receiver algorithms.

1.2.2 Interference-Aware Coordinated Precoding

We propose interference aware-coordinated precoding algorithms to support both private and common messages at the same time. The system model used is a mixture of coordinated beamforming and joint processing in multicell cooperation: base stations transmit both dedicated message and common message and mobile stations receive dedicated message from only one base station while common message can be received from multiple base stations. Under different linear receive processing strategies, we propose coordinated precoding algorithms which are simple but outperform conventional resource segmentation approaches.

1.2.3 Iterative Coordinated Beamforming

We propose novel iterative coordinated beamforming algorithms with limited cooperation for multicell environments. The algorithms are based on MMSE criterion at the transmitters and receivers in the cooperating cells.

The algorithms are designed to update the beamforming vectors iteratively and each node acts to reduce the common network cost. We then extend the algorithms with the limited cooperation where each transmitter and receiver only cooperate with limited adjacent nodes, with synchronous or asynchronous update. By simulation and analysis, the proposed algorithms are shown to achieve better sum throughput than previously proposed coordinated beamforming algorithms and achieve performance close to that of the brute force search algorithm.

1.2.4 Comprehensive Performance Comparison

We provide comprehensive performance comparison between many multicell cooperation techniques with different receiver algorithms. We first compare the sum rate performance between iterative coordinated beamforming and non-iterative coordinated beamforming. A sum rate comparison between coordinated beamforming and joint processing is presented. We also show the performance of multicell coordination in a very densely deployed heterogeneous and small cell network (HetSNets), which is being considered as an enabling technology to achieve the 1000x more data thought for the 5th generation cellular networks, a.k.a, 5G. We also compare the transmitter-centric technique (e.g., massive MIMO) and receiver-centric technique (HetSNets with interference cancellation receivers) when adjacent cells are coordinated.

Chapter 2

Multicell Cooperation with Multiple Receive Antennas

In this chapter, we describe how receive antennas may be used in various multicell cooperative systems and then review receive antenna techniques for different interference conditions. We then investigate the practical issues of receiver processing in emerging standard, followed by the system performance evaluation results.

2.1 Introduction

Multicell cooperative processing has become an important technology for modern cellular networks. To deal with the increasing data traffic due to smart phones, wireless cellular systems such as LTE networks will off-load portions of their traffic onto smaller cells such as picocell, femtocell, and relay, which together with the currently existing macro cells form a heterogenous network. As these cells get smaller and as more cells are packed into the same amount of space, the receiver may see more diverse and stronger out-of-cell interference and thus a novel way of handling the out-of-cell interference is required. To mitigate the effects of out-of-cell interference, multicell cooper-

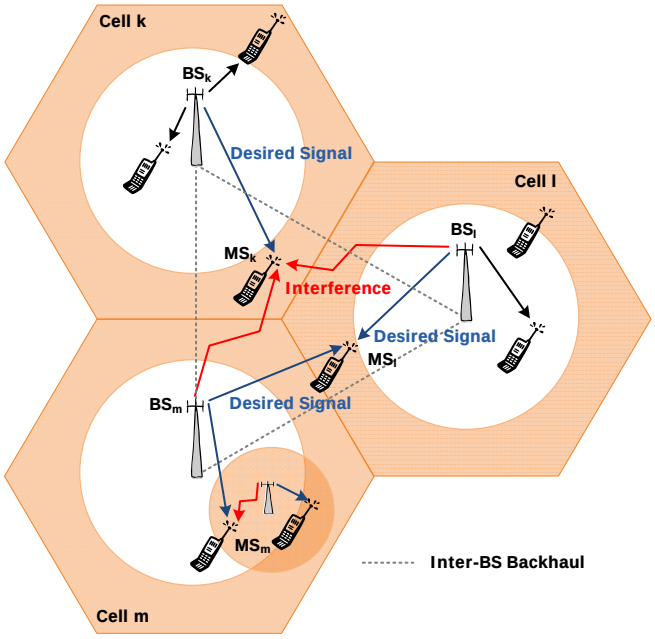

Figure 2.1: Coordinated multicell processing system model (a three cell scenario). The k-th receiver is in a coordinated beamforming scenario, the l-th receiver is under a joint processing scenario, and the m-th receiver is in spatial sensing scenario.

ative processing techniques have been actively investigated [14, 21, 28, 49, 51]. In this regard, multicell cooperative processing is being actively discussed in emerging wireless cellular standards such as the 3GPP LTE-Advanced [3].

In multicell cooperative processing, the transmitters cooperate to jointly combat interference from adjacent cells and fading to receivers. This cooperation requires exchanging some information such as downlink channel information and may require multiple antennas. The barriers to prevent such cooperation has become less costly; the wired communication between transmitters (e.g., X2 interface in the 3GPP LTE-Advanced networks) enable the trans-

mitters to exchange information quite reliably with only marginal delay. The decrease in the price of RF electronic components enable the transmitters and receivers to use MIMO technologies. By combining beamforming/precoding techniques enabled by MIMO with multicell cooperative processing, the post-processing SINR per each receiver can be increased, thus further improving the system throughput.

If the number of data streams designated to a receiver is smaller than the number of receive antennas, the receiver can utilize the receive antennas to combat the other-cell interference. Additional degrees of freedom at each receiver enable such operation, even with the use of linear receive filters [14, 49, 51]. When the number of receive antennas is not greater than the number of streams to decode or transceiver coordination is not feasible due to inaccurate feedback, more advanced receiver algorithms to suppress the other-cell interference can also be used. Advanced receiver algorithms such as the joint maximum likelihood (ML) detector may give better error rate performance through decoding the desired signal and interference signal *jointly* rather than treating the interference as noise [48].

Another potential benefit of using multiple receive antennas in multicell cooperative networks is the measurement of network utility performance. The capacity region of the MIMO interference channel with multiple receive antennas at each receiver–the system model of interest in this article–is still unknown for most cases. The degrees of freedom of the MIMO interference channel has recently been well studied [29] and a better measure of the achiev-

ability that takes interference signal strength into account has been proposed in [27]. Despite its importance, the role of the receive antenna in multicell cooperative coordinated processing has yet to be fully understood.

To achieve this diverse set of objectives, in this chapter, we first introduce basic coordinated beamforming systems, each of which is mainly categorized by the type of information sharing. Next, we investigate the role of multiple receive antennas in coordinated beamforming systems and introduce advanced receivers–processing techniques to efficiently mitigate the other-cell interference. Then we introduce recent theoretical findings on the fundamental limits of cooperation and discuss their expansion to more general multicell scenarios. Finally we review multicell coordinated beamforming in emerging standards, mainly focusing on 3GPP LTE-Advanced systems, and then follow with some conclusions.

2.2 Coordinated Beamforming Systems

Prior work on multicell cooperative processing can be categorized as either 1) coordinated beamforming (CBF), 2) joint processing (JP), or 3) spatial sensing (SS). In this section, we present the key concepts of the three different multicell cooperative processing techniques.

2.2.1 Cellular Networks: CBF with No Data Sharing

In coordinated beamforming, the transmitters exchange only the downlink channel information, and each receiver receives a stream of data from only

one transmitter. The receiver in coordinated beamforming is illustrated as $\mathsf{MS_k}$ in Fig. 2.1. In this case, the multicell MIMO channel is the MIMO interference channel and the goal of the coordinated beamforming is to design jointly optimized transmit and receive beamformers to minimize the effect of the out-of-cell interference. A number of coordinated beamforming algorithms have been proposed in the literature [14, 29], with interference alignment being one of the technical enablers.

In coordinated beamforming, data for a receiver is only available at and transmitted from one cooperating base station for a time-frequency resource. User scheduling and beamforming decisions, however, are made with coordination among transmitters corresponding to the cooperating set. The transmit beamforming and receive combining vectors are generated to reduce the unnecessary interference to other receivers scheduled within the coordinated cell. The scheduler is targeted to maximize the SINR or to minimize the leakage power to other receivers while maximizing the signal power to the desired receiver. The latter is often called Max-SLNR (signal-to-leakgage-plus-noise ratio) scheduler and often leads to better sum rate than the Max-SINR scheduler. Through scheduling, the desired set of receivers is selected so that the transmit and/or receive beamforming vectors are chosen to reduce the interference to/from other neighboring users, while increasing the serving cell's signal strength. The cell edge receiver's SINR can be improved by CBF, resulting in a cell-edge throughput improvement.

When the receivers are equipped with multiple receive antennas, transceiver

algorithms at the cooperating transmitters and receivers need to be jointly optimized to improve the sum rate. In a two-cell system with multiple receive antennas, non-iterative coordinated beamforming algorithms called interference aware-coordinated beamforming (IA-CBF) were proposed in [14]. It was proven that the proposed algorithms are optimal in terms of the degrees of freedom of the two-cell MIMO channel, where the mobile stations have two receive antennas. An asymptotic expression of the achievable sum rate of the proposed system with respect to the number of receive antennas was also derived. Interestingly, as the number of receive antennas increases, the proposed algorithm achieves not only full degrees of freedom but also the sum rate of the point-to-point upper bound.

For the *normalized* matched channel matrix $\boldsymbol{R} = \boldsymbol{H}_k^* \boldsymbol{H}_k / \|\boldsymbol{H}_k\|_F^2$ ($N_t = 2$), which is assumed as i.i.d Rayleigh fading channel, the $\boldsymbol{R}_{kk}$-th entry has a beta distribution with parameters (N_r, N_r) and the real and imaginary parts of the $\boldsymbol{R}_{kl}$-th entry ($k \neq l$) have the same distribution as $\boldsymbol{R}_{kk}$ with a shift by $1/2$. As $N_r \to \infty$, all diagonal entries of $\boldsymbol{R}$ converge to $1/2$ and all non-diagonal entries converges to 0. Therefore, as $N_r \to \infty$, $\boldsymbol{R}$ becomes a 2×2 identity matrix. The *unnormalized* matched channel matrix $\boldsymbol{R} = \boldsymbol{H}_k^* \boldsymbol{H}_k$ thus converges to $N_r \boldsymbol{I}_{N_t}$ as $N_r \to \infty$, which is equivalent to the point-to-point upper bound of the system [14].

Generalization of IA-CBF algorithms to more than two-cell scenarios is also presented in the same paper [14]. The authors proposed a novel (physical) beam-switching mechanism that intentionally creates a beam conflict; a

conflict that in the conventional system was, as much as possible, avoided. A beam sequence optimization problem is NP-hard; simple algorithms are discussed by prioritizing the transmitter to decide the beam index first based on its own channel information. Next the transmitter determines its own beam index that creates a beam conflict with the top priority transmitter. The philosophy used here is that instead of mitigating other-cell interference and treating them as background noise, the transmitters can create a strong interference link and use it to further minimize the background interference. This can be done by additional receiver processing, so the importance of multiple receive antennas in multicell cooperative processing has become more obvious.

2.2.2 Cellular Networks: JP with Perfect Data Sharing

In joint processing, each user receives a data stream from multiple transmitters. To enable it, downlink data streams as well as downlink channel information must be exchanged via inter-transmitter cooperation. The joint processing transforms the MIMO interference channel (in the coordinated case) into the MIMO broadcast channel in a case of ideal cooperation because multiple coordinated transmitters effectively form a distributed super base station. The capacity region of the MIMO broadcast channel has been studied and analyzed [78]. The receiver in joint processing is illustrated as MS_{I} in Fig. 2.1.

Similar to spatial division multiple access (SDMA) technologies in the MIMO broadcast channel, in joint processing, transmit beamforming is performed to eliminate the other-cell interference at the transmitter while the

receivers with single receive antenna performs simple decoding. Typically the transmitter computes a transmit precoding vector using the aggregated channel knowledge. Linear precoding is one of the simplest solutions, although zero-forcing channel inversion linear precoder suffers from excessive power penalty. Regularized channel inversion precoder is hard to find the exact regularization factor. Nonlinear pre-processing such as vector perturbation (VP) [32] or Tomlinson-Harashima precoding (THP) [79] can be applied on top of the linear precoder, showing a better sum rate performance. The role of multiple receive antennas at the receiver side, however, has not been well addressed.

The network coordinated beamforming (N-CBF) algorithm proposed in [15] approaches the joint processing system in different ways. Instead of multiple transmit antennas with a single receive antenna, the paper focuses on the multicell downlink channel where each transmitter is equipped with one transmit antenna and each receiver is equipped with multiple receive antennas. Linear and non-linear coordinated beamforming algorithms are proposed for both clustered broadcast channels and full broadcast channels that achieve near multicell capacity. The proposed algorithms minimize the largest eigenvalue of the inverse of the effective matched channel matrix to minimize the transmit power consumption and simultaneously maximize the effective channel gain. This can be achieved through the fact that the effective channel goes to the identity matrix as the number of receive antennas goes large; the more receive antenna that the system uses, the better throughput can be obtained even with a single transmit antenna. The expansion of this problem

with multiple transmit antennas is nontrivial and may give better sum rate performance.

It is known that joint processing provides higher system throughput than does coordinated beamforming under ideal circumstances, but at the cost of downlink data stream exchange between transmitters. When the signals from multiple base stations arrive in significantly different time[1], the mobile station may not coherently combine the signals from multiple base stations, resulting in poor received SINR. Thus, the joint processing system is enforced by more stringent delay requirements than in the coordinated beamforming system. We note that another down side of joint processing is the requirement that the transmitters exchange downlink data streams. The price to be paid for such additional cooperation, however, may be decreasing. For instance, in 3GPP LTE-Advanced network [3], the transmitters are *already* connected over a wired backhaul line, so data exchange between transmitters is becoming easier. Recent demand for higher data rate support and the use of multiple receive antennas at the receiver changes the aspect of joint processing from classical soft-handoff or macro diversity to joint transmit and receive beamformer/precoder design in multicell cooperative processing.

[1]In typical OFDM-based systems such as 3GPP LTE, the maximum allowable difference is within (extended) cyclic prefix (CP) duration. In 3GPP LTE [4], the extended CP duration under typical 15KHz subcarrier spacing is $16.7us$, whose equivalent distance is $5km$.

2.2.3 Cognitive Networks

So far, we have focused on homogeneous cellular networks and addressed the role of the receive antennas. In this section, we consider cognitive networks and also investigate how much gain can be achieved due to multiple receive antennas. As the standardization of heterogeneous networks become more concrete, cognitive multicell network is also drawing lots of attention. The use of femtocells in a heterogeneous network may use the same licensed band as the macro transmitter, but the femtocell may not be allowed to create any noticeable interference to the legacy receivers. When the primary transmitters are active, the secondary receiver which is attached to the secondary cell (e.g., femtocells) suffers interference from the primary transmitters. This type of interference has motivated new research into joint transceiver designs in cognitive multicell cooperative networks. The receiver MS_m in Fig. 2.1 fits into this scenario.

In cognitive multicell cooperative networks, most prior work has focused on the design of precoding matrices to suppress interference to the primary receivers. In conventional cognitive multicell systems, the secondary receiver treats interference from the primary transmitter as an additive noise. It is thus mainly an interference avoidance approach that minimizes the signal leakage to the primary receivers. The interference to the secondary receivers is considered as a secondary problem, although the secondary receivers are also desired to communicate reliably. Again, multiple receive antennas at the secondary receivers may help to achieve both objectives simultaneously: i) to prevent

interference to the primary receivers and ii) to remove the interference, due to primary transmissions, at the secondary receiver. This can be done by the help of multiple receive antennas at the secondary receiver.

The spatial sensing coordinated beamforming algorithms (SS-CBF), which were proposed in [49], address this problem. With single-antenna primary terminals and two-antenna cognitive terminals, a linear transceiver design has been introduced under a global channel state information (CSI) assumption. Depending on the required information of the secondary transceiver, the approach and the role of multiple receive antennas may be different. If the secondary transceiver has only the local CSI, which consists of the channel knowledge of primary transmitter-secondary receiver and secondary transceivers, the secondary transmitter constructs the projected-channel singular value decomposition (P-SVD) to enable an error-free communication to the secondary receiver. If the channel between primary transceivers is known to the secondary transceiver in addition to the local CSI, the secondary transceivers can adopt a joint transmitter-receiver optimization which has proved to be optimal under the zero-interference constraint both at the secondary transmitter and receiver. If the local CSI and the side information (precoding and postcoding information of the primary transceivers) is known to the secondary transceivers, iterative precoding and decoding is proposed, outperforming the P-SVD approach of the local CSI.

In all of the proposed three SS-CBF algorithms, multiple antennas at the secondary transceiver are used in two ways: to suppress interference to

the primary receivers and from the primary transmitters and as well as to maximize the achievable rate of the secondary link. The conventional approach in cognitive multicell cooperative networks is focused solely on constructing a transmitter by treating the interference from the primary transmissions to the secondary receiver as an additive noise. The proposed SS-CBF jointly designs the secondary transceivers, resulting in the similar achievable rate to that of equivalent point-to-point MIMO channels. As the number of antennas at the second transceivers increase, the performance of SS-CBF with global CSI converges to that of the point-to-point MIMO channel, while the other two SS-CBF algorithms also show the achievable rate very close to that bound.

2.3 Advanced Receiver Algorithms

If the number of receive antennas are insufficient or the full coordination between transmitters and receivers is not feasible, the receiver may utilize its receive antennas in different ways. An advanced receiver technique may also be required when a small group of adjacent interferers are not fully synchronized. So the other-cell interference becomes non-Gaussian [63]. Assuming the receiver can estimate both the desired channel and interference channel, advanced interference mitigation algorithms can be used. Depending on the statistics of interference, the appropriate receiver algorithms can differ. Table 2.1 presents the three possible receiver algorithms under three types of out-of-cell interference, which are MMSE, interference whitening with MMSE (IW-MMSE) or MMSE with interference rejection combining (MMSE-IRC),

Table 2.1: Comparisons of receiver processing. Scenarios are I: Many interferers without dominant one, II: A few interferers with dominant one, and III: Single or a few strong interferers. Interference channel, interference plus noise variance, and interference covariance matrix are respectively denoted by $\boldsymbol{H}_I$, σ_I^2, and $\boldsymbol{R}_I$. MCS represents modulation and coding selection.

Interference	Scenario	Receiver Algorithms	Required Info.
White Gaussian	I	MMSE	σ_I^2
Colored Gaussian	II	IW-MMSE, MMSE-IRC	$\boldsymbol{R}_I$
Modulated symbol	III	Joint Detection	$\boldsymbol{H}_I$, MCS

and joint detection.

In this section, we introduce the advanced receiver algorithms that can be used in multicell cooperative coordinated beamforming systems. Note that the use of advanced receivers is also possible on top of the coordinated beamforming algorithms introduced in Section 2.2. Typically, when the channel is slowly varying so channel knowledge at the transmitter can be accurate, coordinated beamforming can be effectively utilized. In an agile channel condition, the receiver may apply advanced receiver techniques rather than relying on a full coordination. The advanced receive algorithm can thus be a supplementary to coordinated beamforming algorithms, not a competitive one.

2.3.1 White Gaussian Interference: MMSE Filter

If the out-of-cell interference comes from many non-dominant interferers and each of the interference from each interferer is uncorrelated, the aggregated interference seen by the receiver can be assumed as white Gaus-

sian. If the variance of the interference is known or precisely measured by the receiver, the receiver can treat the white Gaussian interference as noise. Since the interference plus noise covariance matrix becomes an identity matrix with the same diagonal entry σ_I^2, it can be treated as additive white Gaussian noise and the MMSE receiver provides the best link quality to the receiver in multicell cooperative systems.

In multicell coordinated system with white Gaussian interference, the MMSE filter performs differently in different SINR levels. If the signal power is noticeably higher than the interference plus noise power, the receiver may ignore the interference and perform as a zero-forcing decorrelator. The detector simply divides the received signal by the serving cell channel gain and then slice it to the nearest signal constellation point. If the interference plus noise power is relatively higher than the signal power, the MMSE receiver matches with the serving cell channel. In the coordinated beamforming system, the MMSE filter maximizes the post-processing SINR when the interference is white Gaussian, regardless of the SINR levels.

2.3.2 Colored Gaussian Interference: IW-MMSE or MMSE-IRC

The noise plus interference term at the receiver may contain either inter-cell interference or intra-cell interference, or a mix of both plus additive Gaussian noise. In general, such interference is not white especially when the number of interferers is small and there is a few dominant interferers. The noise plus interference term is then spatially colored with its covariance ma-

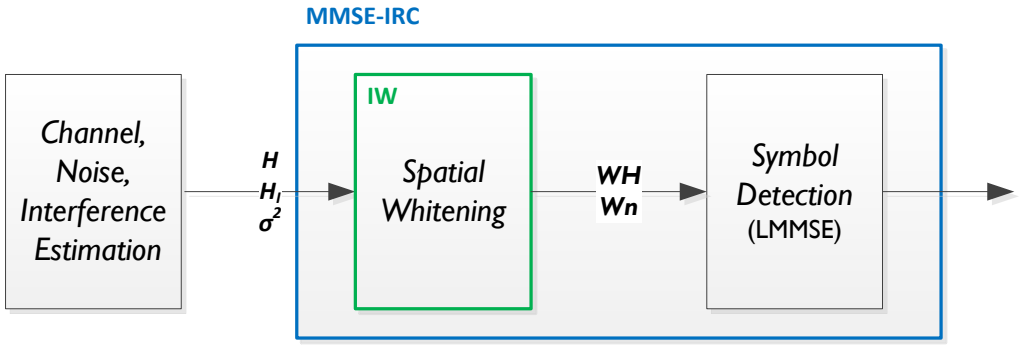

Figure 2.2: An illustration of IW-MMSE and MMSE-IRC processing. IW-MMSE is a two step approach for i) interference whitening and ii) LMMSE, while MMSE-IRC is a combined approach. Under the same estimation error, the two approaches result in the same symbol detection performance.

trix having non-zero off-diagonal terms. The colored interference plus noise term can cause serious problem to the detector and decoder which is generally designed assuming interference and noise is spatially temporally white. Assuming the interference plus noise covariance matrix is non-singular, a spatial whitening filter matrix needs to be applied on the receive signal such that the transformed interference becomes white, with a slight sacrifice to the desired signal strength.

An illustration of IW-MMSE and MMSE-IRC (interference rejection combining) processing is presented in Fig. 2.2. The interference whitening filter $\boldsymbol{W}$ transforms the interference plus noise term $\boldsymbol{n}$ into spatially white Gaussian vector. The transformed noise after whitening $\boldsymbol{Wn}$ has the covariance of an identity matrix, $\mathbb{E}\{\boldsymbol{Wn}(\boldsymbol{Wn})^*\} = \boldsymbol{W}\mathbb{E}\{\boldsymbol{nn}^*\}\boldsymbol{W}^* = \boldsymbol{I}_{N_\mathrm{r}}$. This

yields $\boldsymbol{W}\boldsymbol{R}\boldsymbol{W}^* = \boldsymbol{I}_{N_\mathrm{r}}$ and after taking the eigen-decomposition on the effective channel matrix $\boldsymbol{R}$, $\boldsymbol{R} = \boldsymbol{U}\boldsymbol{\Sigma}\boldsymbol{U}^*$, the whitening matrix can be obtained as $\boldsymbol{W} = \boldsymbol{\Sigma}^{-1/2}\boldsymbol{U}^*$. After the whitening filter is applied, an MMSE detector can be used to eliminate the white Gaussian noise.

An alternative way to detect the symbol with colored interference is to use the interference rejection combining. In the MMSE-IRC filter, the non-diagonal interference covariance matrix $\boldsymbol{R}_I$ is added to the MMSE whitening matrix, enabling the receiver to reject the interference. Note that the MMSE-IRC receiver can be biased or unbiased, depending on the use of normalization factor. The biased MMSE-IRC receiver maximizes the received SINR, while the unbiased MMSE-IRC filter minimizes the MSE. With a proper scaling, however, the two MMSE filters show the identical coded block error rate performance [8]. Thus, we may observe that the two MMSE-IRC filters may result in the similar throughput performance.

The IW-MMSE/MMSE-IRC detector is one of the simplest solutions to combat against (slightly) non-Gaussian interference. By sacrificing the desired channel gain a bit, the interference plus noise can be approximated as Gaussian so conventional detector and decoder can be utilized. The IW-MMSE/MMSE-IRC receiver, however, can perform well only with high modulation order, high code rate in weak to medium interference region. As the signal-to-interference level increases, the packet error rate performance becomes floored. If the interference is highly non-Gaussian, which typically happens for the out-of-cell interference with low modulation order, the IW-MMSE and MMSE-IRC

is not a desirable approach.

2.3.3 Interference with Known Modulation Order: Joint Detection

In practical multicell cooperative systems, the transmit symbols are modulated so the receiver needs to detect the transmitted symbol using a proper demodulator. The modulation order can be changed over time, to adapt the transmission rate close to the instantaneous channel capacity. If the modulation order of both the desired signal and interference signal are known to the receiver, the receiver can attempt to decode the desired symbols by jointly decoding the desired symbol and interference symbol. In [48], a significant performance gain is shown to be obtained if the detectors explicitly take into account the modulation formats of the desired and the interference signals.

Unlike the conventional interference canceler and successive interference canceler, that work well only in noise limited and interference limited regimes, respectively, the joint ML detector can cover variety of interference range. Specifically, the joint ML detector incorporates knowledge of the interfering channel and the finite modulation of the interference, turning interference-limited transmission system into a noise-limited one. The joint ML detector detects the desired and the interfering signals jointly, then discards the detector output for the interference which aids the detection of the desired signal. As the computational complexity can be easily doubled than the interference-ignorant ML detector, less complex joint minimum distance (MD) detector

can also be used. In the multicell cooperative network, however, the joint MD detector is slightly worse than the joint ML detector in low SNR region.

The joint detection approach is beneficial when the channels are fast fading. In such a condition, channel knowledge at the transmitter is easily outdated hence rigorous coordinated processing is somewhat infeasible. The joint detector, however, performs well in such a agile channel condition as it turns an interference-limited channel into a noise-limited channel. It is also shown that the full diversity gains can be achieved with the joint detector even in the presence of interference, so the transmit diversity scheme is advantageous. The joint detector is thus a good complementary good to multicell cooperative coordinated beamforming systems with multiple receive antennas.

2.4 Multicell Cooperation in Emerging Standards

The next generation wireless cellular systems will use coordinated multicell joint processing. In the 3GPP LTE-Advanced systems, coordinated multi-point (CoMP) is considered as one of the strongest and proven tools to improve the cell edge throughput. It is also proven that CoMP gives a higher gain than the traditional approaches of cellular network planning such as frequency reuse, sectoring, or spread spectrum. Despite the standardization of CoMP is still in progress and is scheduled to be finalized in the first half of 2013, it is meaningful to review the practical scenarios and limitations. It is noteworthy that, based on the proposals submitted to Rel-12 LTE-Advanced workshop, CoMP will be further evolved and enhanced to meet the require-

Table 2.2: A summary of the characteristics for each CoMP algorithm.

	CS/CB	JT	DPS
Performance Gain	Medium	High	Medium to High
Feedback Overhead	Medium	High	High
Freq/Time Sync.	Low	High	High
Backhaul Requirement	Medium	High	High
Phase Information at Tx.	Not Required	Required	Not Required
Relative Amplitude Info.	Required	Required	Not Required

ments for so-called 5G systems. In this section, we briefly introduce the scenarios of interest and key challenges when implemented in the real-world multicell cellular systems.

2.4.1 CoMP Algorithms and Scenarios

The scenarios and supported CoMP algorithms in Rel-11 3GPP LTE-Advanced are introduced in [3]. In the standard, both CBF and JP are considered as the main CoMP algorithms and JP is further decomposed into joint transmission and dynamic point selection.

In coordinated scheduling/coordinated beamforming (CS/CB), which contains both coordinated scheduling and CBF, the desired data stream is transmitted only from a transmitter in the CoMP cooperating set. The resource block is assigned to the receiver with CBF by scheduling of the serving cell after a coordination among multiple coordinated cells. The transmit beamforming and receive combining vectors are generated to reduce the unnecessary interference to or from other receiver(s) scheduled within the coordinated cell.

The best serving set of users will be selected so that the transceiver beamforming vectors are chosen to reduce the interference to/from other neighboring receivers, while increasing the serving cell signal strength. The other-cell interference can be mitigated and the cell edge receiver throughput can be improved.

In joint transmission (JT), a data stream is simultaneously transmitted from multiple transmitters to a receiver in a given time-frequency resource. Unlike the CBF receiver, the receiver in joint processing tries to *coherently* combine the symbols from multiple transmitters; if the data streams from multiple transmitters are synchronized, the receiver can have a (coherent) combining gain, which additionally gives both SNR and diversity gains. To enable a coherent combining at the receiver, a strict time-frequency synchronization should be enforced and the phase difference from different transmitters needs to be fed back to the transmitter. In this sense, joint transmission may be more demanding and fragile than coordinated scheduling/coordinated beamforming.

In dynamic point selection (DPS), data is transmitted from one transmitter within the cooperating transmitters in a time-frequency resource and the designated transmitter is dynamically selected. The other transmitter(s) may mute so the receiver do not see out-of-cell interference. The transmitting point may change in time depending on the feedback indicating the most desirable transmitting point by the receiver. Dynamic point selection also includes dynamic cell selection, which is a CoMP transmission scheme that can be seen

as a natural extension of existing scheduler implementations. Unlike the joint transmission, dynamic point selection does not need the inter-point information. Dynamic point selection supports CoMP scenario 3 and 4 (the scenarios will be explained later) where low power remote radio heads (RRHs) are deployed as a heterogeneous network. In situations where the mobile station penetrates across the RRH transmission boundaries, dynamic point selection shows similar gain to joint transmission.

In Table 2.2, the difference of the three CoMP algorithms is presented. It is expected that joint transmission may give the highest throughput gain at the cost of additional feedback and higher use of inter-base station communication. Dynamic point selection is simpler to implement but preferable only for the heterogeneous network scenarios in which the mobile station sees more cell edges so received SINRs are similar to each other. Coordinated scheduling/coordinated beamforming is probably the simplest and one of the most robust schemes with decent performance gain.

The four CoMP scenarios considered in the LTE-Advanced specifications and supported CoMP algorithms are presented in Table 2.3. Scenarios 1 and 2 are designed for classical homogeneous deployments while scenarios 3 and 4 are for the heterogeneous deployment. Scenario 3 targets typical pico-cell heterogeneous deployments and scenario 4 represents a distributed antenna system (DAS) where the points distributed within the macro cell can be thought of as remote radio heads (RRHs). Scenario 4 differs from scenario 3 from the fact that all points belong to the same cell. DAS approach us-

Table 2.3: CoMP scenarios and supported algorithms in 3GPP LTE-Advanced [3]. The scenarios are I: Homogeneous network with intra-site coordination, II: Homogeneous network with high power RRHs, III: Heterogeneous with low power RRHs (different cell IDs) and IV: Heterogeneous with low power RRHs (same cell ID).

Scenarios	Equivalent System	CoMP Algorithms
I	Single-cell Coordination	CS/CB, JT
II	Multi-cell Coordination	CS/CB, JT
III	Macro-Pico Coordination	CS/CB, JT, DPS
IV	Distributed Antenna System (DAS)	CS/CB, JT, DPS

ing RRHs (scenario 4) is easier to handle the out-of-cell interference and to apply the joint processing than the pico-cell (scenario 3) although orthogonal cell-specific pilot sequence design issue ought to be resolved. Note that in all scenarios, two receive antennas is default receive antenna configuration, hence aforementioned multicell coordinated algorithms can be exploited.

2.4.2 Practical Issues in Receiver Processing

The main practical issues of CoMP include feedback channel design and downlink reference signal design as they determine the accuracy of the channel information at the transmitter and receiver, respectively. This receiver processing is also practically important because the receiver needs to learn about the channel with limited reference signals. Although the discussions are still in the consensus–building stage, it is meaningful to learn about the working agreements made so far in the 3GPP LTE-Advanced standard.

Table 2.4: Summary of precoding vector generation metrics in various CoMP and non-CoMP MIMO systems. The channel from the i-th base station to the j-th mobile station is denoted as $\boldsymbol{H}_{ij}$. *vec* and *eig* respectively represent the dominant eigenvector and eigenvalue. For JT with per-point feedback, inter-point phase information needs to be fed back to compute the transmit MCS at the base station.

	Transmit Beamforming Generation
No CoMP SU-MIMO	$\boldsymbol{f} = \arg\max_{\boldsymbol{f}', \|\boldsymbol{f}'\|=1} \|\boldsymbol{H}\boldsymbol{f}'\|^2$
No CoMP MU-MIMO	$\boldsymbol{f}_k = \arg\max_{\boldsymbol{f}', \|\boldsymbol{f}'\|=1} \|\boldsymbol{H}_k\boldsymbol{f}'\|^2$
CS/CB	$\boldsymbol{f}_k = \boldsymbol{v}_{\mathsf{max}}\{\boldsymbol{H}_{kk}^* \boldsymbol{R}_k^{-1} \boldsymbol{H}_{kk}\}$
JT (Per-Point)	$\boldsymbol{f}_{jk} = \boldsymbol{v}_{\mathsf{max}}\{\boldsymbol{H}_{jk}^* \boldsymbol{H}_{jk}\}, \phi_{jk} = \angle(\boldsymbol{H}_{kk}, \boldsymbol{H}_{jk})$
JT (Aggregated)	$\boldsymbol{f}_k = \boldsymbol{v}_{\mathsf{max}}\{[\boldsymbol{H}_{1k}, \cdots, \boldsymbol{H}_{Kk}]^* [\boldsymbol{H}_{1k}, \cdots, \boldsymbol{H}_{Kk}]\}$
DPS	$\boldsymbol{f}_i = \boldsymbol{v}_{\mathsf{max}}\{\boldsymbol{H}_{ik}^* \boldsymbol{H}_{ik}\}, i = \arg\max_j eig\{\boldsymbol{H}_{jk}^* \boldsymbol{H}_{jk}\}$

2.4.2.1 Feedback Channel Design

To enable CoMP operation, each receiver feeds back the necessary information to the transmitter via reliable feedback channel. The channel quality indicator (CQI) is the main feedback information. With CQI, along with other feedback information such as precoding matrix index and rank indicator, the transmitter may be able to learn about the necessary downlink and interference channel and to schedule a transmission with appropriately selected modulation and coding index. As the transmitter solely relies on the information fed back from the receiver, the design of feedback channel is important in CoMP operation.

One of the main issues of the CoMP feedback design is the CQI generation because the definitions of CQI vary in different CoMP algorithms.

The CQI without considering interference is the maximum eigenvalue of the effective downlink channel, while the CQI with interference is the maximum eigenvalue of the effective channel multiplied by the MMSE-IRC whitening matrix. With the use of ML detector, the CQI computation can become more complicated. The CQI thus depends on the receiver algorithm as well as CoMP algorithms.

Increased hypotheses for CQI generation per CoMP scenarios and ambiguity on the CQI metric with certain receiver algorithm may cause a serious problem both to the transmitter and the receiver. One typical issue is what interference should be taken into account in the CQI computation; the interference from cooperating transmitters may be eliminated after a proper coordination, hence it may not be considered while computing the CQI. Interference from non-interfering transmitters should be considered as interference in the CQI computation metric. However, as the cooperating sets may change in time, the reported CQI may not represent the true link quality, and the transmitter may not detect this problem since *the CQI computation metric is not transparent to transmitter*. This makes the feedback design at the receiver harder.

2.4.2.2 Downlink Reference Signal Design

Downlink reference signal is used for the receiver to estimate the multicell channel. The reference signal needs to be carefully designed to meet the performance requirement. If the density of the reference signal in time-

frequency grid is too high, significant spectral efficiency loss occurred. If the reference signals are too sparse, the multicell channel measurement can become very coarse. In 3GPP LTE-Advanced systems, cell-specific reference signal with adequate reference signal density is considered for the CoMP operation. In such a cell-specific reference signal, the scrambling pattern and cyclic-shifting depends on the cell identification (ID) number.

In some CoMP scenarios, especially CoMP scenarios 4 where the RRHs use the same cell IDs, the reference signal from multiple transmission point can be easily collided. Even for the CoMP scenarios with difference cell ID, as the number of transmitting nodes gets higher, the reference signal collision probability gets higher. To provide additional orthogonality between reference signals from different transmitters, the 3GPP LTE-Advanced systems introduce *virtual* cell ID. The reference signal sequence is initiated and scrambled, not by the cell-specific manner using the cell ID, but by the node-specific virtual ID. By doing this, additional orthogonality among reference signal can be obtained.

The second issue is the possibility of different granularity of channel estimation interval in the serving and interfering cells. In general, CoMP operation can be done when the receiver does not move or moves very slowly, so the channel coherence time is strictly longer than the round-trip delay. The issue is that the interference channel does not change significantly in time and its estimation need not to be as accurate as that of the serving cell channel. In most cases, only the covariance of the interference can be utilized. The

interference channel estimation period can be longer, so the receiver can save its power and devote more resources to serving cell channel estimation.

2.4.2.3 Receiver Architecture

In 3GPP LTE-Advanced CoMP, the default receive antenna number is set to two or four. This enables the receiver to apply interference mitigation process. Specifically, the receiver algorithms considered in [3] are MMSE (mandatory) or MMSE-IRC (recommended). For the MMSE-IRC receivers, both biased and unbiased receivers are considered despite the throughput performance difference may be marginal regardless of the biasedness. The performance of the receiver rather depends on the accuracy of the covariance matrix estimation and frequency selectivity of the covariance matrix. Joint detection has yet to be considered in CoMP literature, but it can also be utilized if the modulation order of the interference signal is precisely known to the receiver.

2.4.3 System Performance Evaluation Results

To consider the practical issues discussed in the previous sections, we present the system performance evaluation results. We mostly use the simulation parameters presented in [3]. We use 2×2 antenna configuration with dual polarized antenna and 6ms feedback delay under full buffer traffic. For inter-cell interference modeling, we explicitly consider seven configurable inter-cell interference links to the mobile station and the remaining links are modeled with Rayleigh distribution. Among the scenarios in Table 2.3, we simulate

Table 2.5: Rank statistics - homogeneous (left column) and heterogeneous (right two columns) scenarios

	Homogeneous Network	Heterogeneous Network	
	Macro UE	Macro UE	Pico UE
Rank 1	54.90 %	92.4 %	84.2 %
Rank 2	45.10 %	7.6 %	15.8 %

homogeneous network (Scenario I) and heterogeneous network with low power RRHs with difference cell IDs (Scenario III).

We first present a simulation result for rank statistics with different transmit modulation orders. The rank statistic is an indicator that a mobile station is capable of receiving more than one stream using multiple receive antennas. The benefit of using additional antenna at the receiver can be interpreted as the probability to choose the rank 2 under a good channel condition. The simulation results with the use of the IW receiver is presented in Table 2.5. As shown in the table, the the mobile station tends to choose more than one streams in homogeneous scenario with high probability. The receiver processing with multiple receive antennas can be benefited in such a good channel. For heterogeneous network, however, the UE sees more diverse source of interference. It tends to reject the interference using part of the receive antennas, hence the chances that the mobile station are scheduled with more than one stream is limited. The simulation results show the benefit of using multiple receive antennas in both cases.

Simulation results with different transmitter and receiver techniques

Table 2.6: Cell average and cell edge (5-percentile user) throughput performance comparison in homogeneous (left two columns) and heterogeneous (right two columns) scenarios.

	Average	Edge (5%)	Average	Edge (5%)
IW	1.13 (Mbps)	0.016	9.62	0.054
JD	1.27	0.023	9.89	0.062
CoMP	1.14	0.017	9.58	0.067
CoMP with JD	1.34	0.024	10.09	0.066

discussed in this chapter are also presented in Table 2.6. We compare the cell average throughput and the cell edge throughput (5% user throughput) using the baseline IW receiver with JD and CoMP. By doing so, we show how the way to handle the interference affects the system performance. In Table 2.6, we observe that the use of advanced receive antenna and coordination technique improve the cell edge throughput the most. In homogeneous scenario, the cell edge throughput is improved by 52% when CoMP with joint detection is applied. In heterogeneous scenario, CoMP is the best technique to improve the cell edge user throughput, while CoMP with JD is the best for the average cell throughput. This demonstrates that both multicell cooperative processing and advanced receive technique are good methods to overcome the other-cell interference in practical systems.

2.5 Fundamental Limits of Cooperation

Multicell cooperation is promising as it promises to convert the multicell network from interference-limited to noise-limited. Coordination between

transmitters and receivers or the use of advanced receive algorithm enables the transformation. The use of multiple receive antennas is helpful to alleviate the other-cell interference. The natural question is whether such benefits are still fruitful in a large multicell network. When the cooperating transmitters form a cluster, a recent article [50] derives fundamental limits of cooperation in a general uplink setting. Based on their analysis, the spectral efficiency gets saturated as the transmit power increases in clustered large scale multicell networks.

Surprisingly, in [50], it is shown that saturation of the spectral efficiency at sufficiently high transmit powers is unavoidable in large networks. A key insight used in that paper is that not all channels can be estimated due to time variation, thus there is residual interference that limits the performance. Since the interference power is proportional to the transmit power, increasing the transmit power will not solve the problem. This results in the collapse of the multiplexing gain in higher SNR region. The paper also claims that the fundamental limitations cannot be overcome through any other technological advances. Based on the insights from [50], the discrepancy in terms of throughput gains between theory [14, 15, 49] and practice [3] in multicell cooperative processing comes from this fundamental limit, mainly from the latency of the backhaul link or limited feedback of the practical cellular systems.

The paper [50] provides intuition on how large multicell networks are likely to perform. It would be interesting to study how multiple receive antennas impact the theory derived in [50], for example to show if they can extend

the region of multicell cooperation where capacity scales with SNR. The results in small-scale multicell cooperative systems [14, 15, 49] show that additional receive antennas help achieves a better spectral efficiency. An investigation of the tradeoffs between numbers of antennas at a single transmitter and coordinated of many transmitters is an interesting topic for the purpose of any fundamental preference for centralized (e.g., massive MIMO) or distributed (e.g., distributed antenna systems) architectures. This may give some insights on the evolution of the multicell cooperative network for the next generation cellular standards and the role of the multiple receive antennas therein.

2.6 Discussions

This chapter introduced multicell cooperative systems with multiple receive antennas and advanced receiver techniques. In particular, coordinated beamforming (CBF), joint processing (JP) and spatial sensing (SS) techniques were introduced, explaining their potential use of multiple receive antennas. Asymptotic behavior of the sum rate with increasing number of receive antennas is also analyzed. Advanced receiver algorithms, which include minimum mean square error (MMSE), interference rejection combining (IRC), interference whitening (IW) and joint detection (JD), in different interference statistics were also introduced. Multicell cooperative processing, coordinated multi-point (CoMP), as it is being envisioned by emerging wireless standards, was reviewed. Finally the fundamental limits of cooperation were discussed and the potential role that multiple receive antennas may play was reviewed.

Multiple receive antennas and receiver processing have become more important in multicell cooperative networks both theoretically and practically.

Chapter 3

Interference-Aware Coordinated Precoding

In this chapter, we propose coordinated precoding strategies with linear receiver processing technique. The system model assumes a mixture of coordinated beamforming and joint processing in multicell cooperation, which requires mobile stations to selectively mitigate the signals from other base stations. We propose coordinated precoding algorithms that avoid inefficient time or frequency segmentation.

3.1 Introduction

Mobile users in cellular systems experience degraded performance at the cell edge, due to unfavorable signal-to-interference-plus-noise ratios (SINRs) [20, 70, 82, 84]. Multicell cooperative processing can be used to exploit and thus mitigate the effects of out-of-cell interference [70]. Cooperation is enabled by exchanging necessary information including downlink channel and interference knowledge between base stations.

Multicell cooperation is generally categorized into coordinated beamforming and joint processing [35, 64]. In coordinated beamforming, data for a mobile station is only transmitted from one cooperating base station. Thus the

signals from the other base stations are considered as interference [9, 14, 21]. Mitigating the interference while maintaining desired signal power is the main target. In joint processing, base stations have data for multiple mobile stations. The main objective with joint processing is to provide beamforming and coherent combining gain [15, 44]. The combination of the two multicell cooperation strategies may introduce interesting new problems since the signals from other base stations should be *selectively* mitigated at the mobile stations.

The equivalent channels are the two-user MIMO interference channel (dedicated messages) and two-user MIMO multicast channel (common message). The degrees of freedom region of the MIMO interference channel is presented in [11]. The capacity region (and the degrees of freedom region) of the MIMO multicast channel is specified in [41]. The combined channel, the system model used for the proposed algorithm, is similar to the MIMO X channel [40] except that the messages from BS1 to MS2 and from BS2 to MS1 are identical. The upper bound of the degrees of freedom in MIMO X channel is 4/3M, where M is the number of antennas at each node. However, multicast is fundamentally a different channel model than the MIMO X channel because the mutual information will be different if the common messages from two transmitters are the same.

In this chapter, we consider a system that combines coordinated beamforming and joint processing. Each base station transmits both dedicated (unicast) and common (broadcast or multicast) messages to a mobile station as illustrated in Fig. 3.1(a). The dedicated message is a private message that

is intended for the primary mobile station being served by that base station. The common message is public information that is intended for multiple mobile stations. The simultaneous transmission of a dedicated message (e.g., voice or data) and a common message (e.g. multimedia broadcast multicast services) may provide better user experience, hence it is widely discussed in the next generation mobile standards [2], but the use of dedicated message and common message is often segmented by time or frequency. Another motivation for considering this scenario comes from the heterogeneous network – a mobile station in the vicinity of small cell (e.g., femto or pico) receives the dedicated information from the small cell but may receive the control information also from the macro base station(s) overlaid with the small cells [5].

In this chapter, we propose coordinated precoding strategies to maximize the desired signal and mitigate interference from other cells. The considered cooperative system is a mixture of coordinated beamforming and joint processing. The mobile stations selectively mitigate the non-intended dedicated message portion and attain the beamforming gain from the signal coming from adjacent base stations. By the information that each mobile station can exploit, different *linear* receiver processing techniques are investigated in the multicell cooperative systems.

3.2 System Model

Consider a two-cell MIMO system where the base stations with N_{t} transmit antennas serve the mobile stations equipped with N_{r} receive antennas,

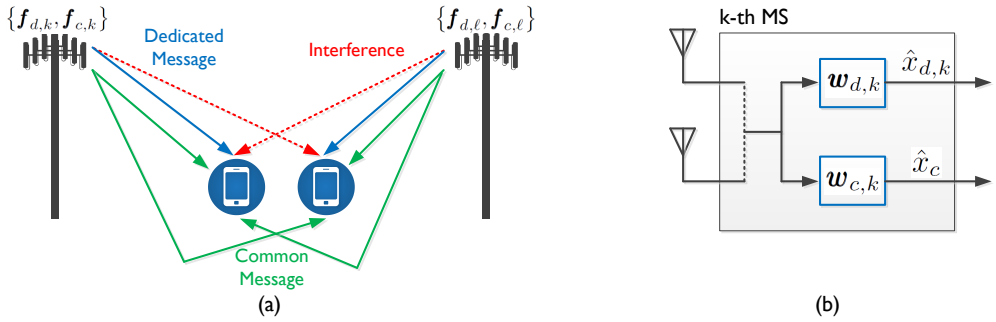

Figure 3.1: Equivalent two-user MIMO interference channel, (a) each base station transmits both dedicated and common messages. The dedicated message is for the desired mobile station, while the common message can be decoded at any mobile station and (b) a linear receiver structure.

as shown in Fig. 1.[1] Let $x_{d,k}$ denote the dedicated complex signal by the k-th base station and x_c denote the common message. The number of transmit antennas is equal to or grater than the number of data streams N_s, which consist of a private message and a common message, thus $N_\mathrm{t} \geq N_\mathrm{s} = 2$. The channel between the k-th base station and the k-th mobile station ($k = 1$ or 2) is represented by $\boldsymbol{H}_k$ of size $N_\mathrm{r} \times N_\mathrm{t}$ with complex entries. The channel between the k-th base station and the ℓ-th mobile station ($k, \ell = 1$ or 2, $k \neq \ell$) is given by the $N_\mathrm{r} \times N_\mathrm{t}$ matrix $\boldsymbol{G}_k$. We assume that the elements in the channel matrices $\boldsymbol{H}_k, \boldsymbol{G}_\ell$, ($k, \ell = 1$ or $2, k \neq \ell$), are i.i.d. random variables. We assume that the k-th mobile station can estimate both $\boldsymbol{H}_k$ and $\boldsymbol{G}_k$ using downlink

[1]Throughout this chapter, we use upper boldface $\boldsymbol{A}$ and lower boldface $\boldsymbol{a}$ as matrices and vectors, respectively. If two vectors $\boldsymbol{a}$ and $\boldsymbol{b}$ are perpendicular, we write $\boldsymbol{a} \perp \boldsymbol{b}$. If they are parallel, we write $\boldsymbol{a} \parallel \boldsymbol{b}$. We denote the inverse, pseudo-inverse, transpose, complex conjugate, Hermitian of matrix $\boldsymbol{A}$ by $\boldsymbol{A}^{-1}$, $\boldsymbol{A}^\dagger$, $\boldsymbol{A}^T$, $\bar{\boldsymbol{A}}$ and $\boldsymbol{A}^*$, respectively. $\|\boldsymbol{a}\|$ and $\|\boldsymbol{A}\|$ denotes vector and matrix 2-norm, respectively, unless otherwise stated.

reference symbols and that the k-th base station is informed of $\boldsymbol{H}_k$ and $\boldsymbol{G}_k$ through a reliable feedback link. We also assume that all channel matrices $\boldsymbol{H}_k$, $\boldsymbol{G}_k$ ($k = 1$ or 2) are full rank. The additive white Gaussian noise at the k-th mobile station is denoted as $\boldsymbol{n}_k$ with distribution $\mathcal{CN}(\mathbf{0}, \boldsymbol{\Sigma}_k)$, where the noise covariance matrix $\boldsymbol{\Sigma}_k = \sigma_k^2 \boldsymbol{I}_{N_\mathrm{r}}$.

We define two unit-norm precoding vectors $\boldsymbol{f}_{d,k} \in \mathcal{C}^{N_\mathrm{t} \times 1}$ and $\boldsymbol{f}_{c,k} \in \mathcal{C}^{N_\mathrm{t} \times 1}$ for the dedicated and common message respectively. As the dedicated message is delivered from the serving base station while the common message is delivered from multiple cooperating base stations, different precoding strategies may be required. To successfully decode the transmitted symbols and eliminate other-cell interference at the mobile station, two linear combining vector, $\boldsymbol{w}_{d,k}$ and $\boldsymbol{w}_{c,k}$ of size $N_\mathrm{r} \times 1$, are applied at the receiver to distinguish the private message and the common message (see Fig. 3.1(b)).

The signaling flow of the proposed algorithm is presented in Fig. 3.2. Although the proposed algorithm may utilize an anchor base station to compute all the beamforming vectors, it is not a limiting assumption. It can a better approach than a distributed approach in 1) reducing the inter-BS feedback overhead and 2) improving the computational efficiency. Assuming the algorithm is fully-distributed, to compute dedicated precoder, BSs need to exchange the downlink channel information. Then BSs need to exchange additional information (e.g., computed dedicated precoder) to compute common precoder and postcoder. It thus requires 2 bi-directional information exchange between BSs. The use of an anchor base station requires only 1 bi-directional

information exchange.

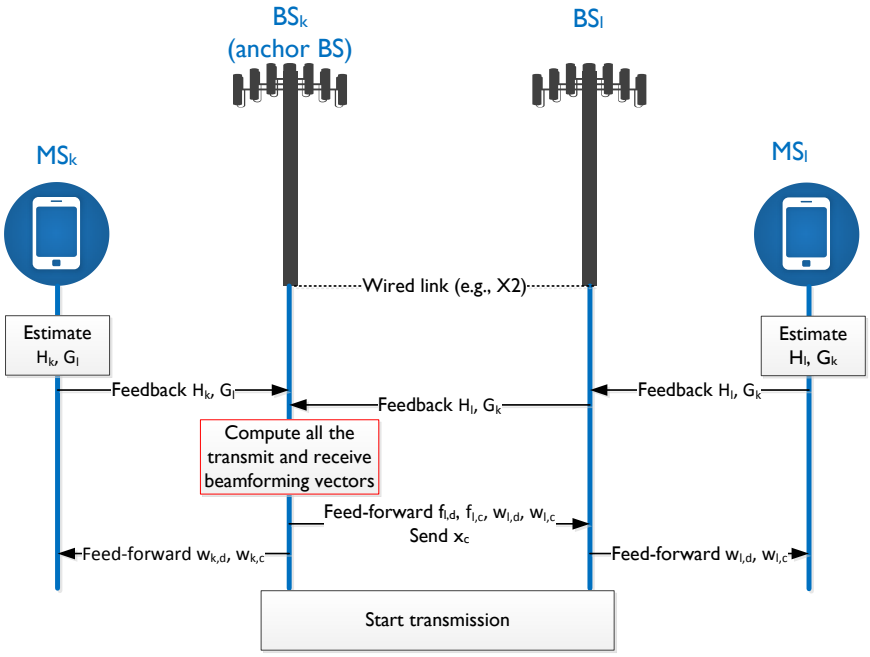

Figure 3.2: Signaling flow chart of the proposed algorithm.

For this system model, the received signal at the k-th mobile station is given by

$$\boldsymbol{y}_k = \boldsymbol{H}_k \boldsymbol{f}_{d,k} x_{d,k} + \left(\boldsymbol{H}_k \boldsymbol{f}_{c,k} + \boldsymbol{G}_\ell \boldsymbol{f}_{c,\ell} \right) x_c + \boldsymbol{G}_\ell \boldsymbol{f}_{d,\ell} x_{d,\ell} + \boldsymbol{n}_k.$$

After applying the receive filters, the two messages become $\hat{x}_{d,k} = \boldsymbol{w}_{d,k}^* \boldsymbol{y}_k$ and $\hat{x}_{c,k} = \boldsymbol{w}_{c,k}^* \boldsymbol{y}_k$. We assume that receiver may adjust the weighting of the received signals from other base station. This assumption is viable by assuming that orthogonal pilot patterns are used per base station for the channel estimation. Let α_k^ℓ denote the weighting factor for the signal from the k-th base station

to the ℓ-th mobile station. Forcing the constraint, $\alpha_k^\ell \leq 1$, we may enforce similar level of noise floor to the equal weighting, $\alpha_k^\ell = 1$ with a sacrifice of the beamforming gain for the common message. As will be shown later, the weighting enables to find the common precoding vectors under a zero-interference condition.

The SINR of the dedicated message at the k-th mobile station is given as

$$\gamma_{d,k} = \frac{|\boldsymbol{w}_{d,k}^* \boldsymbol{H}_k \boldsymbol{f}_{d,k}|^2}{|\boldsymbol{w}_{d,k}^* \left(\boldsymbol{H}_k \boldsymbol{f}_{c,k} + \alpha_k^\ell \boldsymbol{G}_\ell \boldsymbol{f}_{c,\ell}\right)|^2 + |\alpha_k^\ell \boldsymbol{w}_{d,k}^* \boldsymbol{G}_\ell \boldsymbol{f}_{d,\ell}|^2 + \sigma_k^2}.$$

Likewise, the SINR for the common message at the k-th mobile station is

$$\gamma_{c,k} = \frac{|\boldsymbol{w}_{c,k}^* \left(\boldsymbol{H}_k \boldsymbol{f}_{c,k} + \alpha_k^\ell \boldsymbol{G}_\ell \boldsymbol{f}_{c,\ell}\right)|^2}{|\boldsymbol{w}_{c,k}^* \left(\boldsymbol{H}_k \boldsymbol{f}_{d,k} + \alpha_k^\ell \boldsymbol{G}_\ell \boldsymbol{f}_{d,\ell}\right)|^2 + \sigma_k^2}. \tag{3.1}$$

The goal of this chapter is to jointly design precoders and decoders to maximize the achievable sum rate of both messages. We develop coordinated precoding strategies under various assumed linear receiver processing techniques.

3.3 Interference Aware-Coordinated Precoding

It is assumed that the receive beamforming for dedicated and common messages are obtained to meet a zero-interference constraint; the dedicated and the common messages should always be orthogonal to the vector that carries the dedicated messages of other cells. To meet the zero-interference criterion, the interference terms in $\gamma_{d,k}$ and $\gamma_{c,k}$ should be zero for $k, \ell = 1$ or 2, $k \neq \ell$.

For the dedicated postcoder, instead of attempting to cancel out both interference terms in $\gamma_{d,k}$, maximum ratio combining (MRC) is used to maximize the effective channel gain of the dedicated message $|\boldsymbol{w}_{d,k}^{*}\boldsymbol{H}_k\boldsymbol{f}_{d,k}|^2$, hence the dedicated postcoder is given by

$$\boldsymbol{w}_{d,k} = \frac{\boldsymbol{H}_k\boldsymbol{f}_{d,k}}{\|\boldsymbol{H}_k\boldsymbol{f}_{d,k}\|}. \tag{3.2}$$

3.3.1 Dedicated Precoder Design

From (3.2) and the zero-interference condition, the transmit beamforming vectors for the dedicated message satisfy $\boldsymbol{H}_k\boldsymbol{f}_{d,k} \perp \boldsymbol{G}_\ell\boldsymbol{f}_{d,\ell}, \boldsymbol{H}_\ell\boldsymbol{f}_{d,\ell} \perp \boldsymbol{G}_k\boldsymbol{f}_{d,k}$, which is equivalent to

$$\boldsymbol{f}_{d,k}^{*}\boldsymbol{H}_k^{*}\boldsymbol{G}_\ell\boldsymbol{f}_{d,\ell} = 0 = \boldsymbol{f}_{d,\ell}^{*}\boldsymbol{H}_\ell^{*}\boldsymbol{G}_k\boldsymbol{f}_{d,k}. \tag{3.3}$$

This further leads to

$$\boldsymbol{H}_k^{*}\boldsymbol{G}_\ell\boldsymbol{f}_{d,\ell} \parallel \boldsymbol{G}_k^{*}\boldsymbol{H}_\ell\boldsymbol{f}_{d,\ell} \iff \boldsymbol{H}_k^{*}\boldsymbol{G}_\ell\boldsymbol{f}_{d,\ell} = \lambda\boldsymbol{G}_k^{*}\boldsymbol{H}_\ell\boldsymbol{f}_{d,\ell}. \tag{3.4}$$

The problem in (3.4) is known as a generalized eigen problem, where λ is the generalized eigenvalue of $\boldsymbol{H}_k^{*}\boldsymbol{G}_\ell$ and $\boldsymbol{G}_k^{*}\boldsymbol{H}_\ell$. Thus $\{\boldsymbol{f}_{d,\ell}\}$ are generalized eigenvectors of $\boldsymbol{H}_k^{*}\boldsymbol{G}_\ell$ and $\boldsymbol{G}_k^{*}\boldsymbol{H}_\ell$. Likewise, $\boldsymbol{f}_{d,k}$ is a generalized eigenvector of $\boldsymbol{G}_\ell^{*}\boldsymbol{H}_k$ and $\boldsymbol{H}_\ell^{*}\boldsymbol{G}_k$, which can also be simply obtained by finding a vector that meets $\boldsymbol{f}_{d,k} \perp \boldsymbol{H}_k^{*}\boldsymbol{G}_\ell\boldsymbol{f}_{d,\ell}$ when $N_\mathrm{t} = 2$. The chosen dedicated precoder pair $\{\boldsymbol{f}_{d,k}, \boldsymbol{f}_{d,\ell}\}$ is unique up to complex multiplication when $N_\mathrm{t} = 2$ [14]. For $N_\mathrm{t} > 2$, $\boldsymbol{f}_{d,k}$ lies on the intersection of an N_t-dimensional plane and an N_t-dimensional hypersphere. As $\boldsymbol{H}_k^{*}\boldsymbol{G}_\ell$ and $\boldsymbol{G}_k^{*}\boldsymbol{H}_\ell$ are $N_\mathrm{t} \times N_\mathrm{t}$ full rank matrices

with probability one, there exists N_{t} generalized eigenvectors that meet the condition in (3.4) and the pair $\{\boldsymbol{f}_{d,k}, \boldsymbol{f}_{d,\ell}\}$ that maximizes the achievable sum rate $\gamma_{d,k}$ is chosen.

3.3.2 Common Precoder Design

Since $\boldsymbol{f}_{d,k}$, $\boldsymbol{f}_{d,\ell}$ are uniquely given, the common precoder for receiver k depends only upon the weighting factor and the ℓ-th receiver's common precoder. To mitigate the remaining interference in the dedicated message, the two perpendicularity conditions, $\boldsymbol{w}_{d,k} \perp \left(\boldsymbol{H}_k \boldsymbol{f}_{c,k} + \alpha_k^{\ell} \boldsymbol{G}_{\ell} \boldsymbol{f}_{c,\ell}\right)$ and $\boldsymbol{w}_{d,\ell} \perp \left(\boldsymbol{H}_{\ell} \boldsymbol{f}_{c,\ell} + \alpha_{\ell}^{k} \boldsymbol{G}_k \boldsymbol{f}_{c,k}\right)$, need to be met. This yields the zero-interference condition $\boldsymbol{f}_{d,k}^{*} \boldsymbol{H}_k^{*} \boldsymbol{H}_k \boldsymbol{f}_{c,k} + \alpha_k^{\ell} \boldsymbol{f}_{d,k}^{*} \boldsymbol{H}_k^{*} \boldsymbol{G}_{\ell} \boldsymbol{f}_{c,\ell} = 0$, for $k, \ell = 1$ or $2, k \neq \ell$. Thus,

$$\boldsymbol{f}_{c,k} = -\alpha_k^{\ell} \left(\boldsymbol{f}_{d,k}^{*} \boldsymbol{H}_k^{*} \boldsymbol{H}_k\right)^{\dagger} \left(\boldsymbol{f}_{d,k}^{*} \boldsymbol{H}_k^{*} \boldsymbol{G}_{\ell}\right) \boldsymbol{f}_{c,\ell} \tag{3.5}$$

for $k, \ell = 1$ or $2, k \neq \ell$. Rewriting $\boldsymbol{f}_{c,\ell}$ with $\boldsymbol{f}_{c,k}$ gives

$$\boldsymbol{f}_{c,k} \ = \lambda_{c,k} \boldsymbol{A}_k \boldsymbol{B}_k \boldsymbol{f}_{c,k} \tag{3.6}$$

where the square matrices $\boldsymbol{A}_k$ and $\boldsymbol{B}_k$ are given as $\boldsymbol{A}_k = \left(\boldsymbol{f}_{d,k}^{*} \boldsymbol{H}_k^{*} \boldsymbol{H}_k\right)^{\dagger} \left(\boldsymbol{f}_{d,k}^{*} \boldsymbol{H}_k^{*} \boldsymbol{G}_{\ell}\right)$ and $\boldsymbol{B}_k = \left(\boldsymbol{f}_{d,\ell}^{*} \boldsymbol{H}_{\ell}^{*} \boldsymbol{H}_{\ell}\right)^{\dagger} \left(\boldsymbol{f}_{d,\ell}^{*} \boldsymbol{H}_{\ell}^{*} \boldsymbol{G}_k\right)$. The generalized eigenvalue of $\boldsymbol{I}_{N_{\mathrm{t}}}$ and $\boldsymbol{A}_k \boldsymbol{B}_k$ is given by $\lambda_{c,k} = \frac{\alpha_k^{\ell}}{\alpha_{\ell}^{k}}$. The common precoder $\boldsymbol{f}_{c,k}$, therefore, is one of the normalized principal eigenvectors of $(\boldsymbol{I}_{N_{\mathrm{t}}}, \boldsymbol{A}_k \boldsymbol{B}_k)$. In a similar way,

$$\boldsymbol{f}_{c,\ell} \ = \lambda_{c,\ell} \boldsymbol{B}_k \boldsymbol{A}_k \boldsymbol{f}_{c,\ell}, \tag{3.7}$$

where $\boldsymbol{f}_{c,\ell}$ is the normalized principal eigenvectors of $(\boldsymbol{I}_{N_{\mathrm{t}}}, \boldsymbol{B}_k \boldsymbol{A}_k)$ which corresponds to the unique non-singular eigenvalue $\lambda_{c,\ell} = \frac{\alpha_k^{\ell}}{\alpha_{\ell}^{k}}$. As the non-singular

generalized eigenvalue of $\boldsymbol{A}_k\boldsymbol{B}_k$ and $\boldsymbol{B}_k\boldsymbol{A}_k$ is the same, so is $\lambda_{c,k}$ and $\lambda_{c,\ell}$. With measured channels and given dedicated precoders, therefore, the common postcoders and appropriate weighting at each mobile station can be determined.

3.3.3 Common Postcoder Design

To maintain the zero-interference condition, the common postcoders should completely nullify the interference that comes from the dedicated messages. We may not obtain MRC-type postcoders for the common message while maintaining such a condition since the common precoders are already obtained. We thus focus only on the interference nulling common postcoder design. The zero-interference condition yields $\boldsymbol{w}_{c,k} \perp (\boldsymbol{H}_k\boldsymbol{f}_{d,k} + \boldsymbol{G}_\ell\boldsymbol{f}_{d,\ell})$ and $\boldsymbol{w}_{c,\ell} \perp (\boldsymbol{H}_\ell\boldsymbol{f}_{d,\ell} + \boldsymbol{G}_k\boldsymbol{f}_{d,k})$.

If $N_\mathrm{r} = 3$, the solutions are $\mu\overline{\boldsymbol{H}_k\boldsymbol{f}_{d,k}} + \phi\boldsymbol{G}_\ell\boldsymbol{f}_{d,\ell}$ for some $\mu, \phi \in \mathbb{C}$ [15], where $\overline{\boldsymbol{H}_k\boldsymbol{f}_{d,k}}$ is the complex conjugate of $\boldsymbol{H}_k\boldsymbol{f}_{d,k}$. A sufficient and numerically simple solution is to find $\boldsymbol{w}_{c,k}$ which satisfies $\boldsymbol{f}_{d,k}^*\boldsymbol{H}_k^*\boldsymbol{w}_{c,k} = 0 = \boldsymbol{f}_{d,\ell}^*\boldsymbol{G}_\ell^*\boldsymbol{w}_{c,k}$ for $k, \ell = 1$ or $2, k \neq \ell$. If $N_\mathrm{r} = 3$, the vectors $\boldsymbol{H}_k\boldsymbol{f}_{d,k}$ and $\boldsymbol{G}_\ell\boldsymbol{f}_{d,l}$ are in $\mathbb{C}^3$, so the unnormalized common decoder $\boldsymbol{w}'_{c,k}$ is defined as the cross product of $\boldsymbol{H}_k\boldsymbol{f}_{d,k}$ and $\boldsymbol{G}_\ell\boldsymbol{f}_{d,\ell}$, i.e.,

$$\boldsymbol{w}'_{c,k} = \boldsymbol{H}_k\boldsymbol{f}_{d,k} \times \boldsymbol{G}_\ell\boldsymbol{f}_{d,\ell}, \tag{3.8}$$

where $(\boldsymbol{a} \times \boldsymbol{b})$ indicates a cross product of $\boldsymbol{a}$ and $\boldsymbol{b}$. Among two vectors in opposite direction, the vector that maximizes the effective channel gain of the common message $|\boldsymbol{w}_{c,k}^*(\boldsymbol{H}_k\boldsymbol{f}_{c,k} + \boldsymbol{G}_\ell\boldsymbol{f}_{c,\ell})|^2$ is selected. Likewise, $\boldsymbol{w}'_{c,\ell} =$

$\boldsymbol{H}_\ell \boldsymbol{f}_{d,\ell} \times \boldsymbol{G}_k \boldsymbol{f}_{d,k}$ and the one that maximize the effective channel gain is selected. To obtain the normalized dedicated postcoder $\boldsymbol{w}_{c,k}$, we scale $\boldsymbol{w}'_{c,k}$ by $\|\boldsymbol{H}_k \boldsymbol{f}_{d,k}\| \|\boldsymbol{G}_\ell \boldsymbol{f}_{d,\ell}\|$ or directly by $\left|\boldsymbol{H}_k \boldsymbol{f}_{d,k} \times \boldsymbol{G}_\ell \boldsymbol{f}_{d,\ell}\right|$. The normalized postcoder for the ℓ-th receiver's common mssage is $\boldsymbol{w}_{c,\ell} = \boldsymbol{w}'_{c,\ell} / \left(\|\boldsymbol{H}_\ell \boldsymbol{f}_{d,\ell}\| \|\boldsymbol{G}_k \boldsymbol{f}_{d,k}\|\right)$.

When $N_\mathrm{r} > 3$ many solutions exist that and the solutions lie on the intersection of an N_r-dimensional plane and an N_r-dimensional hypersphere. Finding one such vector is not difficult [14], but finding the one that maximizes $\gamma_{c,k}$ is not trivial.

3.4 Coordinated Precoding with MMSE-IRC

Instead of forcing the zero interference constraint, another coordinated precoding strategy is to maximize the received SINR via minimum mean squared error-interference rejection combining (MMSE-IRC) filter [64]. From (3.1), the received filter that maximizes the SINR for the dedicated message (before normalization) is

$$\boldsymbol{w}_{d,k} = \boldsymbol{R}_{d,k}^{-1} \boldsymbol{H}_k \boldsymbol{f}_{d,k}, \tag{3.9}$$

where the interference plus noise whitening matrix is $\boldsymbol{R}_{d,k} = \boldsymbol{H}_k \boldsymbol{f}_{c,k} \boldsymbol{f}_{c,k}^* \boldsymbol{H}_k^* + \boldsymbol{G}_\ell \boldsymbol{f}_{c,\ell} \boldsymbol{f}_{c,\ell}^* \boldsymbol{G}_\ell^* + \boldsymbol{G}_\ell \boldsymbol{f}_{d,\ell} \boldsymbol{f}_{d,\ell}^* \boldsymbol{G}_\ell^* + \sigma_k^2 \boldsymbol{I}_{N_\mathrm{r}}$. Likewise, the received filter that maximizes the effective gain of the common message (before normalization) is

$$\boldsymbol{w}_{c,k} = \boldsymbol{R}_{c,k}^{-1} \left(\boldsymbol{H}_k \boldsymbol{f}_{c,k} + \boldsymbol{G}_\ell \boldsymbol{f}_{c,\ell}\right), \tag{3.10}$$

where $\boldsymbol{R}_{c,k} = \boldsymbol{H}_k \boldsymbol{f}_{d,k} \boldsymbol{f}_{d,k}^* \boldsymbol{H}_k^* + \boldsymbol{G}_\ell \boldsymbol{f}_{d,\ell} \boldsymbol{f}_{d,\ell}^* \boldsymbol{G}_\ell^* + \sigma_k^2 \boldsymbol{I}_{N_\mathrm{r}}$.

As the zero-interference condition is not enforced, non-iterative coordinated beamforming may not be utilized. Instead, one strategy for transmit beamforming vector design is to minimize the *leakage* of the dedicated message to the non-intended mobile station, while maximizing the signal strength to the intended user [17]. This yields the following transmit beamforming vector design rule:

$$\boldsymbol{f}_{d,k} = \left(\boldsymbol{G}_{\ell}^{*}\boldsymbol{w}_{d,\ell}\boldsymbol{w}_{d,\ell}^{*}\boldsymbol{G}_{\ell} + \sigma_{k}^{2}\boldsymbol{I}_{N_{\mathrm{t}}}\right)^{-1}\boldsymbol{H}_{k}^{*}\boldsymbol{w}_{d,k}. \tag{3.11}$$

Regarding the common precoder, maximum ratio transmission (MRT) is a good strategy since the common message is intended to all of the mobile stations. With appropriate feedback, the common precoder at the k-th base station is

$$\boldsymbol{f}_{c,k} = \boldsymbol{H}_{k}^{*}\boldsymbol{w}_{c,k} + \boldsymbol{G}_{k}^{*}\boldsymbol{w}_{c,\ell}. \tag{3.12}$$

The transmit and receive beamforming vector design based on MMSE-IRC may lead to an iterative solution: if the receive filters are updated, the transmit precoders can also be updated. This approach is applicable for coordinated precoding with the more than two base stations.

3.5 Simulations

For numerical comparisons, we define the sum rate as a combination of the broadcast channel and the multicast, which is given by $R_{\mathrm{sum}} = \mathsf{E}\left[\gamma_{d,k} + \gamma_{d,\ell} + \min\left\{\gamma_{c,k}, \gamma_{c,\ell}\right\}\right]$ as the multicast performance is limited by the

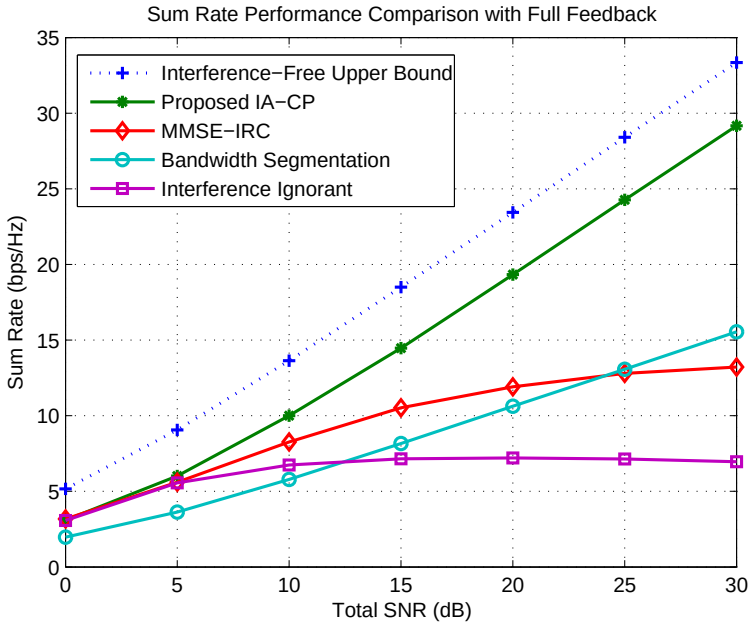

Figure 3.3: Sum rate performance comparison with full feedback.

worst channel user [42]. As a reference, interference-free upper bound is presented assuming no out-of-cell interference. The transmit and receive vectors are thus, respectively, the left and right principal singular vectors of the desired channel. Interference ignorant assumes the same precoding strategy but in presence of the crosstalk. Bandwidth Segmentation is the one being used in 3GPP LTE [64]: dedicated and common messages are segmented in time or frequency.

In Fig. 3.3, sum rate comparison results are presented. We could see that the proposed precoder design achieves the full degrees of freedom (DoF 3) of the given channel. Note that we observe 3 DoF are achieved in the simulations but we have been unable to prove the result. There is power

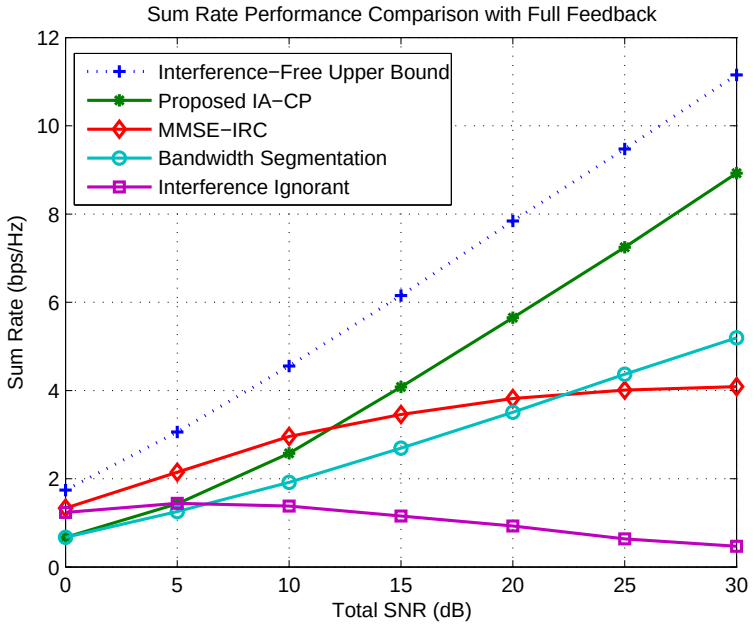

Figure 3.4: Sum rate performance (common only).

penalty to the common signal in (3.1) due to the weighting factor that is required to maintain the zero-interference condition. MMSE-IRC approach achieves higher sum rate as the signal-to-interference-ratio (SIR) improves. Bandwidth Segmentation achieves less sum rate due to an inefficiency of the segmentation even though there is no cross-signal interference between the dedicated message and the common message. Sum rate with just common message is presented in Fig. 3.4. We followed the definition of the multicast channel capacity [42]: the sum rate performance of the common message is limited by the worst user's achievable rate.

In Fig. 3.5, performance comparison of the proposed algorithms with limited feedback is illustrated. Instead of having a full channel knowledge

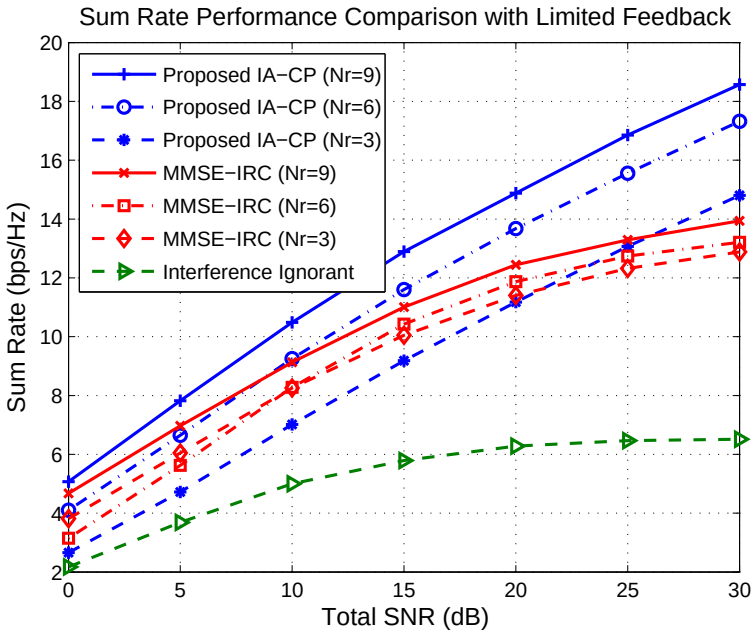

Figure 3.5: Sum rate comparison with limited feedback. For the simulation, a non-uniform codebook with 3 bit quantization per real entry is used.

at the transmitter, the receivers send only quantized channel information so the downlink channel knowledge at the base stations is limited. To quantize the effective channel, we have utilized the non-uniform vector quantization methods described in [16]. This can be done since all elements of $\boldsymbol{H}_k^* \boldsymbol{G}_\ell$ and $\boldsymbol{G}_k^* \boldsymbol{H}_\ell$ are beta distributed with a shift by $1/2$ and the diagonal terms of $\boldsymbol{H}_k^* \boldsymbol{H}_k$ and $\boldsymbol{G}_\ell^* \boldsymbol{G}_\ell$ are also beta distributed with parameters $(N_{\mathrm{r}}, (N_{\mathrm{t}} - 1)N_{\mathrm{r}})$, so the proposed codebook design methods nicely quantize the effective channel. Using this quantization method, the amount of feedback can also be reduced as the number of receive antenna increases.

As shown in Fig. 3.5, quantization errors degrade the sum rate. Unlike

the receive filter that is designed using perfect channel knowledge, the transmit precoders rely on limited feedback, resulting in a loss in SINR. As the number of receive antennas increases, the quantization error diminishes with the same number of quantization bits [16]. We can observe that the gain in the proposed IA-CP algorithm is high as the number of receive antennas increases. The gain in MMSE-IRC algorithm is not big since the optimum quantization of $\boldsymbol{H}_k^* \boldsymbol{w}_{d,k}$ and $\boldsymbol{G}_k^* \boldsymbol{w}_{c,k}$ are not explicitly known, which is one of the main drawbacks of the algorithm.

3.6 Discussions

In this chapter, interference aware-coordinated precoding algorithms were presented. Assuming both private and common messages were sent from each base station to each desired mobile station, we proposed novel coordinated precoding algorithms to nullify undesired interference and maximize the effective channel gain through generalized eigen decomposition, interference alignment, and maximum ratio combining techniques. For future work, we will consider the asymptotic behavior of the proposed algorithms when i) the number of receive antenna increases, ii) the number of messages increases under more practical multi-cell cooperation scenario with processing delay and latency during the coordination.

Chapter 4

Iterative Coordinated Beamforming

For a K-user interference channel with multiple antennas, the network utility such as (weighted) sum rate is one of the most commonly considered performance measures. Under this objective, many algorithms have been proposed for the purpose of the sum mean square error (MSE) minimization [66], MMSE interference alignment [62], max-min weighted SINR [12], interference-aware coordinated beamforming [14], and iterative precoder optimization [74]. The cost of cooperation was often neglected in most of the previously proposed algorithms thus the study of CBF algorithms with limited but efficient cooperation is desired.

Besides the mobility management (e.g., handover), the limiting factor of BS cooperation in hyper-dense network is a lack of wired backhaul connection between small cells. This often limits the ability of cooperation between small cells. In indoor environment, the small cells are typically deployed in different rooms and the path loss exponent is high. Over-the-air backhaul connection thus suffers from higher attenuation so the cooperation is limited to the base stations in close proximity.

In this chapter, we propose novel iterative CBF algorithms that work

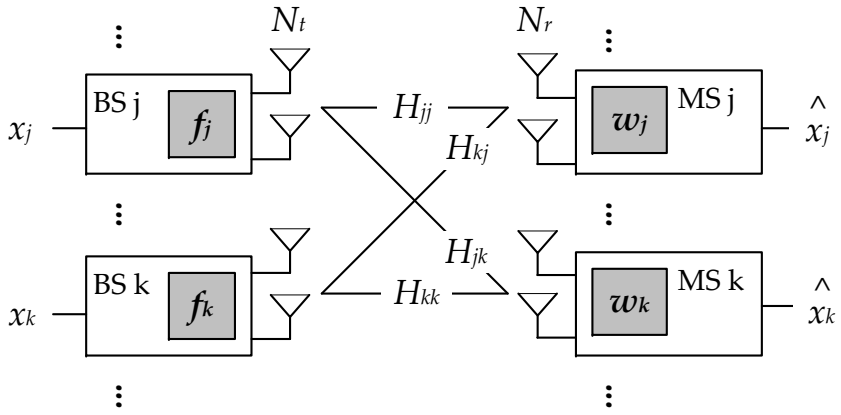

Figure 4.1: K User, K cell MIMO coordinated beamforming system model.

with arbitrary K and multiple transmit and receive antennas, with a limited cooperation between cells. We propose three different algorithms that lead a better sum rate performance than previously proposed algorithms. We then propose limited cooperation algorithms, where the update of the beamforming vectors can be done synchronously or asynchronously. We finally confirm the performance of the proposed algorithms via simulation and analysis.

4.1 System Model and Problem Statement

Consider a K-user, K-cell MIMO downlink system model with N_{t} transmit and N_{r} receive antennas as illustrated in Fig. 4.1. We assume that each BS transmits only one stream of data to its serving MS. At the k-th BS, a normalized transmit symbol x_k is multiplied by the normalized beamforming vector $\boldsymbol{f}_k \in \mathcal{C}^{N_{\mathrm{t}} \times 1}$ and then transmitted over the $N_{\mathrm{r}} \times N_{\mathrm{t}}$ channel $\boldsymbol{H}_{kk}$. A matrix $\boldsymbol{H}_{jk}$ of size $N_{\mathrm{r}} \times N_{\mathrm{t}}$ is used to denote the interference from the j-th

BS to the k-th MS. We further assume that each base station uses the same fixed power P/K, where P is the total transmit power used in the system. This equal power approach achieves performance close to that of a brute force search algorithm, which we present in the later section.

The received signal at the k-th MS is given by

$$\boldsymbol{y}_k = \sqrt{\frac{P}{K}}\boldsymbol{H}_{kk}\boldsymbol{f}_k x_k + \sum_{j\neq k}\sqrt{\frac{P}{K}}\boldsymbol{H}_{jk}\boldsymbol{f}_j x_j + \boldsymbol{n}_k, \tag{4.1}$$

where $\boldsymbol{n}_k$ is an $N_\mathrm{r}\times 1$ additive white Gaussian noise with variance σ_k^2 per entry. After applying a *linear* receive filter $\boldsymbol{w}_k$ of size $N_\mathrm{r}\times 1$, the estimated signal at the k-th MS is given by $\tilde{x}_k = \boldsymbol{w}_k^*\boldsymbol{y}_k$, where $\boldsymbol{w}_k^*$ is Hermitian of $\boldsymbol{w}_k$. The corresponding post-processing SINR at the k-th MS is

$$\gamma_k = \frac{\frac{P}{K}|\boldsymbol{w}_k^*\boldsymbol{H}_{kk}\boldsymbol{f}_k|^2}{\sum_{j\neq k}\frac{P}{K}|\boldsymbol{w}_k^*\boldsymbol{H}_{jk}\boldsymbol{f}_j|^2 + \|\boldsymbol{w}_k\|_2^2\sigma_k^2}, \tag{4.2}$$

and the achievable sum rate of all K MSs is given by

$$\mathcal{R}_{\mathsf{SUM}} = \sum_{k=1}^{K}\log_2(1+\gamma_k). \tag{4.3}$$

The goal of the chapter is to *jointly* determine $\boldsymbol{f}_k$ and $\boldsymbol{w}_k$, $k = 1,\cdots,K$, to maximize the sum throughput $\mathcal{R}_{\mathsf{SUM}}$. It is known that each γ_k can be maximized when the linear MMSE receive combining vector is used [47]. If the objective is related to the throughput maximization, therefore, MMSE-based receive combining vector may yield a better solution than the zero-forcing (ZF) approach in [14]. It is also proved that the sum rate maximization problem and MSE minimization problem can be equivalent [75]. We thus focus on the

design of MMSE-type beamforming vectors, despite it may yield to iterative coordinated beamforming algorithms for $K > 2$.

4.2 Iterative CBF Algorithms

In this section, we present iterative-CBF algorithms based on the three different objectives, Max-SINR, Max-SLNR (signal-to-leakage-and-noise ratio) and Min-SMSE (sum MSE). These metrics are well-known variants of the throughput maximization problem. Based on the objectives, the optimal beamforming vectors can also be obtained differently.

4.2.1 Maximizing Per-MS SINR

Maximizing per-MS SINR can be seen as a partial cooperation technique because each transceiver pair maximizes its own link quality using the transmit beamforming vector(s) at other BS(s). With given receive combining vector $\boldsymbol{w}_k$, the post-processing SINR (4.2) at the k-th MS becomes

$$\gamma_k = \frac{\boldsymbol{w}_k^* \boldsymbol{H}_{kk} \boldsymbol{f}_k \boldsymbol{f}_k^* \boldsymbol{H}_{kk}^* \boldsymbol{w}_k}{\boldsymbol{w}_k^* \left(\sum_{j \neq k} \boldsymbol{H}_{jk} \boldsymbol{f}_j \boldsymbol{f}_j^* \boldsymbol{H}_{jk} + \frac{K}{P} \sigma_k^2 \right) \boldsymbol{w}_k}. \tag{4.4}$$

The filter $\boldsymbol{w}_k$ that maximizes γ_k in (4.4) is known as the principal singular vector of $\frac{\boldsymbol{H}_{kk} \boldsymbol{f}_k \boldsymbol{f}_k^* \boldsymbol{H}_{kk}^*}{\sum_{j \neq k} \boldsymbol{H}_{jk} \boldsymbol{f}_j \boldsymbol{f}_j^* \boldsymbol{H}_{jk}^* + \frac{K}{P} \sigma_k^2 \boldsymbol{I}_{N_\mathrm{r}}}$, which yields

$$\boldsymbol{w}_k = \alpha_k \left(\sum_{j \neq k} \boldsymbol{H}_{jk} \boldsymbol{f}_j \boldsymbol{f}_j^* \boldsymbol{H}_{jk}^* + \frac{K}{P} \sigma_k^2 \boldsymbol{I}_{N_\mathrm{r}} \right)^{-1} \boldsymbol{H}_{kk} \boldsymbol{f}_k, \tag{4.5}$$

with the normalization parameter $\alpha_k = \frac{1}{(\boldsymbol{H}_{kk} \boldsymbol{f}_k)^* \boldsymbol{R}_k^{-1} (\boldsymbol{H}_{kk} \boldsymbol{f}_k)}$. The proposed receive filter that maximizes per-MS SINR relates the k-th MS's MSE and the

k-th MS's SINR (4.4) as

$$\begin{aligned}\epsilon_k &= \mathbb{E}\left[|\hat{x}_k - x_k|^2\right] \\ &= \frac{1}{|\boldsymbol{w}_k^* \boldsymbol{H}_{kk} \boldsymbol{f}_k|^2} \left(\sum_{j \neq k} |\boldsymbol{w}_k^* \boldsymbol{H}_{jk} \boldsymbol{f}_j|^2 + \frac{K}{P} \boldsymbol{w}_k^* \boldsymbol{w}_k \sigma_k^2 \right) \\ &= \frac{\sum_{j \neq k} \boldsymbol{f}_j^* \boldsymbol{H}_{jk}^* \boldsymbol{w}_k \boldsymbol{w}_k^* \boldsymbol{H}_{kj} \boldsymbol{f}_j + \frac{K}{P} \boldsymbol{w}_k^* \boldsymbol{w}_k \sigma_k^2}{\boldsymbol{f}_k^* \boldsymbol{H}_{kk}^* \boldsymbol{w}_k \boldsymbol{w}_k^* \boldsymbol{H}_{kk} \boldsymbol{f}_k} = \frac{1}{\gamma_k}.\end{aligned} \tag{4.6}$$

This receiver filter (4.5) is often referred to as MMSE interference rejection combiner (IRC). Note that the normalization factor does not give any impact on the per-link SINR. The proposed receive filter is, however, not the optimum in the sense that minimizes the k-th MS's MSE as we specify later.

Applying (4.6), the k-th MS's SINR γ_k is given by

$$\gamma_k = \boldsymbol{f}_k^* \boldsymbol{H}_{kk}^* \left(\sum_{j \neq k} \boldsymbol{H}_{jk} \boldsymbol{f}_j \boldsymbol{f}_j^* \boldsymbol{H}_{jk}^* + \frac{K}{P} \sigma_k^2 \boldsymbol{I}_{N_\mathrm{r}} \right)^{-1} \boldsymbol{H}_{kk} \boldsymbol{f}_k. \tag{4.7}$$

Given $\boldsymbol{w}_k$ and by letting $\boldsymbol{R}_k = \sum_{j \neq k} \boldsymbol{H}_{jk} \boldsymbol{f}_j \boldsymbol{f}_j^* \boldsymbol{H}_{jk}^* + \sigma_k^2 \boldsymbol{I}_{N_\mathrm{r}}$, $\boldsymbol{f}_k$ that maximizes per-MS SINR is obtained by

$$\boldsymbol{f}_k = \boldsymbol{v}_{\max} \left\{ \boldsymbol{H}_{kk}^* \boldsymbol{R}_k^{-1} \boldsymbol{H}_{kk} \right\}, \tag{4.8}$$

where $\boldsymbol{v}_{\max}\{\boldsymbol{A}\}$ is the dominant singular vector of $\boldsymbol{A}$. This is known as a generalized Rayleigh quotient and $\boldsymbol{f}_k$ generally depends on the transmit beamforming vectors chosen by other BSs if $K > 2$ [14].

An iterative update of transmit vectors may improve the system performance. As the transmit beamforming vector $\boldsymbol{f}_k$ depends on other BS's transmit beamformer vectors but not the receive combining vectors, iteration

can be done among transmit beamforming vectors only. If a global channel state information is available at one of the BS, the computation is done at that BS and then the beamforming vector can be feed-forwarded to each BS (possibly via inter-BS wired connection such as an X2 interface). The received filter is simply applied once at each receiver when the iteration is done.

4.2.2 Maximizing Per-BS SLNR

Maximizing per-BS SLNR is similar to maximizing per-MS SINR: the role of transmitter and receiver is simply changed. The *leakage* is defined as the power dissipation from a BS to all undesired MSs. If the leakage level is high, it cause higher interference to adjacent MSs, degrading the system performance. Minimizing the leakage is thus another good strategy to improve the overall system performance [17, 61, 80].

The k-th BS's SLNR is defined as

$$\eta_k = \frac{|\boldsymbol{w}_k^* \boldsymbol{H}_{kk} \boldsymbol{f}_k|^2}{\sum_{j \neq k} |\boldsymbol{w}_j^* \boldsymbol{H}_{kj} \boldsymbol{f}_k|^2 + \frac{P}{K} \bar{\sigma}_k^2} \tag{4.9}$$

$$= \frac{\boldsymbol{f}_k^* \boldsymbol{H}_{kk}^* \boldsymbol{w}_k \boldsymbol{w}_k^* \boldsymbol{H}_{kk} \boldsymbol{f}_k}{\boldsymbol{f}_k^* \left(\sum_{j \neq k} \boldsymbol{H}_{kj}^* \boldsymbol{w}_j \boldsymbol{w}_j^* \boldsymbol{H}_{kj} + \frac{K}{P} \bar{\sigma}_k^2 \right) \boldsymbol{f}_k} \tag{4.10}$$

where $\bar{\sigma}_k^2$ is the average noise variance at all the MSs but the k-th MS. The term $\sum_{j \neq k} |\boldsymbol{w}_j^* \boldsymbol{H}_{kj} \boldsymbol{f}_k|^2$ is the leakage from the k-th BS to all non-serving MSs. The transmit beamforming vector that maximizes the SLNR is

$$\boldsymbol{f}_k = \beta_k \left(\sum_{j \neq k} \boldsymbol{H}_{kj}^* \boldsymbol{w}_j \boldsymbol{w}_j^* \boldsymbol{H}_{kj} + \frac{K}{P} \bar{\sigma}_k^2 \boldsymbol{I}_{N_t} \right)^{-1} \boldsymbol{H}_{kk}^* \boldsymbol{w}_k, \tag{4.11}$$

with the beamforming normalization parameter $\beta_k = \frac{1}{(\boldsymbol{H}_{kk}^* \boldsymbol{w}_k)^* \boldsymbol{L}_k^{-1} (\boldsymbol{H}_{kk}^* \boldsymbol{w}_k)}$, where $\boldsymbol{L}_k = \sum_{j \neq k} \boldsymbol{H}_{kj}^* \boldsymbol{w}_j \boldsymbol{w}_j^* \boldsymbol{H}_{kj} + \frac{K}{P} \bar{\sigma}_k^2 \boldsymbol{I}_{N_\mathrm{t}}$. The received combining vector that maximizes per-BS SLNR is thus

$$\boldsymbol{w}_k = \boldsymbol{v}_{\max} \left\{ \boldsymbol{H}_{kk} \boldsymbol{L}_k^{-1} \boldsymbol{H}_{kk}^* \right\}. \tag{4.12}$$

The transmit beamforming vector in Max-SLNR algorithm is similar to the receive filter in Max-SINR algorithm as it is based on the generalized Rayleigh quotient. For multi-user MIMO channel, the SLNR in the dual uplink channel is equivalent to the downlink SINR, if $\bar{\sigma}_k = \sigma_k$. It is understood as a dual of the downlink channel, by exchanging the role of transmitter and receiver and $\boldsymbol{H}_{jk}$ with $\boldsymbol{H}_{kj}^*$ for all j, k [73]. However, in multi-cell MIMO networks, the interference to the k-th MS and the interference from the k-th BS are not the same [31]. We thus need to verify how does the SNLR approaches can maximize the sum rate as the Max-SINR did. The discussion is introduced in the next section.

We may define the MSE at the uplink receiver (BS) side: similar to Max-SINR approach in Eq. (4.6), the proposed transmit filter relates uplink MSE and SLNR as

$$\epsilon_k^{\mathsf{UL}} = \mathbb{E}\left[|\hat{x}_k - x_k|^2 \right] = \frac{1}{\eta_k}, \tag{4.13}$$

and in this regard, the proposed Max-SLNR approach maximizes the k-th BS's uplink throughput.

Note that the receive combining vector $\boldsymbol{w}_k$ can be updated iteratively. When the iteration is done, the transmit beamforming vector in (4.11) can

Table 4.1: Channel matrices, noise variances and beamforming vectors required to compute the transmit beamforming and receive combining vectors at the base station and the mobile station

	Max-SINR	Max-SLNR	Min-SMSE
MS k	$\boldsymbol{H}_{jk}\boldsymbol{f}_j$, σ_k^2	$\boldsymbol{L}_k^{-1/2}\boldsymbol{H}_{kk}^*$	$\boldsymbol{H}_{jk}\boldsymbol{f}_j$, σ_k^2
MS k to BS k	$\boldsymbol{R}_k^{-1/2}\boldsymbol{H}_{kk}$	$\boldsymbol{H}_{kk}\boldsymbol{w}_k$, σ_k^2	$\boldsymbol{H}_{kk}\boldsymbol{w}_k$, σ_k^2
Other BSs to BS k	-	$\boldsymbol{H}_{kj}\boldsymbol{w}_j, j \neq k$, $\bar{\sigma}_k^2$	$\boldsymbol{H}_{kj}\boldsymbol{w}_j, j \neq k$, $\bar{\sigma}_k^2$

finally be applied at each BS before it sends the data stream. The MS does not need to know about the final transmit beamforming vector if the MS can estimate the downlink channel from the pilot symbols *weighted* by the trasnmit beamforming vector.

4.2.3 Minimizing Sum-MSE (SMSE)

Max-SINR and Max-SLNR are good objectives that maximize the individual link performance in each MS and BS, respectively. However, this do not necessarily lead to better sum rate in multi-antenna multicell networks. To achieve a better sum rate in such networks, different objective needs to be investigated. The SMSE maximization, which was proposed in multi-user MIMO literature in [75], is proven to lead a similar result to minimizing the product of MSE (PMSE), which is equivalent to maximizing the sum throughput at the high SNR regime [77]. In this section, we expand the equivalence of the two objectives to multicell networks under the max-SINR and max-SLNR constraints and then propose iterative beamforming strategies to achieve higher

sum rate.

The receive filter for the k-th MS in Eq. (4.5) minimizes the MSE of the k-th MS independently with other MSs. This means that the choice of the receive beamforming vector at each MS is *irrelevant* to the choice of receive beamforming vectors by other MS. Thus,

$$\{\hat{\boldsymbol{w}}_1, \cdots, \hat{\boldsymbol{w}}_K\} = \underset{\{\boldsymbol{w}_1, \cdots, \boldsymbol{w}_K\}}{\operatorname{argmin}} \sum_k \epsilon_k = \sum_k \underset{\{\boldsymbol{w}_k\}}{\operatorname{argmin}} \epsilon_k \tag{4.14}$$

and

$$\underset{\{\boldsymbol{w}_1, \cdots, \boldsymbol{w}_K\}}{\operatorname{argmin}} \sum_k \epsilon_k = \underset{\{\boldsymbol{w}_1, \cdots, \boldsymbol{w}_K\}}{\operatorname{argmin}} \prod_k \epsilon_k. \tag{4.15}$$

If each MS minimizes its own MSE, not only the SMSE but also PMSE are minimized. For the transmitter side, the transmit filter for the k-th BS in Eq. (4.11) minimizes the MSE in Eq. (4.13) but independent with the MSE at other BSs. It thus leads to the similar conclusion: the proposed beamforming in Eq. (4.11) minimizes not only the SMSE but also the PMSE of the all the BSs,

$$\left\{\hat{\boldsymbol{f}}_1, \cdots, \hat{\boldsymbol{f}}_K\right\} = \underset{\{\boldsymbol{f}_1, \cdots, \boldsymbol{f}_K\}}{\operatorname{argmin}} \sum_k \eta_k = \prod_k \underset{\{\boldsymbol{f}_k\}}{\operatorname{argmin}} \eta_k. \tag{4.16}$$

An iterative CBF algorithm consists of two update steps, receive filter update stage and the transmit beam forming vector update stage that minimizes the SMSE at each side, is proposed. With the estimated symbol $\tilde{x}_k$ in

(4.1), the MSE for the k-th MS is defined as

$$\begin{aligned}\epsilon_k &= \mathbb{E}\left[|\hat{x}_k - x_k|^2\right] \\ &= \boldsymbol{w}_k^* \boldsymbol{R} \boldsymbol{w}_k + (1 - \boldsymbol{w}_k^* \boldsymbol{H}_{kk} \boldsymbol{f}_k - (\boldsymbol{H}_{kk} \boldsymbol{f}_k)^* \boldsymbol{w}_k) \\ &= \left(\boldsymbol{w}_k^* - (\boldsymbol{H}_{kk} \boldsymbol{f}_k)^* \boldsymbol{R}^{-1}\right) \boldsymbol{R} \left(\boldsymbol{w}_k^* - (\boldsymbol{H}_{kk} \boldsymbol{f}_k)^* \boldsymbol{R}^{-1}\right)^* \\ &+ \left(1 - \boldsymbol{f}_k^* \boldsymbol{H}_{kk}^* \boldsymbol{R}^{-1} \boldsymbol{H}_{kk} \boldsymbol{f}_k\right),\end{aligned} \tag{4.17}$$

where the total covariance matrix is given by

$$\boldsymbol{R} = \sum_j \boldsymbol{H}_{jk} \boldsymbol{f}_j \boldsymbol{f}_j^* \boldsymbol{H}_{jk}^* + \sigma_k^2 \boldsymbol{I}_{N_\mathrm{r}} \triangleq \boldsymbol{R}_k + \boldsymbol{H}_{kk} \boldsymbol{f}_k \boldsymbol{f}_k^* \boldsymbol{H}_{kk}^*. \tag{4.18}$$

The filter that minimize the MSE (4.17) is obtained by [47]

$$\boldsymbol{w}_k = \boldsymbol{R}^{-1} \boldsymbol{H}_{kk} \boldsymbol{f}_k = \frac{1}{1 + \alpha_k^{-1}} \boldsymbol{R}_k^{-1} \boldsymbol{H}_{kk} \boldsymbol{f}_k, \tag{4.19}$$

Since $\mathbb{E}[\hat{x}_k - x_k] = \boldsymbol{w}_k^* \boldsymbol{H}_{kk} \boldsymbol{f}_k - 1 \neq 0$, $\boldsymbol{w}_k$ in (4.19) is a biased estimator. As $\epsilon_k = 1 - \boldsymbol{f}_k^* \boldsymbol{H}_{kk}^* \boldsymbol{R}^{-1} \boldsymbol{H}_{kk} \boldsymbol{f}_k = 1 - \frac{(\boldsymbol{f}_k^* \boldsymbol{H}_{kk}^* \boldsymbol{R}^{-1} \boldsymbol{H}_{kk} \boldsymbol{f}_k)^2}{\boldsymbol{f}_k^* \boldsymbol{H}_{kk}^* \boldsymbol{R}^{-1} \boldsymbol{H}_{kk} \boldsymbol{f}_k}$, the MSE can be modified by

$$\begin{aligned}\epsilon_k &= 1 - \frac{\boldsymbol{f}_k^* \boldsymbol{H}_{kk}^* \boldsymbol{w}_k \boldsymbol{w}_k^* \boldsymbol{H}_{kk} \boldsymbol{f}_k}{\boldsymbol{w}_k^* \boldsymbol{R} \boldsymbol{w}_k} \\ &= \frac{\boldsymbol{w}_k^* \boldsymbol{R} \boldsymbol{w}_k - \boldsymbol{f}_k^* \boldsymbol{H}_{kk} \boldsymbol{w}_k \boldsymbol{w}_k^* \boldsymbol{H}_{kk} \boldsymbol{f}_k}{\boldsymbol{w}_k^* \boldsymbol{R} \boldsymbol{w}_k},\end{aligned} \tag{4.20}$$

and taking the inverse of the MSE yields

$$\begin{aligned}\frac{1}{\epsilon_k} &= 1 + \frac{\boldsymbol{f}_k^* \boldsymbol{H}_{kk}^* \boldsymbol{w}_k \boldsymbol{w}_k^* \boldsymbol{H}_{kk} \boldsymbol{f}_k}{\boldsymbol{w}_k^* \boldsymbol{R} \boldsymbol{w}_k - \boldsymbol{f}_k^* \boldsymbol{H}_{kk}^* \boldsymbol{w}_k \boldsymbol{w}_k^* \boldsymbol{H}_{kk} \boldsymbol{f}_k} \\ &= 1 + \frac{|\boldsymbol{w}_k^* \boldsymbol{H}_{kk} \boldsymbol{f}_k|^2}{\boldsymbol{w}_k^* \boldsymbol{R}_k \boldsymbol{w}_k} = 1 + \gamma_k,\end{aligned} \tag{4.21}$$

which is equivalent to $\epsilon_k = \frac{1}{1+\gamma_k}$. Thus the MMSE filter used in (4.19) indeed minimizes the MSE of MS. This MMSE filter, the principal singular vector

of $\frac{\boldsymbol{H}_{kk}\boldsymbol{f}_k\boldsymbol{f}_k^*\boldsymbol{H}_{kk}^*}{\sum_j \boldsymbol{H}_{jk}\boldsymbol{f}_j\boldsymbol{f}_j^*\boldsymbol{H}_{jk}^* + \frac{K}{P}\sigma_k^2\boldsymbol{I}_{N_\mathrm{r}}}$, seems to be inequivalent to the SINR formula (4.4). However, the biased MMSE estimator (4.19) *does* also maximize the k-th MS's post-processing SINR as [8]

$$\begin{aligned}
[\boldsymbol{w}_k]_{\mathsf{MMSE}} &= \left(\boldsymbol{H}_{kk}\boldsymbol{f}_k\boldsymbol{f}_k^*\boldsymbol{H}_{kk}^* + \boldsymbol{R}_k\right)^{-1}\boldsymbol{H}_{kk}\boldsymbol{f}_k \\
&= \left(\boldsymbol{R}_k^{-1} - \frac{\boldsymbol{R}_k^{-1}\boldsymbol{H}_{kk}\boldsymbol{f}_k(\boldsymbol{H}_{kk}\boldsymbol{f}_k)^*\boldsymbol{R}_k^{-1}}{1+\alpha_k^{-1}}\right)\boldsymbol{H}_{kk}\boldsymbol{f}_k \\
&= \boldsymbol{R}_k^{-1}\boldsymbol{H}_{kk}\boldsymbol{f}_k - \frac{\boldsymbol{R}_k^{-1}\boldsymbol{H}_{kk}\boldsymbol{f}_k(\boldsymbol{H}_{kk}\boldsymbol{f}_k)^*\boldsymbol{R}_k^{-1}\boldsymbol{H}_{kk}\boldsymbol{f}_k}{1+\alpha_k^{-1}} \\
&= \boldsymbol{R}_k^{-1}\boldsymbol{H}_{kk}\boldsymbol{f}_k - \frac{\boldsymbol{R}_k^{-1}\boldsymbol{H}_{kk}\boldsymbol{f}_k\alpha_k^{-1}}{1+\alpha_k^{-1}} \\
&= \frac{\alpha_k}{1+\alpha_k}\boldsymbol{R}_k^{-1}\boldsymbol{H}_{kk}\boldsymbol{f}_k = \frac{\alpha_k}{1+\alpha_k}\left[\boldsymbol{w}_k\right]_{\mathsf{Max\text{-}SINR}}.
\end{aligned}$$

Since the biased MMSE filter that minimizes the MSE is a *scaled* version of unbiased MMSE filter that maximizes SINR, from (4.4) where the scaling term $\frac{\alpha_k}{1+\alpha_k}$ in numerator and denominator can be canceled out, the biased MMSE filter also maximizes the link SINR. With a proper scaling, as pointed out in [8], both $[\boldsymbol{w}_k]_{\mathsf{MMSE}}$ and $[\boldsymbol{w}_k]_{\mathsf{Max\text{-}SINR}}$ filters yield the same symbol (soft) decoding performance.

After the received beamforming vectors are updated, the transmit beamforming vector can be chosen to minimize the uplink MSE. The uplink MSE is defined by

$$\epsilon_k^{\mathsf{UL}} = \mathbb{E}\left[|\hat{x}_k - x_k|^2\right] = 1 - \boldsymbol{H}_{kk}^*\boldsymbol{w}_k\boldsymbol{L}^{-1}\boldsymbol{w}_k^*\boldsymbol{H}_{kk}, \tag{4.22}$$

where the uplink total covariance matrix is given by

$$\boldsymbol{L} = \sum_j \boldsymbol{H}_{kj}^*\boldsymbol{w}_j\boldsymbol{w}_j^*\boldsymbol{H}_{kj} + \frac{K}{P}\bar{\sigma}_k^2\boldsymbol{I}_{N_\mathrm{t}} \triangleq \boldsymbol{L}_k + \boldsymbol{H}_{kk}^*\boldsymbol{w}_k\boldsymbol{w}_k^*\boldsymbol{H}_{kk}. \tag{4.23}$$

The choice of the transmit beamforming vector, which is also the MMSE filter, is thus

$$\boldsymbol{f}_k = \boldsymbol{L}^{-1}\boldsymbol{H}_{kk}^{*}\boldsymbol{w}_k = \frac{1}{1+\beta_k^{-1}}\boldsymbol{L}_k^{-1}\boldsymbol{H}_{kk}^{*}\boldsymbol{w}_k. \tag{4.24}$$

The biasedness of (4.24) can be removed by multiplying the normalization factor $\frac{\beta_k}{1+\beta_k}$, making the filter equivalent to the filter in Max-SLNR algorithm. By applying (4.19) and (4.24) iteratively, the individual MSE is minimized. After each iteration, the vectors are updated only when the stopping condition $\Delta(\text{SMSE})_{i-1} - \Delta(\text{SMSE})_i > th > 0$ is not met. The stopping condition enables to achieve a higher sum rate as iteration goes by.

Note that the proposed iterative CBF achieves higher sum rate than Max-SINR and Max-SLNR which optimize only one side, as will be shown in Section 4.4. As iteration is progressed, the beamforming strategies at BSs and MSs decrease the MSE, which yields sum throughput increase. Remaining questions are 1) how does the Max-SLNR beamforming is related to the MMSE transmit filter, 2) the convergence of the proposed iterative CBF, and 3) the comparison with non-iterative joint transmit-receive beamforming strategy.

4.2.3.1 Max-SLNR beamforming and the transmit MMSE filter

Although the proposed Max-SLNR beamforming is a method to achieve the minimum MSE of the virtual uplink, one may think it is unclear how it is related to the transmit MMSE filter [45, 54]. Let us recall the Max-SLNR

transmit beamforming in (4.24). Applying the Sherman-Morrison formula [33],

$$\begin{aligned}
\boldsymbol{f}_k &= \boldsymbol{L}^{-1}\boldsymbol{H}_{kk}^{*}\boldsymbol{w}_k \\
&= \boldsymbol{L}_k^{-1}\boldsymbol{H}_{kk}^{*}\boldsymbol{w}_k - \frac{\boldsymbol{L}_k^{-1}\boldsymbol{H}_{kk}^{*}\boldsymbol{w}_k\boldsymbol{w}_k^{*}\boldsymbol{H}_{kk}\boldsymbol{L}_k^{-1}}{1+\boldsymbol{w}_k^{*}\boldsymbol{H}_{kk}\boldsymbol{L}_k^{-1}\boldsymbol{H}_{kk}^{*}\boldsymbol{w}_k}\boldsymbol{H}_{kk}^{*}\boldsymbol{w}_k \qquad (4.25)\\
&= \frac{\boldsymbol{L}_k^{-1}\boldsymbol{H}_{kk}^{*}\boldsymbol{w}_k}{1+\boldsymbol{w}_k^{*}\boldsymbol{H}_{kk}\boldsymbol{L}_k^{-1}\boldsymbol{H}_{kk}^{*}\boldsymbol{w}_k}, \qquad (4.26)
\end{aligned}$$

which is a scaled version of the transmit Wiener filter of the same channel [45, 54].

In general, maximizing SLNR at the BSs does not necessarily lead to sum rate maximization with multiple data streams per user [17]. In a beamforming system considered in this chapter, the sum rate maximization can be much simpler though. But since the Min-SMSE uplink-downlink duality in multiuser MIMO systems [68] is no longer applied to multi-cell MIMO systems, the direct proof of the optimality of Max-SLNR beamforming for the downlink sum rate is not easy. In [81], it was shown that the transmit beamforming vectors found through the SLNR maximization reaches the rate region boundary for a two-cell scenario. As in [81], our proposed transmit beamformer balances between leakage minimization ($\boldsymbol{L}_k^{-1}$) and signal power maximization ($\boldsymbol{H}_{kk}^{*}\boldsymbol{w}_k$). As the proposed algorithm is equivalent to the transmit Weiner filter as well, we thus conclude that the proposed algorithm is a good choice to achieve close-to-optimal downlink sum rate at least for the multicell channel with similar level of interference power.

4.2.3.2 Proof of convergence:

Note that either the SMSE or the PMSE is not jointly convex on all the input variables, so showing the global convergence may not be feasible. However, as indicated in [85], it is convex over each of the transmitter and receiver matrices which may guarantee that the proposed algorithm could converge to a local minimum.

A proof for the convergence in adaptive weighted sum MSE algorithm can be found in [62]. In the adaptive weighted sum MSE algorithm in [62], the transmit beamformer is weighted and the noise scaling factor is chosen so that the transmit beamforming vector has a unit norm. In our proposed Min-SMSE transmit beamforming, although we keep the noise variance to $\frac{K}{P}\bar{\sigma}_k^2$, we keep the beaoforming vector $\boldsymbol{f}_k$ be normalized to one by multiplying $1/(1+\beta_k^{-1})$. Thus, although the method to obtain the weight and noise variance are different, we may apply the proof in [62] to our proposed algorithm. The monotonic decrease condition however does not guarantee convergence; it should be followed by a contraction condition to prove a convergence to a fixed point.

The proof of the contraction condition is as follows. For the i-th iteration, we define $f(\epsilon(i)) = -\log_2(\prod_k \epsilon_k(i))$ and $f(\epsilon(i-1)) = -\log_2(\prod_k \epsilon_k(i-1))$ for the $i-1$-th iteration. As $\log_2(x)$ is monotonically increasing function and its slope is strictly smaller than 1 for $x > 1/\ln(2)$,

$$\frac{|f(\epsilon(i)) - f(\epsilon(i-1))|}{|\epsilon(i) - \epsilon(i-1)|} < 1, \tag{4.27}$$

which implies that there exists a constant $k < 1$ s.t.

$$|f(\epsilon(i)) - f(\epsilon(i-1))| < k|\epsilon(i) - \epsilon(i-1)|, \tag{4.28}$$

for all $\epsilon(i)$ and $\epsilon(i-1)$ that satisfies $\prod_k \epsilon_k(i)) > 1/\ln 2$. This is also related to the stopping condition, $\Delta(\text{SMSE})_{i-1} - \Delta(\text{SMSE})_i > th > 0$, meaning that the non-negative threshold th can enable that the iterative update algorithm to satisfy the contraction condition.

In the proposed algorithm, the utility cannot decrease over consecutive beamforming vector updates. At each iteration step, the SMSE or PMSE is monotonically decreasing so the utility is at least maintained. After enough iteration, any stationary point corresponds to a local optimum. The proof of the global convergence from any initial points is still an open problem in this iterative approach though.

4.2.3.3 Comparison with non-iterative joint CBF:

Although the iterative CBF may achieve good sum rates, the performance needs to be compared with optimal approach. The capacity region of the MIMO interference channel is still an open problem except a few special cases [27]. As indicated in [21], numerical optimization of achievable rate regions with with sum power constraint across all the BSs is a difficult problem in general. Finding sum rate optimum beamforming in multicell MIMO networks is known as NP-hard for more than two-cell scenarios [14].

One easy way to compare the proposed iterative CBF algorithms with

the best non-iterative joint CBF algorithms is to utilize the random vector quantization (RVQ) method. As the beamforming vectors we achieve have a unit norm, we can randomly generate vectors under the same constraint. As the number of candidate vectors increase, we may assume that the non-iterative optimal beamforming vectors can be found within the set. This can be done numerically and we present the performance comparison in Section 4.4.

4.3 Iterative CBF with Limited Cooperation

The full cooperation presented in the previous section is sometimes inefficient and very costly in practical cellular networks. For instance, large information exchange between BSs requires additional protocols and may cause significant delay to the system. Also, the need of a centralized entity to compute the transmit beamforming vectors and receive combining vectors is often impractical. We therefore present distributed asynchronous update mechanisms with limited cooperation, where limited cooperation means that BSs cooperate only when strong interference is caused to an MS. The optimality of this approach is shown for multi-cell network with single receive antenna per MS [86], which the maximum achievable rates for all BSs are bounded by finite Pareto-optimal values. It is also shown that the optimal high-SNR sum rate slope can be achievable with limited amount of information [67]. The MS measures the strength of interference and then informs to the serving BS about the interfering BS index, and the BS informs to the interfering BS(s)

Algorithm 1 Centralized Limited Cooperation

Compute the initial $\boldsymbol{f}_k$ using (4.11) for $k = 1, \cdots, K$
BS k: Informs $\boldsymbol{f}_k$ to MS k
MS k: Initialize $\boldsymbol{R}_k$ and
for $j = 1$ **to** K **do**
  if $|\boldsymbol{H}_{jk}\boldsymbol{f}_j|^2 > \gamma|\boldsymbol{H}_{kk}\boldsymbol{f}_k|^2$ **then**
    Update $\boldsymbol{R}_k = \boldsymbol{R}_k + \boldsymbol{H}_{jk}\boldsymbol{f}_j\boldsymbol{f}_j^*\boldsymbol{H}_{jk}^*$
  end if
end for
MS k: Report $\boldsymbol{R}_k$ to the central entity
Central Entity: Compute $\boldsymbol{f}_k$ and $\boldsymbol{w}_k$ using (4.11) and (4.5) interchangeably for $k = 1 \cdots, K$
Central Entity: Forward $\boldsymbol{f}_k$ to BS k
MS k: Update $\boldsymbol{w}_k$

with updated transmit beamforming vector. This limited cooperation can be done synchronously in the central entity or asynchronously in a distributed manner.

In the proposed iterative-CBF algorithms, limited cooperation is a valid approach because of the following reasons. First, as the channel estimation error is generally proportional to the inverse of the receive signal power [47], the measured channel can be inaccurate if the received power is weak. Second, a weak interference does not contribute much to the beamforming vector design. From Eq. (4.24), the interference rejection combiner can autonomously ignore whose power level is low. Sharing of such unnecessary information that may not be used for computing the beamforming vector is thus redundant.

Based on above observation, we propose a limited cooperation mechanism for more efficient communication. Both centralized and distributed

Algorithm 2 Distributed Limited Cooperation

Compute the initial $\boldsymbol{f}_k$ using (4.11) for $k = 1, \cdots, K$
BS k: Informs $\boldsymbol{f}_k$ to MS k
MS k: Initialize $\boldsymbol{R}_k$ and
for $j = 1$ **to** K **do**
  if $|\boldsymbol{H}_{jk}\boldsymbol{f}_j|^2 > \gamma|\boldsymbol{H}_{kk}\boldsymbol{f}_k|^2$ **then**
    Update $\boldsymbol{R}_k = \boldsymbol{R}_k + \boldsymbol{H}_{jk}\boldsymbol{f}_j\boldsymbol{f}_j^*\boldsymbol{H}_{jk}^*$
    Store j to $\mathfrak{I}_k$
  end if
end for
MS k: Report $\boldsymbol{R}_k$ to BS k
BS k: Compute $\boldsymbol{f}_k$ using (4.11) and inform $\boldsymbol{f}_k$ to the BS(s) in the stored index $\mathfrak{I}_k$
BS(s) in the index $\mathfrak{I}_k$: Update beamforming vector and inform the change to the BS(s) that cause interference to the serving MS
BS(s): Update until either there is no update or timer expires

algorithms are presented in Alg. 1 and Alg. 2, respectively. The degree of cooperation can be adjusted by changing the cutoff threshold γ adaptively: γ can be associated with either the SNR, the target SINR or the number of cooperating nodes. The key differences between centralized and distributed cooperation is on the update timing. The distributed algorithm updates the beamforming vectors asynchronously, while the centralized one updates synchronously. Note that although for the asynchronous update, after enough iteration, the performance may converge to that of synchronous update. This is because the proposed iterative-CBF algorithm is designed to minimize the MSE at each node per iteration. Even after updating the beamforming vectors in each cell asynchronously, as long as other beamforming vectors that are affected by the change are also updated, the sum MSE cannot be increased.

4.4 Performance Comparison

In this section, the performance of the proposed iterative-CBF algorithms are presented. The reference algorithms that we compare with are point-to-point upper bound (PP-UB) and non-coordinated beamforming. The PP-UB is the sum throughput when the crosstalk between cells are zero, i.e., $\boldsymbol{H}_{jk} = 0$ if $j \neq k$. As no other cell interference exists, each mobile station tries to maximize its own received signal power. In the beamforming system, such approach is known as (single-cell) eigen-beamforming. The beamforming vectors $\boldsymbol{w}_k$ and $\boldsymbol{f}_k$ are respectively the principal left and right singular vectors of $\boldsymbol{H}_{kk}$. In this case, the achievable sum rate is given as

$$\mathcal{R}_{\mathsf{PP}} = \sum_k \log_2 \left(1 + \frac{P}{K} \frac{|\boldsymbol{w}_k^* \boldsymbol{H}_{kk} \boldsymbol{f}_k|^2}{\sigma_k^2} \right). \tag{4.29}$$

In the non-coordinated beamforming, beamforming vectors are chosen to maximize its own effective channel gain after treating all the other-cell interference as noise. The MS is equipped with the MMSE-IRC filter to maximize the link SINR, but the BS does not cooperatively update its transmit beamforming vectors. This approach is useful for cell-interior MSs whose INR level is much lower than the SNR level. As the mobile station moves to the cell boundary, however, INR becomes higher and this non-coordinated approach may become unsuitable.

The last algorithm we compare is the non-coordinated beamforming with interference-ignorant receiver. In this case, both BS and MS put no effort on mitigating the inter-cell interference. The transmit beamforming

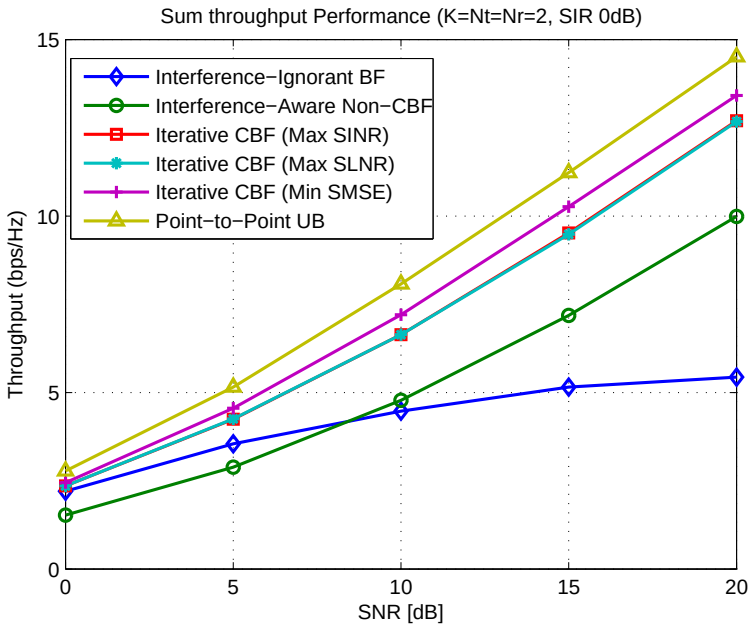

Figure 4.2: Sum rate comparison (SIR=0 dB, $K = N_{\mathrm{t}} = N_{\mathrm{r}} = 2$).

vector $\boldsymbol{f}_k$ is the dominant right singular vector of $\boldsymbol{H}_{kk}$. The receive filter performs the maximum ratio combining, $\boldsymbol{w}_k = \frac{\boldsymbol{H}_{kk}\boldsymbol{f}_k}{\|\boldsymbol{H}_{kk}\boldsymbol{f}_k\|}$, to maximize its own effective channel gain.

In Fig. 4.2, sum throughput performance comparison with $K = N_{\mathrm{t}} = N_{\mathrm{r}} = 2$ at SIR=0 dB is presented. The proposed Max-SINR and Max-SLNR algorithms outperform the non-cooperative algorithms, but are worse than the Min-SMSE algorithm. The Min-SMSE algorithm is closest to the PP-UB, thanks to the joint optimization of transmitter and receiver to improve both SINR and SLNR iteratively.

To see the achievability of the proposed algorithms, we randomly gen-

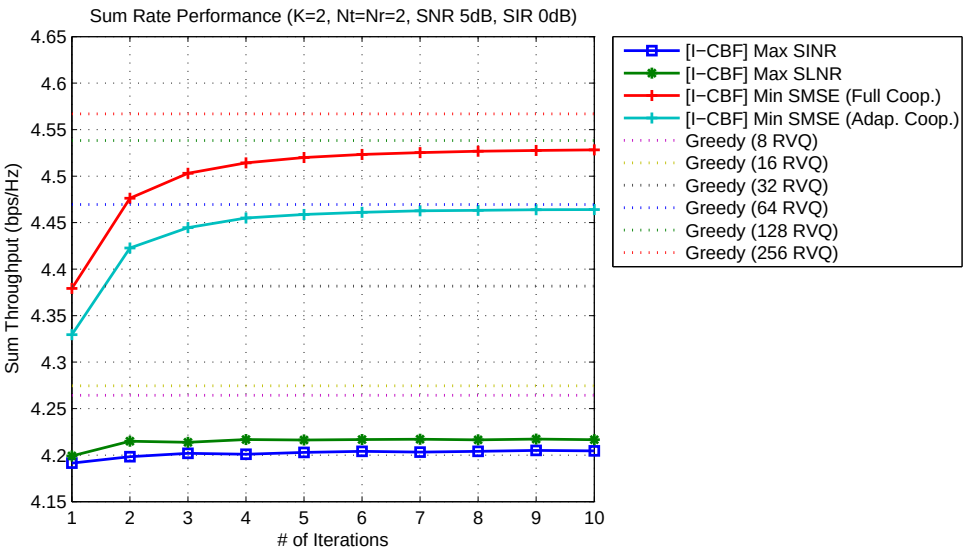

Figure 4.3: Sum rate under different numbers of iterations I - SNR at 5dB.

erate a number of unit-norm vectors and take an exhaustive, greedy search over them. With given set of greedy vectors $\mathcal{M} = \{\boldsymbol{g}_1, \cdots, \boldsymbol{g}_M\}$, $\|\boldsymbol{g}_k\|_2^2 = 1$, the greedy algorithm chooses the beamforming vectors that maximize the sum throughput (4.3). The method to generate vectors is often referred to as random vector quantizer (RVQ). The computational complexity of the greedy search algorithm is M^K and as M goes to infinity, it can be understood that the set of chosen vectors are close to optimum. The simulation results with greedy search approach are presented in Fig. 4.3 and Fig. 4.4. In Fig. 4.3, when SNR is fixed at 5dB, the proposed Min-SMSE algorithm is close to the greedy search algorithm with $M = 256$ per node. When SNR is fixed at 20dB, as shown in Fig. 4.4, the proposed Min-SMSE algorithm is close to 64 RVQ greedy search, although we observe a slower convergence speed than low SNR

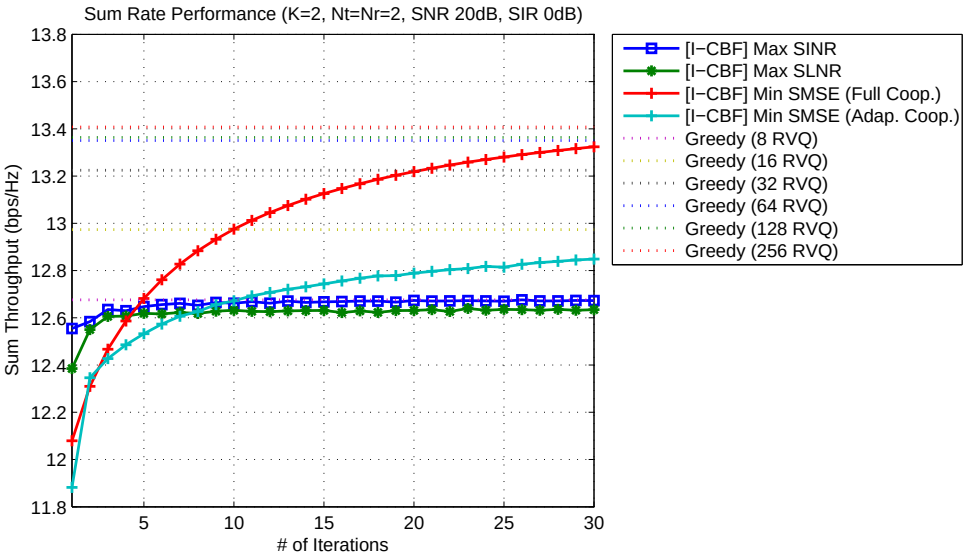

Figure 4.4: Sum rate under different numbers of iterations II - SNR at 20dB.

region. Based on the simulation results, we observe that the proposed Min-SMSE iterative CBF algorithm is very close to the achievable bound of the system, although more rigorous mathematical derivations should be investigated.

A new comparison with fractional frequency reuse (reuse factor 1/2) is presented in Fig. 4.5. When $K = 2$, the fractional frequency reuse with reuse factor 1/2 eliminate all the other-cell interference at the cost of resource segmentation. Each base station and mobile station pair can apply optimal eigen-beamforming. Although there is no outer-cell interference, the penalty for the fractional use of the resource limits the sum rate performance.

In Fig. 4.6, the throughput performance with limited cooperation is

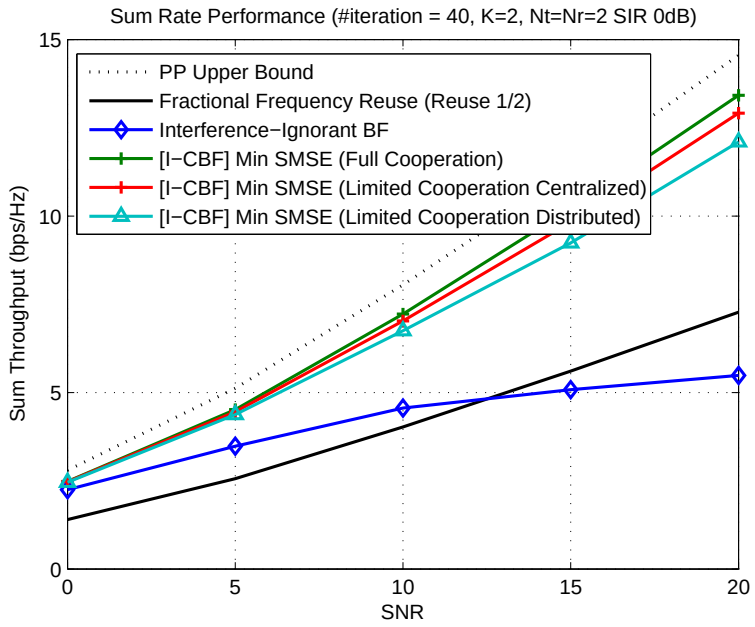

Figure 4.5: Sum throughput performance of proposed iterative CBF with limited cooperation.

presented. We assume that the channel estimation error is proportional to the inverse of the received power. The cutoff threshold γ is set at 6 dB, so the interference whose power is more than 6 dB lower than the desired signal can be neglected. From the simulation results, we observe that the adaptive limited cooperation shows very close performance to the full cooperation and clearly outperforms the fixed limited cooperation with fixed number of interference $(K/2)$ to compute the filters. Note that the average number of interference links that is shared for cooperation is approximately 45% of the all the interfering nodes. This percentage could be lower if a more sophisticated cutoff parameter optimization for limited cooperation is applied.

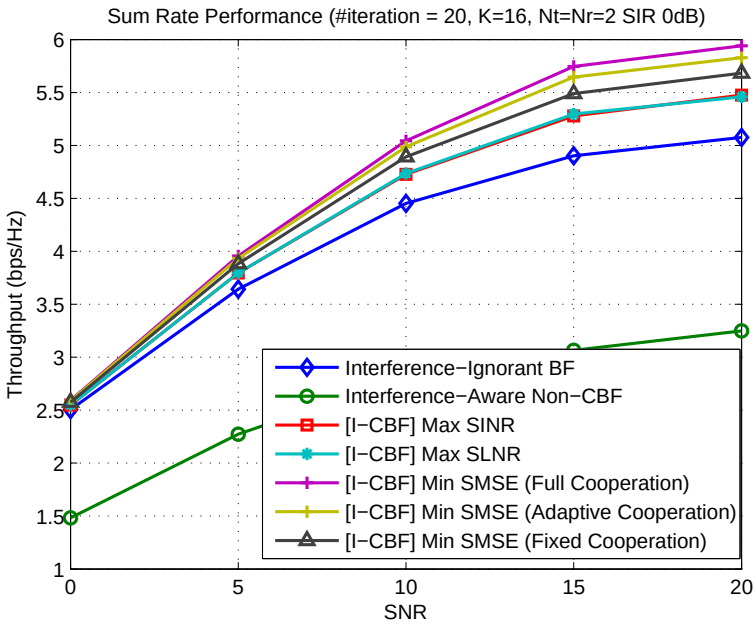

Figure 4.6: Sum rate with limited cooperation ($K = 16, N_{\mathrm{t}} = N_{\mathrm{r}} = 4$).

4.5 Discussions

In this chapter, we investigated the sum rate maximizing issue in multi-cell MIMO cellular networks and proposed iterative coordinated beamforming algorithms with limited cooperation. The proposed iterative CBF algorithms, which are based on Max-SINR, Max-SLNR or Min-SMSE objectives, show enhanced performance than the non-cooperative or interference-ignorant approaches. Especially, the Min-SMSE algorithm achieved performance close to that of a brute force search algorithm after enough iterations. We then proposed synchronous and asynchronous limited feedback algorithms that are more efficient and adequate in practical cellular networks. In the future work,

we will provide a more rigorous proof of the convergence of the proposed distributed cooperation algorithm and investigate an expansion of the proposed algorithms for joint precoding multicell systems with novel joint power optimization technique.

Chapter 5

Comprehensive Performance Comparison

In this chapter, comprehensive performance comparisons among various algorithms are presented. We compare the sum rate of 1) coordinated beamoforming with realistic assumptions, 2) coordinated beamforming and joint processing, and 3) multicell coordination in a common heterogeneous network setting.

Throughout this chapter, we assume perfect channel state information at transmitter and receiver unless stated otherwise. For the coordinated beamforming, we assume that an anchor base station has the global knowledge of downlink and interference channels, so the computation can be done within that base station. The anchor base station feed-forwards the computed beamforming vectors to other base stations. For joint processing, we assume that the timing of the signals from multiple base stations to a mobile station is within the coherence time of the system (e.g., within the cyclic prefix duration in OFDM systems). For the distribution of small cells in heterogeneous networks, we use the stochastic geometry model in [7, 10]. Specific assumptions are explained in the subsections.

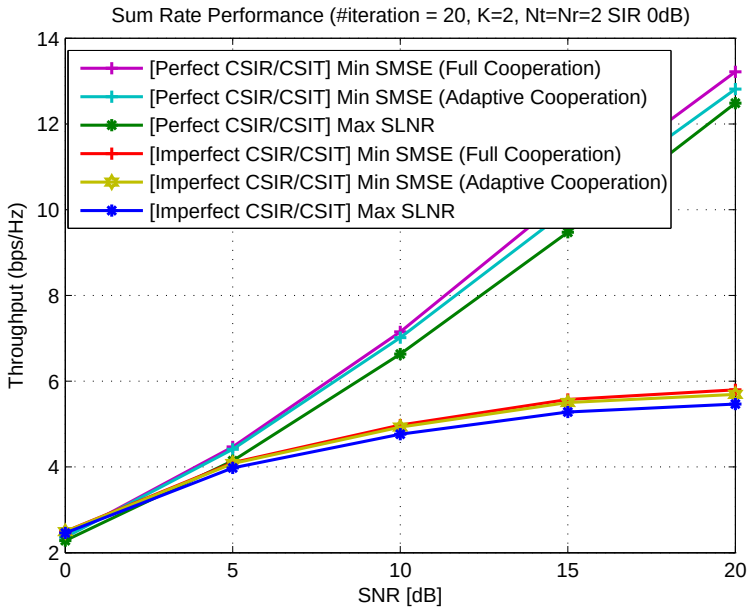

Figure 5.1: Comparison of iterative coordinated beamforming algorithms with imperfect CSIR/CSIT due to channel estimation error and limited feedback.

5.1 Further Evaluation of Coordinated Beamforming

In Chapter 4, we presented simulation results mostly in ideal conditions. In this section, we present performance comparison under realistic conditions in practical cellular systems. In practical multicell cellular systems with practical receiver processing, there are typically two impairments during the coordination process: one is channel estimation error that causes imperfect channel state information at the receiver (CSIR) and the other is limited feedback that results in imperfect channel state information at the transmitter (CSIT). The imperfect CSIR makes the computation of receive beamforming be inaccurate, while the imperfect CSIT results in impairments in computing

transmit beamforming vectors.

We assume that the channel estimation error is proportional to the inverse of the received signal power, which is a typical assumption by the definition of MSE and shown in Eq. (4.22). For the limited feedback, we have utilized the non-uniform vector quantization methods described in [15]. The simulation results with the two impairments are presented in Fig. 5.1. As we may have expected, the sum performance of the coordinated beamforming is highly degraded due to imperfect CSIR/CSIT. The is because the computation of Max-SINR and Max-SLNR requires rigorous knowledge on both the channel and the interference. Even with a small imperfection, therefore, we may achieve only a fraction of the performance gain (e.g., about 30% of the the cell throughput improvement in [3, 39]) instead of the ideal K-times throughput gain.

The sum rate performance comparison between iterative and non-iterative coordinated beamforming[1] algorithms is presented in Fig. 5.2. Note that the non-iterative coordinated beamforming algorithms exist mostly in a two-cell scenario [14], so we compared in the simplest multicell MIMO systems ($N_{\mathrm{r}} = N_{\mathrm{t}} = K = 2$). The iterative coordinated beamforming is based on the Max-SMSE algorithm in Chapter 4.

[1] In [14], two interference-aware coordinated beamforming (IA-CBF) approaches that jointly optimized MMSE and ZF MIMO transceiver algorithms, are presented. The two algorithms are non-iterative for a two-cell, two user MIMO system. The MMSE IA-CBF is obtained by using a lower bound of the achievable product rate. The ZF IA-CBF is developed under the zero other-cell interference constraint and is proven to be optimal in the two-cell two-antenna system.

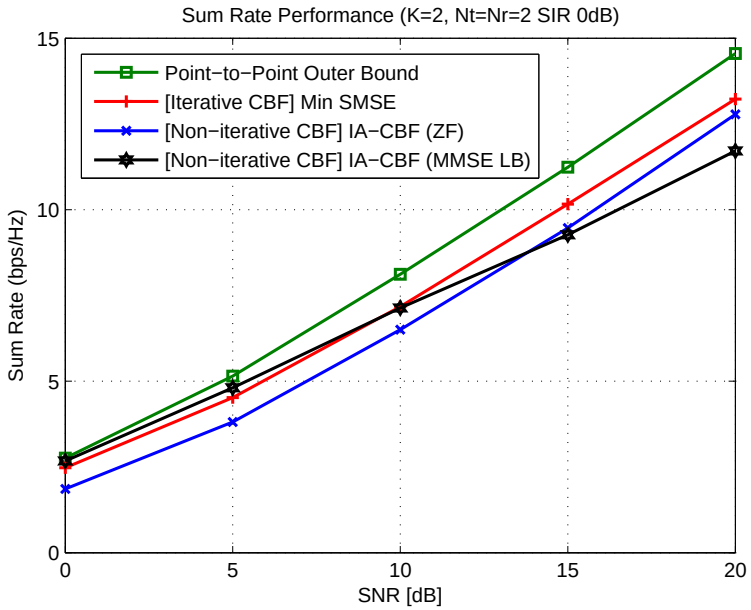

Figure 5.2: Comparison between iterative and non-iterative coordinated beamforming algorithms in $N_{\mathrm{t}} = N_{\mathrm{r}} = K = 2$.

In Fig. 5.2, we can observe the proposed iterative CBF outperforms in non-iterative CBF algorithms. The Min-SMSE algorithm gives higher sum rate than the ZF IA-CBF algorithm because MSE is better minimized at every node under the Min-SMSE algorithm. When SNR is low to medium, forcing zero other-cell interference actually degrades the sum rate. The gap between the Min-SMSE beamforming and ZF IA-CBF asymptotically disappears as the MMSE beamforming acts as ZF decorrelator in very high SNR regions with fixed interference power. If the out-of-band interference also increases as the SNR increases, the gap will be maintained. Comparing iterative and non-iterative MMSE beamforming, the iterative algorithm outperforms non-

iterative MMSE IA-CBF in high SNR region. This is because the non-iterative algorithm in [14] only achieves a lower bound of the product rate, while the iterative algorithm achieves the minimum SMSE in all SNR regions.

5.2 Coordinated Beamforming vs. Joint Processing

Unlike the coordinated beamforming systems in Fig. 4.1, in joint processing, base stations not only share the downlink channel information but also the information about the transmit data streams, and a mobile station can receive data symbols from multiple base stations. The joint processing transforms the MIMO interference channel into a MIMO broadcast channel because multiple coordinated BSs effectively form a distributed super-BS whose capacity region is well known [13, 76, 78]. The joint processing provides higher system throughput than the coordinated beamforming, but at the cost of downlink data stream exchange between BSs. It also requires a more stringent synchronization in time, frequency (phase) among multiple streams to a desired mobile station.

The block diagram of a multicell joint processing system is illustrated in Fig. 5.3. The n-th mobile station's effective channel (before passing though the receive beamforming vector) is $\tilde{\boldsymbol{H}}_n = [\boldsymbol{H}_{n1}\boldsymbol{f}_1 \cdots \boldsymbol{H}_{nK}\boldsymbol{f}_K]_{N_\mathrm{r}\times K}$, where $\boldsymbol{H}_{nm} \in \mathcal{C}^{N_\mathrm{r}\times N_\mathrm{t}}$ is the channel matrix from m-th cell to n-th user and $\boldsymbol{f}_k \in \mathcal{C}^{N_t\times 1}$ and $\boldsymbol{w}_k \in \mathcal{C}^{N_r\times 1}$ are the k-th BS's unit-norm transmit vector and the k-th MS's receive beamforming vector, respectively. It is assumed that each element of $\boldsymbol{H}_{nm}$ is i.i.d and distributed as $\mathcal{CN}(0,1)$. The $K \times K$ aggregated effective

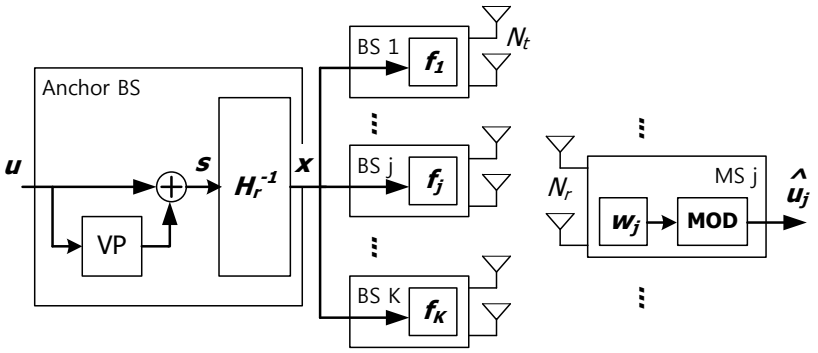

Figure 5.3: Block diagram of the proposed multicell joint processing.

channel is then given by

$$\boldsymbol{H}_r = \left[\left(\boldsymbol{w}_1^* \tilde{\boldsymbol{H}}_1 \right)^T \cdots \left(\boldsymbol{w}_k^* \tilde{\boldsymbol{H}}_k \right)^T \cdots \left(\boldsymbol{w}_K^* \tilde{\boldsymbol{H}}_K \right)^T \right]^T, \tag{5.1}$$

whose (m, n)-th element is $\boldsymbol{w}_m^* \boldsymbol{H}_{mn} \boldsymbol{f}_n$. We assume that $\boldsymbol{H}_r$ is a full rank matrix. The received signal is then given as

$$\boldsymbol{y} = \boldsymbol{H}_r \boldsymbol{x} + \boldsymbol{n} = \boldsymbol{H}_r \frac{\boldsymbol{s}}{\sqrt{\gamma}} + \boldsymbol{n}, \tag{5.2}$$

where $\boldsymbol{s} = [s_1 \ \cdots \ s_K]^T \in \mathcal{C}^{K \times 1}$ is an *unnormalized* precoded signal vector, $\gamma = \|\boldsymbol{s}\|^2$ and $\boldsymbol{n} = [n_1 \ \cdots \ n_K]$. With the normalization by γ, the transmit vector $\boldsymbol{x} = \boldsymbol{s}/\sqrt{\gamma}$ obeys the unit-norm constraint, i.e., $\|\boldsymbol{x}\|^2 = 1$.

The performance difference between coordinated beamforming and joint processing can be understood in terms of the eigenvalue distribution . For K-user, K-cell joint processing system, the largest eigenvalue of $K \times K$ aggregated effective channel increases as the number of antennas or the number of cells for joint processing increases [25]. This is the gain over coordinated beamform-

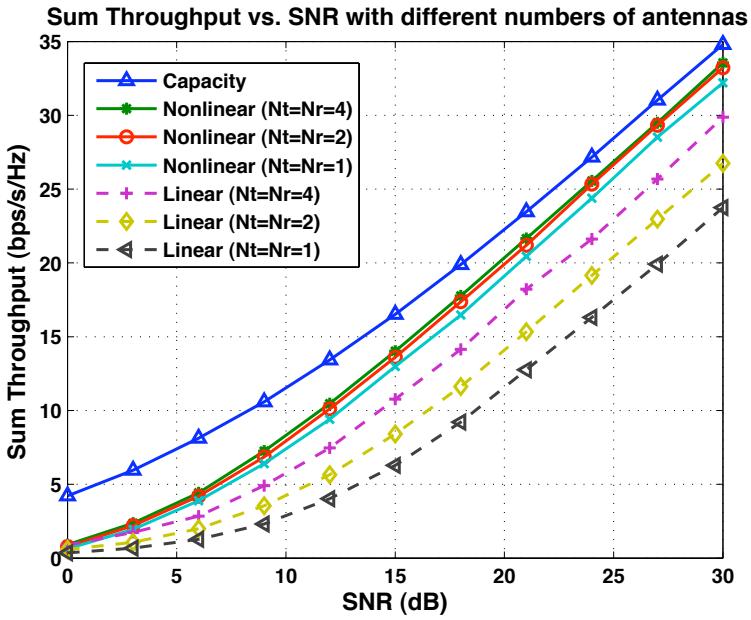

Figure 5.4: Sum throughput of linear and nonlinear joint processing with different numbers of antennas. The capacity with nonlinear precoding is obtained using the sum power iterative water-filling process [43]. Vector perturbation (VP) [32] is used as nonlinear precoding technique.

ing where additional cells in the cooperating system increase the out-of-cell interference.

Fig. 5.4 compares the achievable sum rate of the joint processing with different N_{t} and N_{r}. As a reference, the sum capacity obtained using the sum power iterative water-filling process [43] is presented. From Fig. 5.4, we observe that the sum rate is improved as $N_{\mathrm{t}}, N_{\mathrm{r}}$ increase. The gain due to larger number of antennas is obvious in the linear joint processing algorithm. In the nonlinear precoding, vector perturbation [32] is being utilized so that higher sum throughput gain can be achieved. The performance can be compared

with coordinated beamforming in [14, 37], showing the joint processing can give much higher throughput at the cost of additional information exchange between base stations.

5.3 Multicell Coordination in Heterogeneous Networks

There have been two different approaches to achieving a much higher throughput in the future wireless systems. The first approach is to use more antennas to achieve higher spatial gain in outdoor macro base stations. The second approach is to deploy more small cells to cope with increasing traffic demand from both indoors and outdoors. A deployment of many antenna in a base station is called massive MIMO. The second approach often referred to as a viral proliferation of small cell or hyper-dense heterogeneous and small cell networks (HetSNets) [38]. Multicell cooperation is closely related to hyper-dense HetSNets since inter-cell interference cancellation and coordination is the key in that system.

5.3.1 Massive MIMO

Massive MIMO is an emerging technology that uses a large excess of base station antennas (up to a few hundred antennas) to serve a number of users in the same time-frequency resource simultaneously [34]. In massive MIMO systems, as the aperture of the array grows with the number of antennas, the resolution of the array also increases, and hence the transmitted power can be sharply focused into a small area, allowing the transmitter to use less

transmit power to achieve a given SNR at the receiver. It was thus expected that massive MIMO can provide a significant capacity gain and improve the energy efficiency.

However, the performance of massive MIMO is limited by the finite and potentially correlated scattering given the space constraints of the transmit antenna array [34]. With insufficient scattering and correlation among different scattering clusters, the degrees of freedom may be saturated to certain values which limits the performance [56, 57]. Also, the number of orthogonal pilots may be limited by the finite channel coherence time even in TDD system. This results in a high reuse of pilots among adjacent cells, making the pilots contaminated and thus resulting in corrupted uplink channel estimation [53]. As a result, massive MIMO can be more attractive in time-division duplex (TDD) systems where downlink channel training and feedback do not constrain the number of transmit antennas. In addition, high deployment cost of large arrays with many RF chains is a problem. It is expected, therefore, that the throughput gain and application of massive MIMO is fundamentally limited and massive MIMO may not be a single dominant approach to meet the ever-increasing traffic demands.

5.3.2 Hyper-Dense HetSNets

Hyper-dense HetSNets are motivated by rethinking of the network deployment principle – to bring the network close to the users to offer unprecedented capacity. There are several advantages of this approach over macro cell

enhancements. First, the cost of deployment in HetSNets is much lower than that of the macro cells. Unlike the macro cell where a significant portion of the recurring cost comes from fiber to each cell site location, power usage and real estate, there is no big operating cost in user deployed HetSNets. Second, HetSNets are energy efficient as they can be utilized intelligently and opportunistically. Depending on the traffic demand, small cells can be in dormant state so the energy consumption and the interference can be minimized. Third, hyper-dense HetSNets can realize the *always best connected* principle by seamless handover and smart offloading. Proximity based over-the-air congestion control and fast inter-cell load balancing in HetSNets increase the overall spatial reuse [1]. As many small cells are deployed indoor, offloading the indoor user traffic to indoor small cells may provide a huge gain.

The macro base stations can also stretch their antennas closer to the users. Instead of deploying expensive macro base stations with many antennas and digital baseband processing units, the radio processing units can be deployed in remote locations. Such cells are called remote radio heads (RRHs), which are parts of the distributed antenna systems (DAS) [58]. DAS/RRH may provide additional throughput gain by filling up the coverage hole due to disruption of obstacles. The Cloud RAN approach extends this to a network-wide scale. In these centrally controlled networks, extensive requirements for high capacity fiber connections to/from the RRHs and fast adaptation capability to the agile traffic demands need to be properly addressed. Despite the similarity in the physical appearance, HetSNets operate in a distributed man-

ner by allowing enough intelligence to each cell to organize and coordinate autonomously. Current deployment of millions of femtocells is suggestive of initial preference for small cells. Technology enhancements for HetSNets with distributed intelligence are actively promoting this further.

5.3.3 Simulation Assumptions

To apply multicell cooperation algorithms to K-tier hyper-dense HetSNets in real-world deployment, one of the biggest concerns is how to model the base station distribution. One proven way is the use of the stochastic geometry [7, 10]: the location of small cell base stations can be drawn from a stochastic process because most small cells are deployed in unplanned positions. Poisson point process (PPP), which is a useful mathematical tool based on stochastic geometry, provides an accurate and tractable analytical model [24]. Recently, repulsive cell planning strategies based on Matern hard core process (MHP) where the constituent nodes are forbidden to lie closer than a certain minimum distance are proposed [18, 19]. MHP is a thinning of the PPP ensuring a desired minimum distance between base stations. Specifically, distributed control [18] and centralized control [19] of minimum separation distance in MHP enables the number of active base stations to be adjusted, improving the coverage probability, throughput and load balancing.

The two multi-cell modeling methods, PPP and MHP, are compared and illustrated in Fig. 5.5. As shown in the figures, MHP makes the base station distribution more uniform than PPP and the coverage probability for

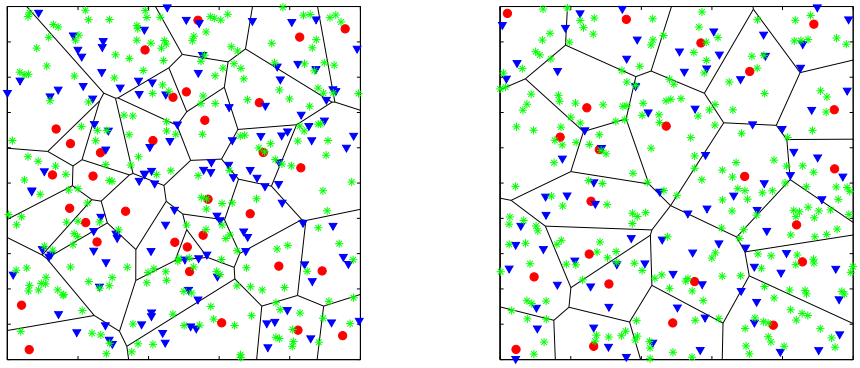

(a) PPP

(b) MHP

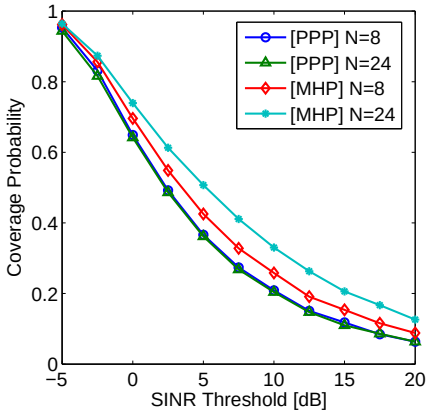

(c) CCDF of SINR

Figure 5.5: An illustration of base station distribution for 3-tier (red: macro, blue: pico, green: femto) HetSNets in (a) PPP and (b) MHP with voronoi tessellation of macro cells, and (c) their cell coverage performance comparison. In both cases, $\lambda_3 = 4\lambda_2 = 8\lambda_1$, where λ_i is the i-th tier's base station density. In MHP, the minimum distance in each tier is inversely proportional to its transmit power and the cell coverage performance is improved as the number of cells (N) in unit area is increased.

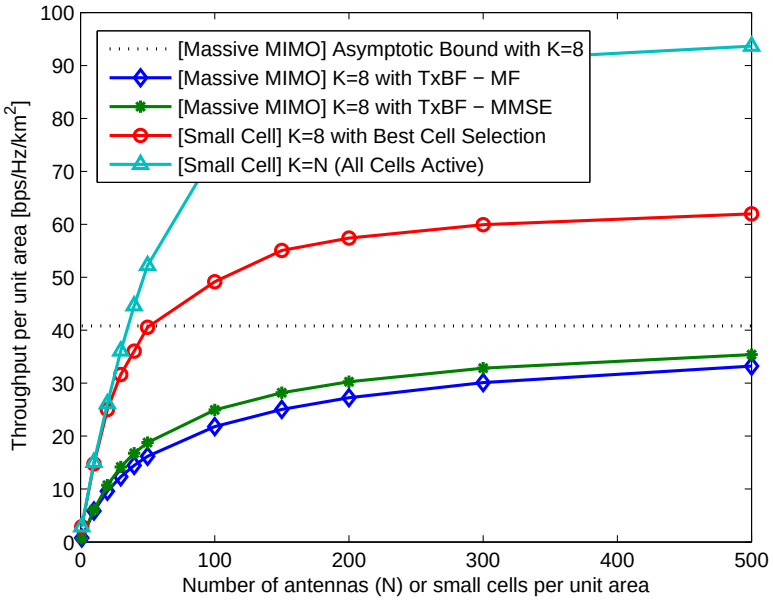

Figure 5.6: Performance comparison - massive MIMO (number of users per cell $K = 8$, number of cells $L = 4$, and inter-cell interference factor $\alpha = 0.1$) vs. dense small cells (1-tier, base stations are distributed by MHP with minimum distance $85m$, path loss exponent $\gamma = 4$). 'Best cell selection' means that each user selects the nearest base station and the unchosen base stations are turned off.

a given SINR requirement higher. Further advantages of the MHP approach such as improved load balancing capability are analyzed in [18, 19]. As a next step of performance evaluation in practical cellular systems in [3], the performance of various multicell cooperation techniques need to be compared using these tractable models.

5.3.4 Performance Comparison

We present the performance gain of many enabling technologies, focusing on the performance comparison between massive MIMO and hyper-dense HetSNets. In theory, massive MIMO achieves a high throughput by achieving a high beamforming gain, while hyper-dense HetSNets improves the performance by bringing base stations closer to the target mobile stations. With a massive antenna array at the base station with appropriate transmit beamforming such as MF (matched filter) or MMSE, the effective SNR increases linearly with the array size N as long as the size of the antenna array is scaled accordingly [34]. In hyper-dense HetSNets with N small cells per unit area, the average distance from the base station is decreased by $\sqrt{N}$ so $\sqrt{N}^{\gamma}$ gain can be achieved where γ is the pathloss exponent. Typically γ is greater than 2[2] in most propagation conditions (especially in indoor environments). Therefore, the gain achieved by bringing the network closer to the mobile station $N^{\gamma/2}$ is greater than the massive array gain N.

In Fig. 5.6, the throughput performance of massive MIMO and hyper-dense HetSNets are presented for $\gamma = 4$. In massive MIMO, the deterministic equivalent model based on random matrix theory [34] tells that the maximum achievable average rate it limited because of pilot contamination and correlated scattering, as indicated by the black dashed line in Fig. 5.6. In hyper-dense HetSNets with the number of users ($K = 8$), the network throughput scales

[2] $\gamma = 2$ is the path loss exponent in free space.

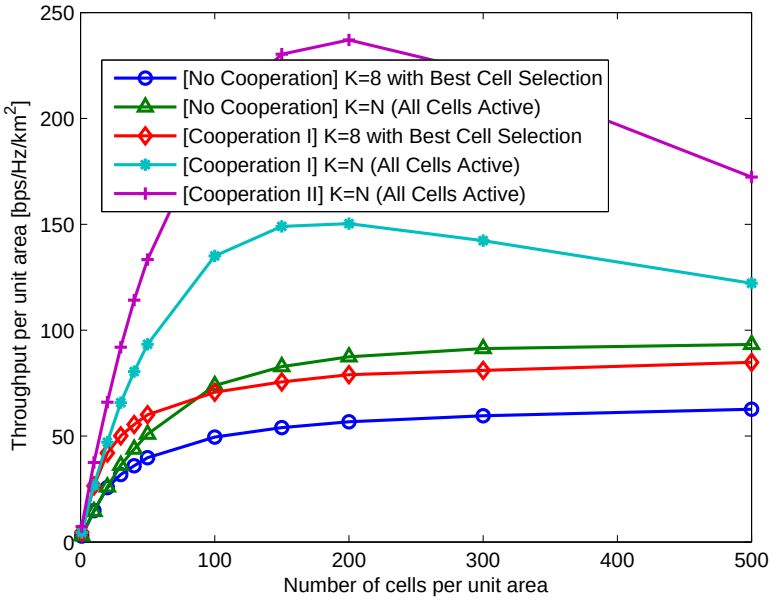

Figure 5.7: Performance comparison - dense small cells with and without multicell cooperation. In multicell Cooperation I, we assumed that each mobile station is capable of mitigating one dominant interferer, which is the strongest interference. In Coooperation II, each mobile station is capable of mitigating two dominant interferers.

to a higher value as the hyper-densification takes place. We also plotted the scenario where the number of users scales according to N (i.e., $K = N$), where a significantly higher gain is observed. The performance gain of hyper-dense HetSNets can be improved even further with novel adjacent-cell interference mitigation schemes [1, 23].

In Fig. 5.7, the throughput performance of hyper-dense HetSNets with and without multicell coordination is presented. We keep the same simulation assumptions for the small cells – 1-tier, base stations are distributed by

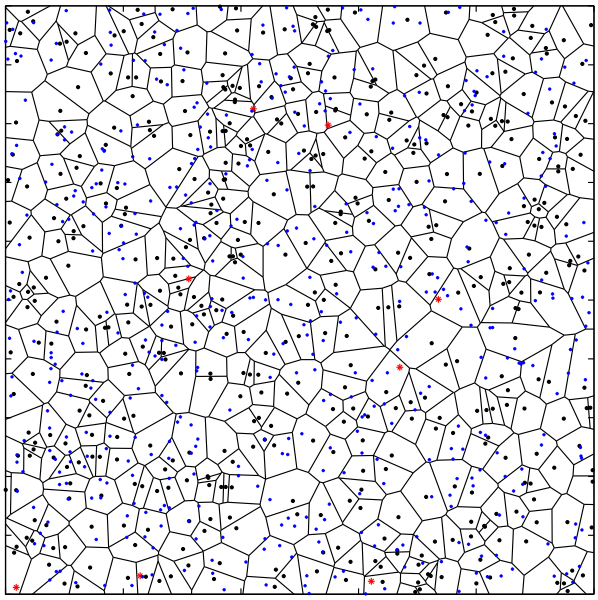

Figure 5.8: PPP with $N = 500$ with voronoi tessellation of small cells. Blue dots represent mobile stations (500 users) and red dots represent the 8 mobile stations.

MHP with minimum distance $85m$, path loss exponent $\gamma = 4$ – as in Fig. 5.6. For multicell cooperation, we assume that each mobile station is capable of mitigating one strongest interferer (Cooperation I) or two dominant interferers (Cooperation II). The simulation results show very interesting trend: the throughput per unit area increases and then decreases as the number of small cells per unit area increases, when all the cells are active.

To figure out the hidden limiting factor in Fig. 5.7, a set of new simulations is conducted. First, a simulation with PPP (lifting the minimum

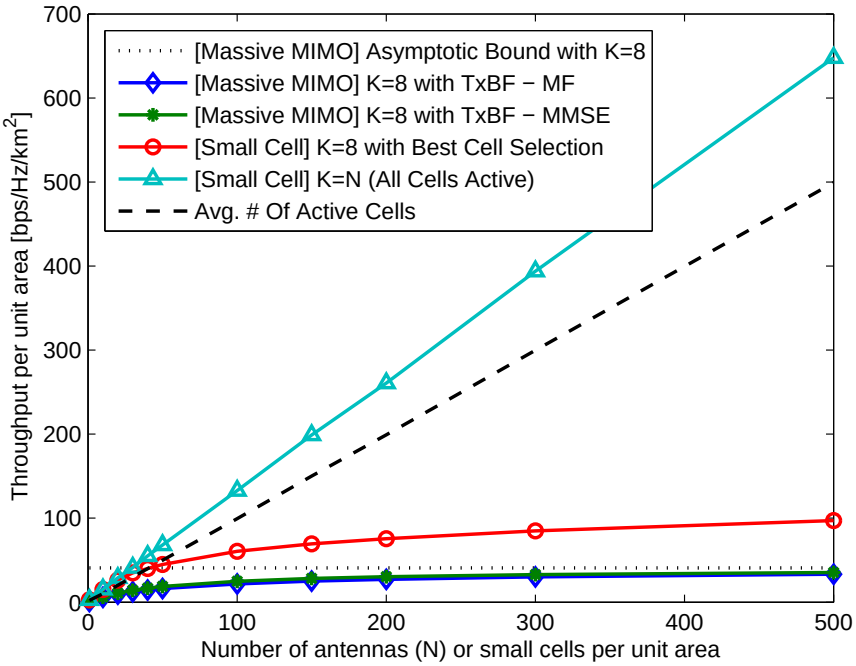

Figure 5.9: Area throughput with PPP distribution of small cells.

distance enforcement off between small cells) in Fig. 5.8 shows the small cell and user distribution with $K = N = 500$. The red dots represent $K = 8$ for a comparison with massive MIMO. As can be shown in Fig. 5.9, the area throughput monotonically increases due to reduced distance from the serving cell with high pass loss exponent ($\gamma = 4$). As we assume that the mobile station can choose the nearest base station as the serving cell, some cells do not have serving mobile station. In such a case, those unchosen small cells go into a dormant state. The difference between N and 'Avg # of Active Cells' in Fig. 5.9 represents the number of cells in dormancy. From the simulation, we may see the limiting factor shown in Fig. 5.7 comes from enforcing the

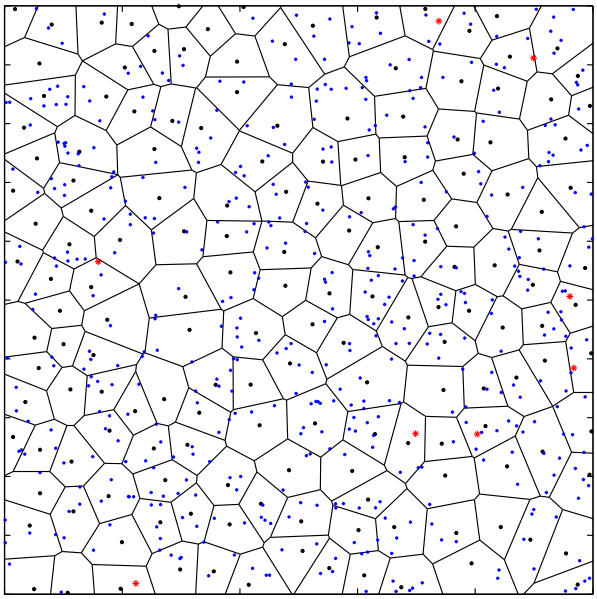

Figure 5.10: MHP with $N = 500$ with voronoi tessellation of small cells. Blue dots represent mobile stations (500 users) and red dots represent the 8 mobile stations. $50m$ minimum distance is enforced between small cells. The path loss exponent is 4.

minimum distance between small cells.

Additional simulations with MHP to figure out the reason of the decrease in the area throughput as densification is progressed are presented in Fig. 5.10 and Fig. 5.11. Note that the thinning is done practically rather than theoretically; newly added small cell may not be turned on if the distance from nearest *existing* base station is shorter than the predefined minimum distance. Although this is not an efficient way of thinning to maximize the area throughput or a user-centric per-user throughput, this is the way that a prac-

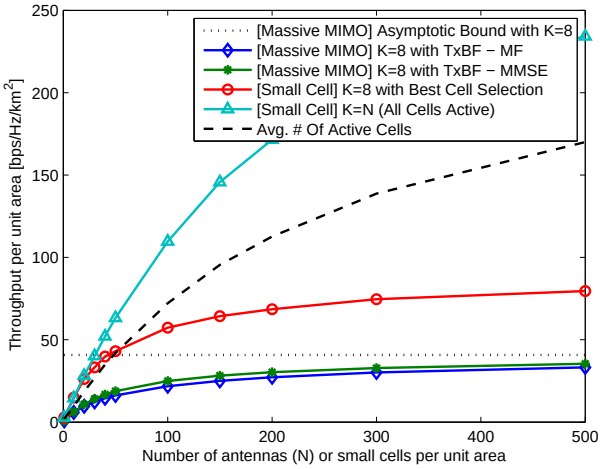

(a) Without Cooperation

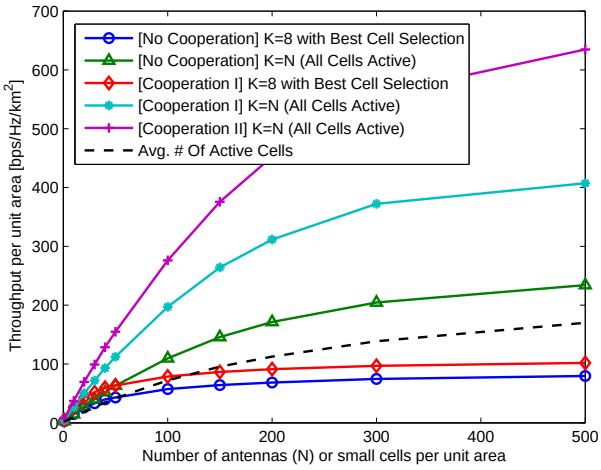

(b) With Cooperation

Figure 5.11: Area throughput with MHP distribution of small cells. $50m$ minimum distance is enforced between small cells.

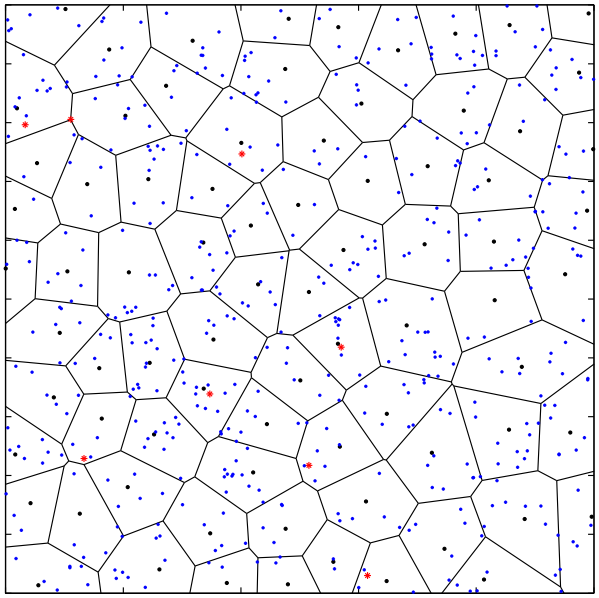

Figure 5.12: MHP with $N = 500$ with voronoi tessellation of small cells. Blue dots represent mobile stations (500 users) and red dots represent the 8 mobile stations. $85m$ minimum distance is enforced between small cells.

tical self-optimizing network (SON) is operated [38]. This realistic assumption is used to see the area throughput in the following simulations.

Fig. 5.10 and Fig. 5.11 are respectively the simulation results for cell/user distribution and the area throughput with $50m$ minimum distance between small cells. As can be seen in Fig. 5.10, the cell size and shape becomes more uniform than the cells distributed by the PPP shown in Fig. 5.8. This reduces the number of active cells in the given area, as we may be seen in the dashed line in Fig. 5.11(b). This would limit the area throughput

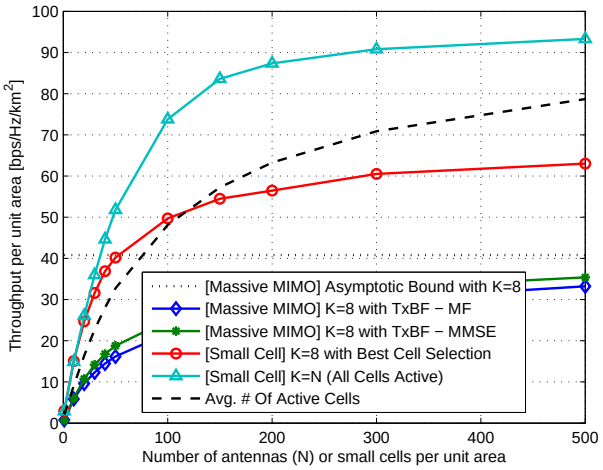

(a) Without Cooperation

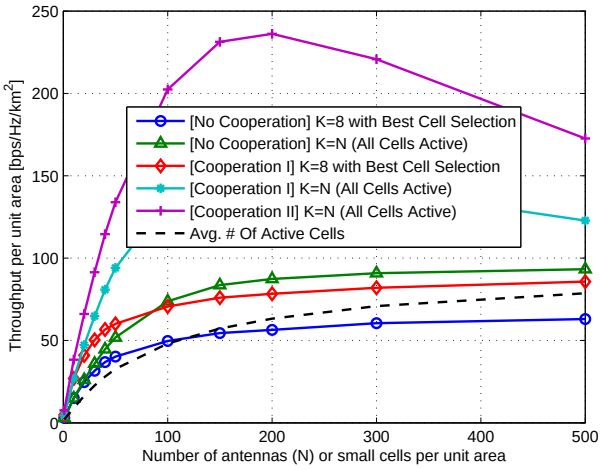

(b) With Cooperation

Figure 5.13: Area throughput with MHP distribution of small cells. $85m$ minimum distance is enforced between small cells.

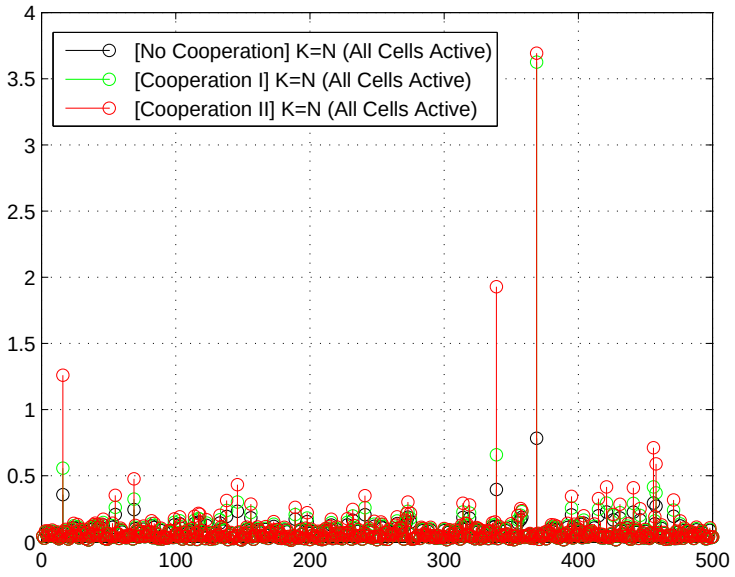

Figure 5.14: SINR distribution.

gain as densification is progressed.

When a more stringent minimum distance is enforced ($85m$), we could observe that the area throughput is actually decreasing as number of active cells increase. The results can be found in Fig. 5.12 and Fig. 5.13. In Fig. 5.12, the average number of active cells is significantly reduced, compared to $50m$ distance enforcement in Fig. 5.10 and PPP in Fig. 5.8. This results in the performance saturation in Fig. 5.13(a). When multicell cooperation is applied, the area throughput decreases as the densification is progressed, meaning that the gain by dominant interference cancellation is decreased. This comes from the saturation of active base stations (at around 70); as the number of mobile stations (K) is increased, the chances that a base station serves more

than one mobile station increases as shown in Fig. 5.12. This would lead to increased *intra-cell interference* and eliminating one or two dominant *intra-cell interferer(s)* does not give any more throughput improvement since the average number of inter-cell interferers is much more than that. For instance, when $K = 500$, there are $500/70 \approx 7$ mobile stations per base station in average, so there are 6 intra-cell mobile stations that compete for resource and cause strong interference. As K increases, therefore, without mitigating the intra-cell interference or a novel scheduling algorithm, the SINR per mobile station significantly decreases, which results in the degradation of the area throughput.

Finally, we presented the SINR distribution of all mobile stations ($K = 500$), with and without eliminating the dominant interferer(s) in Fig. 5.14. In Fig. 5.14, SINR$<$ 1 means that the overall interference power is greater than the signal power as the system operates in interference-limited (not noise limited) region. Cooperation improve the SINR for a few mobile stations whose dominant *intra-cell interferer(s)* are one or two, but it would give marginal gain on most of the mobile stations' SINR. This is the reason why the gain by cooperation may not prevail the loss by increased number of dominant *intra-cell interferer(s)* when the number of active cells is limited but the number of active mobiles stations keeps increasing.

The extensive simulation results explain that in not-so-dense HetSNets, even simple multicell cooperation (e.g., dominant interference mitigation) may improve the area throughput. In hyper-dense HetSNets, however, advanced

multicell coordination and intra-cell interference mitigation techniques are required because the likelihood of mobile stations having multiple dominant interferers gets high due to the enforcement of minimum distance between base stations. Small cell clustering is one viable solution, but the number of small cells need to be increased in hyper-dense HetSNets to provide the similar level of mobility management performance.[3] As mobile stations are limited in estimating interference channel, as indicated in [50], the channel gains outside the (cooperating) cluster of interest cannot be known. In hyper-dense HetSNets, even the estimation of interference channel may be limited when the number of dominant interferers increases[4], resulting in degradation of the area throughput. From the results in Fig. 5.7, it seems obvious that there are fundamental limits of hyper-densification which may be governed by the fundamental limits of cooperation in [50].

[3]One of the reasons of forming a small cell cluster is to improve the mobility management performance. It is known that the handover performance in HetNet deployments is not as good as in pure macro deployments [52]. To keep average time of stay (ToS), a.k.a cell sojourn time, per cell, the small cell cluster size depends on the area, not the number of small cells. Therefore, the number of small cells in a cluster keeps increasing as the small cell densification is progressed.

[4]For instance, in 3GPP LTE systems [4], due to the modulo-6 frequency shift of the cell reference signal, reference signals from interfering cells may collide with the reference signal in the serving cell if the number of dominant interfering cells with two transmit antennas is greater than 2.

Chapter 6

Conclusions and Future Work

6.1 Conclusions

In dense cellular networks where other-cell interference is the key capacity limiting factor, multicell cooperation may dramatically enhance the system performance. Understanding the role of the multiple receive antennas and receiver processing in multicell cooperative systems is important to achieve the full benefits of such systems because transmitter and receiver beamforming design is often closely coordinated. In this dissertation, we have investigated the role of receive antenna and receiver processing techniques in multicell MIMO cooperative systems. We have then proposed coordinated beamforming and joint processing algorithms based on the investigated receiver techniques, providing not only higher system throughput but also the practical advantages such as simplified receiver processing, scalability, and limited cooperation.

In Chapter 2, we have first introduced multicell cooperative systems with multiple receive antennas and advanced receiver techniques. Three representative multicell cooperation techniques have been introduced, explaining their potential use of multiple receive antennas and asymptotic behavior of the sum rate with increasing number of receive antennas. Advanced receiver algo-

rithms in different interference statistics have also been introduced. Multicell cooperative processing, CoMP, as it is being envisioned by emerging wireless standards, has been reviewed and simulated, showing the gains of CoMP and advanced receiver techniques.

In Chapter 3, interference aware-coordinated precoding algorithms with different linear receive processing techniques have been presented. Assuming both private and common messages were sent from each base station to each desired mobile station, we have proposed novel coordinated precoding algorithms to nullify undesired interference and maximize the effective channel gain through generalized eigen decomposition, interference alignment and maximum ratio combining techniques.

In Chapter 4, we have proposed iterative CBF algorithms, which are based on Max-SINR, Max-SLNR or Min-SMSE objectives, and showed enhanced performance than the non-cooperative or interference-ignorant approaches. Especially, the Min-SMSE algorithm have achieved performance close to that of a brute force search algorithm after enough iterations. We have then proposed synchronous and asynchronous limited feedback algorithms that are more efficient and adequate in practical cellular networks.

To sum up, in this dissertation, we have identified the role of multiple receive antennas in multicell cooperative systems. Multiple receive antennas may provide not only additional degrees of freedom to combat out-of-cell interference but also provide better channel state information to the transmitter with the same number of feedback bits. Many receiver processing techniques

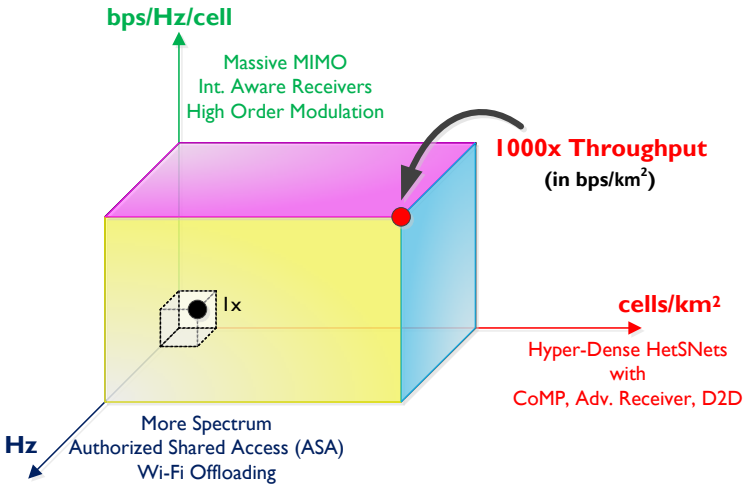

Figure 6.1: The 1000x data challenge in three domains.

have then proposed to provide not only higher link throughput (e.g., per-link SINR) but also higher system throughput (e.g., sum rate) in multicell systems. As the mobile stations may experience higher interference power due to smaller cell size, the needs for multicell cooperation become obvious and so does the use of multiple receive antennas and advanced receiver processing.

6.2 Future Work

Mobile data traffic has just started exploding: the amount of traffic usage has been doubling each year during the last few years due to increasing popularity of smart phones and new types of mobile computing devices. Now the wireless industry is preparing for even a bigger challenge, an astounding 1000x increase in the data traffic is expected in this decade [1].

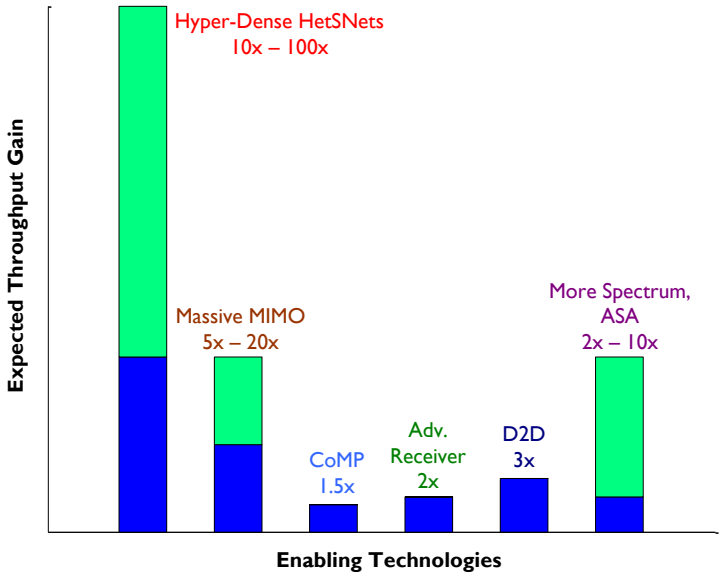

Figure 6.2: Multiple paths to the 1000x data throughput with projected gains.

A set of new radio access technologies is required to satisfy future requirements of 1000x capacity [38]. The required capacity is in bps/km^2, which is equivalent to $bps/Hz/cell \times Hz \times cell/km^2$. Higher utilization of spectrum ($bps/Hz/cell$) in given frequency resources per cell is difficult; recent results show that at least point-to-point link throughput is very close to the theoretical limits. Utilization of more bandwidth (Hz) is a very costly solution, unless devices can utilize additional radio access technologies for unlicensed bands with seamless aggregation and offloading. The final and probably one of the most promising frontiers to achieve the goal is to increase $cell/km^2$ by deploying more cells of different types/technologies in a given area. Heterogeneous and small cell networks (HetSNets), whose goal is to maximize the

utilization of existing spectrum by deploying more cells, are thus expected to be an important part of the future of cellular networks [6, 23]. In hyper-dense HetSNets, multicell coordination with multiple receive antennas plays a key role in achieving unprecedented capacity. Fig. 6.1 shows the 1000x challenge in three domains and shows the hyper-densification of small cells needs to be accompanied by multicell cooperation with advanced receiver techniques.

The projected throughput gains of different enabling technologies are presented in Fig. 6.2. Note that the blue bars presented in Fig. 6.2 are rough estimates based on the current status of the technologies [38]. Each green bar represents the expected throughput gain of the technology: with further technological advances, a higher gain (the blue bar) can be achieved. Based on the investigation made in this dissertation, we are confident that *HetSNets with novel multicell cooperation techniques can provide the data throughput required in the upcoming decade.*

There are many potential research topics related to our work here on multicell cooperative networks. We highlight a few of them here.

- Multicell cooperation in viral proliferation of small cells: As the deployment of small cell is mostly unplanned, how to apply multicell cooperation to and from the new small cells is of interest. As shown in [19], enforcing a certain minimum distance between cells is desirable for better coverage and load balancing. This enforcement, however, can be relaxed by utilizing novel multicell coordination algorithms discussed in

this dissertation. A possible future topic could be practical ways of promoting/enforcing multicell coordination between unplanned small cells in a distributed manner.

- Multicell cooperation with advanced receivers: As indicated in Chapter 2, in an agile channel condition, the receiver may apply advanced receiver techniques rather than relying on a full coordination. The advanced receive algorithm can thus supplement to the coordinated beamforming algorithms. How to combine the multicell cooperation and advanced receive antenna under different channel conditions would provide interesting guidelines in practical multicell systems.

- Multicell Cooperation in Massive MIMO and mmWave MIMO: MIMO technologies are clearly heading from coordinated multi-cell MIMO to massive MIMO and mmWave MIMO. Unlike the current cellular systems in busy microwave frequencies, future 5G system may (at leat partially) utilize under-utilized mmWave bands [26, 55, 59, 60]. The possibility of multicell coordination techniques in such mmWave bands is another interesting research topic.

- Fundamental Limits of Hyper-Densfication: Despite the fundamental limits of cooperation are shown due to the time required for aggregated interference channel estimation, feedback reporting and coordination among cells exceeds the channel coherence time [50], their expansion to multi-tier HetSNets overlaid on existing macrocellular networks

are not fully understood. We presented some primitive results in Section 5.3, showing that the reuse of the capacity in hyper-dense HetSNets does not grow indefinitely as long as the user density grows accordingly. The area sum throughput is saturated at some point due to distinct interference characteristics, channel properties, growing overhead (e.g., handover overhead), and most importantly, fundamental limits of cooperation. Then, what is the role of receiver processing and multiple receive antennas in such hyper-dense HetSNets?

Bibliography

[1] Qualcomm Incorporated (2012, Oct.). The 1000x data challenge [Online]. available at http://www.qualcomm.com/1000x/.

[2] 3GPP LTE TR 36.300 (V11.7.0). Evolved universal terrestrial radio access (E-UTRA) and evolved universal terrestrial radio access network (E-UTRAN); overall description; stage 2. *Third Generation Partnership Projects*, Sep. 2013.

[3] 3GPP LTE TR 36.819 (V11.2.0). Coordinated multi-point operation for lte physical layer aspects (release 11). *Third Generation Partnership Projects*, Sep. 2013.

[4] 3GPP LTE TS 36.211 (V11.4.0). Physical channels and modulation (release 11). *Third Generation Partnership Projects*, Sep. 2013.

[5] 3GPP TR 36.814. Further advancements for E-UTRA: physical layer aspects. *The 3rd Generation Partnership Project (3GPP)*, 9.0.0, Mar. 2010.

[6] J. G. Andrews. Seven ways that HetNets are a cellular paradigm shift. *IEEE Comm. Mag.*, 51(3):136–144, 2013.

[7] T. Bai and R. W. Heath, Jr. Asymptotic coverage probability and rate in massive MIMO networks. *submitted to IEEE Trans. Comm. Lett.*, 2013. available at http://arxiv.org/abs/1305.2233.

[8] Z. Bai, B. Badic., S. Iwelski., T. Scholand, R. Balraj, G. Bruck, and P. Jung. On the equivalence of MMSE and IRC receiver in MU-MIMO systems. *IEEE Comm. Lett.*, 15(12):1288–1290, Dec. 2011.

[9] R. Bhagavatula and R. W. Heath, Jr. Adaptive limited feedback for sum-rate maximizing beamforming in cooperative multicell systems. *IEEE Trans. Sig. Proc.*, 59(2):800–811, 2011.

[10] T. X. Brown. Cellular performance bounds via shotgun cellular systems. *IEEE Jour. Select. Areas in Comm.*, 18(11):2443–2455, 2000.

[11] V. Cadambe and S. Jafar. Interference alignment and the degrees of freedom for the K-user interference channel. *IEEE Trans. on Info. Theory*, 54(8):3425–3441, July 2008.

[12] D. Cai, T. Quek, C. Tan, and S. Low. Max-min weighted SINR in coordinated multicell MIMO downlink. In *International Symposium on Modeling and Optimization in Mobile, Ad Hoc and Wireless Networks (WiOpt 2011).*, pages 286 –293, May 2011.

[13] G. Caire and S. Shamai (Shitz). On the achievable throughput of a multi-antenna Gaussian broadcast channel. *IEEE Trans. Info. Th.*, 43(7):1691–1706, July 2003.

[14] C. B. Chae, I. Hwang, R. W. Heath, Jr., and V. Tarokh. Interference aware-coordinated beamforming in a multi-cell system. *IEEE Trans. Wireless Comm.*, (99):1–12, Sep. 2012.

[15] C. B. Chae, S. Kim, and R. W. Heath, Jr. Network coordinated beamforming for cell-boundary users: Linear and non-linear approaches. *IEEE Journal of Selected Topics in Signal Processing (J-STSP)*, 2009.

[16] C. B. Chae, D. Mazzarese, N. Jindal, and R. W. Heath, Jr. Coordinated beamforming with limited feedback in the MIMO broadcast channel. *IEEE Jour. Select. Areas in Comm.*, 26(8):1505–1515, Oct. 2008.

[17] P. Cheng, M. Tao, and W. Zhang. A new SLNR-based linear precoding for downlink multi-user multi-stream MIMO systems. *IEEE Comm. Lett.*, 14(11):1008–1010, 2010.

[18] S. Cho and W. Choi. Coverage and load balancing in heterogeneous cellular networks with minimum cell separation. *IEEE Transactions on Mobile Computing*, 99:1, 2013.

[19] S. Cho and W. Choi. Energy-efficient repulsive cell activation for heterogeneous cellular networks. *IEEE Jour. Select. Areas in Comm.*, 31(5):870–882, 2013.

[20] W. Choi and J. G. Andrews. The capacity gain from intercell scheduling in multi-antenna systems. *IEEE Trans. on Wireless Communications*, 7(2):714–725, Feb. 2008.

[21] H. Dahrouj and W. Yu. Coordinated beamforming for the multicell multi-antenna wireless systems. *IEEE Trans. Wireless Comm.*, 9(5):1748–1795, May 2010.

[22] H. Dai and V. Poor. Asymptotic spectral efficiency of multicell MIMO systems with frequency-flat fading. *IEEE Trans. on Sig. Proc.*, 51(11):2976–2988, Nov. 2003.

[23] A. Damnjanovic, J. Montojo, Y. Wei, T. Ji, T. Luo, M. Vajapeyam, T. Yoo, O. Song, and D. Malladi. A survey on 3GPP heterogeneous networks. *IEEE Wireless Commun.*, 18(3):10–21, Jun. 2011.

[24] H. S. Dhillon, R. K. Ganti, F. Baccelli, and J. G. Andrews. Modeling and analysis of K-tier downlink heterogeneous cellular networks. *IEEE Jour. Select. Areas in Comm.*, 30(3):550–560, Apr. 2012.

[25] Alan Edelman. Eigenvalues and condition number of random matrices. *Ph.D. dissertation, Dept. Mathematics, MIT, Cambridge, MA*, 1989.

[26] O. El-Ayach, S. Rajagopal, S. Abu-Surra, Z. Pi, and R. W. Heath, Jr. Spatially sparse precoding in millimeter wave MIMO systems. *submitted to IEEE Trans. Wireless Comm.*, 2013. available at http://arxiv.org/abs/1305.2460.

[27] R. Etkin, D. Tse, and H. Wang. Gaussian interference channel capacity to within one bit. *IEEE Trans. Info. Th.*, 54(12):5534–5562, Dec. 2008.

[28] D. Gesbert, S. Hanly, H. Huang, S. Shamai (Shitz), O. Simeone, and W. Yu. Multi-cell MIMO cooperative networks: a new look at interference. *IEEE Jour. Select. Areas in Comm.*, 28(9):1380–1408, Dec. 2010.

[29] T. Gou and S. A. Jafar. Degrees of freedom of the K user $M \times N$ MIMO interference channel. *IEEE Trans. Info. Th.*, 56(12):6040–6057, Dec. 2010.

[30] J. He and M. Salehi. Low-complexity coordinated interference-aware beamforming for MIMO broadcast channels. *Proc. IEEE Veh. Technol. Conf.*, pages 685–689, 2007.

[31] Z. Ho and D. Gesbert. Balancing egoism and altruism on interference channel: The MIMO case. In *Proc. IEEE Int. Conf. on Comm.*, pages 1–5, 2010.

[32] B. M. Hochwald, C. B. Peel, and A. L. Swindlehurst. A vector-perturbation technique for near capacity multiantenna multiuser communication - part II: perturbation. *IEEE Trans. on Commun.*, 53:537–544, March 2005.

[33] R. A. Horn and C. R. Johnson. *Matrix Analysis*. University of Cambridge Press, New York, 4th edition, 1990.

[34] J. Hoydis, S. ten Brink, and M. Debbah. Massive MIMO: How many antennas do we need? In *49th Annual Allerton Conference on Communication, Control, and Computing (Allerton)*, pages 545–550, Sep. 2011.

[35] I. Hwang, C. B. Chae, J. Lee, and R. W. Heath, Jr. Multicell cooperative systems with multiple receive antennas. *IEEE Wireless Commun.*, 20(1):50–58, 2013.

[36] I. Hwang, C. B. Chae, and R. W. Heath, Jr. Interference-aware coordinated precoding strategies with common and privte messages. *to be submitted to IEEE Comm. Lett.*, 2013.

[37] I. Hwang, B. Song, and R. W. Heath, Jr. Iterative coordinated beamforming with limited cooperation for multi-antenna multicell networks. *to be submitted to IEEE Trans. Wireless Comm.*, 2013.

[38] I. Hwang, B. Song, and S. S. Soliman. A holistic view on hyper-dense heterogeneous and small cell networks. *IEEE Comm. Mag.*, 51(6):20–27, 2013.

[39] R. Irmer, H. Droste, P. Marsch, M. Grieger, G. Fettweis, S. Brueck, H. P Mayer, L. Thiele, and V. Jungnickel. Coordinated multipoint: Concepts, performance, and field trial results. *IEEE Comm. Mag.*, 49(2):102–111, 2011.

[40] S.A. Jafar and S. Shamai. Degrees of freedom region of the MIMO X channel. *IEEE Trans. on Info. Theory*, 54(1):151–170, Jan. 2008.

[41] N. Jindal and Z.-Q. Luo. Capacity limits of multiple antenna multicast. *Proc. IEEE Int. Symp. Info. Th.*, pages 1841–1845, July 2006.

[42] N. Jindal and Z. Q. Luo. Capacity limits of multiple antenna multicast. *IEEE International Symposium on Information Theory (ISIT)*, July 2006.

[43] N. Jindal, W. Rhee, S. Vishwanath, S. Jafar, and A. Goldsmith. Sum power iterative water-filling for multi-antenna gaussian broadcast channels. *IEEE Trans. on Info. Theory*, 51(4):1570–1580, 2005.

[44] S. Jing, D. Tse, J. Soriaga, J. Hou, J. Smee, and R. Padovani. Multicell downlink capacity with coordinated processing. *EURASIP J. Wireless Comm. and Networking*, 2008(Article ID 586878):1–19, 2008.

[45] M. Joham, K. Kusume, M. Gzara, W. Utschick, and J. Nossek. Transmit Wiener filter for the downlink of TDD DS-CDMA systems. In *in Proc. IEEE ISSSTA*, pages 9–13, 2002.

[46] E. Katranaras, M. Imran, and C. Tzaras. On the capacity of variable density cellular systems under multicell decoding. *IEEE Commun. Lett.*, 12(7):496–498, Jul. 2008.

[47] Steven M. Kay. *Fundamentals of statistical signal processing: estimation theory*. Prentice-Hall, Inc., Upper Saddle River, NJ, USA, 1993.

[48] J. Lee, D. Toumpakaris, and W. Yu. Interference mitigation via joint detection. *IEEE Jour. Select. Areas in Comm.*, 29(6):1172–1184, June 2011.

[49] K. Lee, C.-B. Chae, R. W. Heath, Jr., and J. Kang. MIMO transceiver designs for spatial sensing in cognitive radio networks. *IEEE Trans. Wireless Comm.*, 10(11):3570–3576, Nov. 2011.

[50] A. Lozano, R. W. Heath, Jr., and J. G. Andrews. Fundamental limits of cooperation. *IEEE Trans. Info. Th.*, 59(9):5213–5226, 2013.

[51] P. Marsch and G. P. Fettweis. *Coordinated Multi-Point in Mobile Communications: From Theory to Practice.* Cambridge University Press, 2011.

[52] 3GPP Technical Specification Group Radio Access Network. Mobility enhancements in heterogeneous networks (release 11). *Technical Report 3GPP TR 36.839*, 2012.

[53] H. Ngo, E. Larsson, and T. L. Marzetta. Energy and spectral efficiency of very large multiuser MIMO systems. *submitted to IEEE Trans. Comm.*, 2011. available at http://arxiv.org/abs/1112.3810.

[54] C. B. Peel, B. M. Hochwald, and A. L. Swindlehurst. A vector-perturbation technique for near capacity multiantenna multiuser communication - part I: channel inversion and regularization. *IEEE Trans. on Commun.*, 53:195–202, Jan. 2005.

[55] Z. Pi and F. Khan. An introduction to millimeter-wave mobile broadband systems. *IEEE Comm. Mag.*, 49(6):101–107, 2011.

[56] A. Poon, R. Brodersen, and D. Tse. Degrees of freedom in multiple-antenna channels: A signal space approach. *IEEE Trans. Info. Th.*, 51:523–536, 2005.

[57] A. Poon, D. Tse, and R. Brodersen. Impact of scattering on the capacity, diversity, and propagation range of multiple-antenna channels. *IEEE Trans. Info. Th.*, 52(3):1087 –1100, Mar. 2006.

[58] R. W. Heath, Jr., S. Peters, Y. Wang, and J. Zhang. A current perspective on distributed antenna systems for the downlink of cellular systems. *IEEE Comm. Mag.*, 51(4):161–167, 2013.

[59] T. Rappaport, F. Gutierrez, E. Ben-Dor, J. Murdock, Y. Qiao, and J. Tamir. Broadband millimeter-wave propagation measurements and models using adaptive-beam antennas for outdoor urban cellular communications. *IEEE Trans. Antennas Propagat.*, 61(4):1850–1859, 2013.

[60] T. Rappaport, S. Sun, R. Mayzus, H. Zhao, Y. Azar, K. Wang, G Wong, J. Schulz, M. Samimi, and F. Gutierrez. Millimeter wave mobile communications for 5G cellular: It will work! *Access, IEEE*, 1:335–349, 2013.

[61] M. Sadek, A. Tarighat, and A. H. Sayed. A leakage-based precoding scheme for downlink multi-user MIMO channels. *IEEE Trans. Wireless Comm.*, 6(5):1711–1721, 2007.

[62] D. A. Schmidt, C. Shi, R. A. Berry, M. L. Honig, and W. Utschick. Minimum mean squared error interference alignment. In *Proc. of Asilomar*

Conf. on Sign., Syst. and Computers, pages 1106–1110, 2009.

[63] C. Seol and K. Cheun. A statistical inter-cell interference model for downlink cellular OFDMA networks under log-normal shadowing and multipath Rayleigh fading. *IEEE Trans. Comm.*, 57(10):3069–3077, Oct. 2009.

[64] Stefania Sesia, Issam Toufik, and Matthew Baker. *LTE - The UMTS Long Term Evolution: From Theory to Practice.* Wiley, 2nd edition, 2011.

[65] S. Shamai and B.M. Zaidel. Enhancing the cellular downlink capacity via co-processing at the transmitting end. *Proc. IEEE Vehicular Technology Conference (VTC)*, 3:1745–1749, 2001.

[66] H. Shen, B. Li, M. Tao, and X. Wang. MSE-based transceiver designs for the MIMO interference channel. *IEEE Trans. Wireless Comm.*, 9(11):3480–3489, Nov. 2010.

[67] C. Shi, D.A. Schmidt, R.A. Berry, M.L. Honig, and W. Utschick. Distributed interference pricing for the MIMO interference channel. In *Proc. IEEE Int. Conf. on Comm.*, pages 1–5, 2009.

[68] S. Shi, M. Schubert, and H. Boche. Downlink MMSE transceiver optimization for multiuser MIMO systems: Duality and Sum-MSE minimization. *IEEE Trans. Sig. Proc.*, 55(11):5436–5446, 2007.

[69] S. Shim, J. S. Kwak, R. W. Heath, Jr., and J. G. Andrews. Block diagonalization for multi-user MIMO with other-cell interference. *IEEE Trans. Wireless Comm.*, 7(7):2671–2681, July 2008.

[70] O. Simeone, O. Somekh, H. V. Poor, and S. S. (Shitz). Local base station cooperation via finite-capacity links for the uplink of wireless networks. *IEEE Trans. on Info. Theory*, 55(1):190–204, Jan. 2009.

[71] O. Simeone, O. Somekh, H. V. Poor, and S. Shamai. Downlink multicell processing with limited-backhaul capacity. *EURASIP Journal on Advances in Signal Processing*, 2009(3), Feb. 2009.

[72] O. Somekh, B.M. Zaidel, and S. Shamai. Sum rate characterization of joint multiple cell-site processing. *IEEE Trans. on Info. Theory*, 53(12):4473 –4497, dec. 2007.

[73] B. Song, R. Cruz, and B. Rao. Network duality for multiuser MIMO beamforming networks and applications. *IEEE Trans. Commun.*, 55(3):618–630, March 2007.

[74] H. Sung, K. Lee, S. Park, and I. Lee. An iterative precoder optimization method for k-user interference channel systems. In *Proc. IEEE Glob. Telecom. Conf.*, Dec. 2009.

[75] A. J. Tenenbaum and R. S. Adve. Linear processing and sum throughput in the multiuser MIMO downlink. *IEEE Trans. Wireless Comm.*, 8(5):2652–2661, May 2009.

[76] S. Vishwanath, N. Jindal, and A. Goldsmith. Duality, achievable rates, and sum capacity of Gaussian MIMO broadcast channels. *IEEE Trans. on Info. Theory*, 49:2658–2668, Aug. 2003.

[77] P. Viswanath, V. Anantharam, and D. Tse. Optimal sequences, power control, and user capacity of synchronous CDMA systems with linear MMSE multiuser receivers. *IEEE Trans. Info. Th.*, 45(6):1968–1983, Sep. 1999.

[78] H. Weingarten, Y. Steinberg, and S. Shamai. The capacity region of the Gaussian multiple-input multiple-output broadcast channel. *IEEE Trans. Info. Th.*, 52(9):3936–3964, Sept. 2006.

[79] R. Wesel and J. Cioffi. Achievable rates for Tomlinson-Harashima precoding. *IEEE Trans. Info. Th.*, 44(2):824 –831, Mar 1998.

[80] M. Yoon, M. Kim, and C. Lee. Decentralized precoding algorithm with weighted SLNR for limitedly coordinated network. *IEEE Comm. Lett.*, 16(3):318–320, 2012.

[81] R. Zakhour, Z. Ho, and D. Gesbert. Distributed beamforming coordination in multicell MIMO channels. In *Vehicular Technology Conference, 2009. VTC Spring 2009. IEEE 69th*, pages 1–5, 2009.

[82] H. Zhang and H. Dai. Cochannel interference mitigation and cooperative processing in downlink multicell multiuser MIMO networks. *EURASIP*

Journal on Wireless Communications and Networking, 2004(2):222–235, 2004.

[83] H. Zhang, H. Dai, and Q. Zhou. Base station cooperation for multiuser MIMO: joint transmission and BS selection. *in Proc. Conference on Informations Sciences and Systems (CISS)*, March 2004.

[84] J. Zhang and J. Andrews. Adaptive spatial intercell interference cancellation in multicell wireless networks. *IEEE Jour. Select. Areas in Comm.*, 28(9):1455–1468, 2010.

[85] J. Zhang, Y. Wu, S. Zhou, and J. Wang. Joint linear transmitter and receiver design for the downlink of multiuser MIMO systems. *IEEE Comm. Lett.*, 9(11):991–993, 2005.

[86] R. Zhang and S. Cui. Cooperative interference management with MISO beamforming. *IEEE Trans. Sig. Proc.*, 58(10):5450–5458, 2010.

Vita

Insoo Hwang obtained his M.S. degree from University of Southern California, Los Angeles in 2005 and B.S. degree from Pohang University of Science and Technology (POSTECH), Pohang, Korea in 2003, both in electrical engineering. He enrolled at The University of Texas at Austin to pursue a doctoral degree in the department of electrical and computer engineering in 2007.

He has more than 7 years of experience in wireless systems research and design at Qualcomm Research (San Diego), Samsung Electronics US R&D Center (San Diego) and Telecommunications R&D Center (Korea), and Samsung Advanced Institute of Technology (Korea). He is (co)author of over 70 issued patents and published patent applications. At Qualcomm Research San Diego (Office of the Chief Scientist), he has been working toward next generation cellular systems and standards, focusing on investigation of the limits and challenges in large-scale heterogeneous and small cell networks. He is actively seeking for the fundamental limits of such networks via hyper-dense deployment of small cells, multicell cooperation, and advanced receiver processing.

Permanent address: San Diego, USA (insoo.hwang@gmail.com)

This dissertation was typeset with LaTeX[†] by the author.

[†]LaTeX is a document preparation system developed by Leslie Lamport as a special version of Donald Knuth's TeX Program.